Russian Chemical Reviews **74** (6) 489 – 520 (2005) © 2005 Russian Academy of Sciences and Turpion Ltd

DOI 10.1070/RC2005v074n06ABEH000897

Magnetic nanoparticles: preparation, structure and properties

S P Gubin, Yu A Koksharov, G B Khomutov, G Yu Yurkov

Contents

I.	Introduction	489
II.	Nanoparticles and materials based on them (classification, definitions)	490
III.	Methods for the preparation of magnetic nanoparticles and nanomaterials	491
IV.	The most widely encountered magnetic nanoparticles	497
V.	Methods of nanoparticle stabilisation	499
VI.	Types of materials containing magnetic nanoparticles	500
VII.	Magnetic nanoparticles in biological objects	502
VIII.	Physical methods for determination of the composition and dimensions of nanoparticles	503
IX.	Characteristic features of the nanoparticle magnetism (theory)	505
X.	Magnetic characteristics of nanoparticles (experimental data)	510
XI.	Further prospects for the study of magnetic nanoparticles	513
XII.	Conclusion	514

Abstract. The key methods for the preparation of magnetic nanoparticles are described systematically. The experimental data on their properties are analysed and generalised. The main theoretical views on the magnetism of nanoparticles are considered. The bibliography includes 416 references.

I. Introduction

In the last two decades, new terms with the prefix 'nano' have rushed into the scientific vocabulary — nanoparticle, nanostructure, nanotechnology, nanomaterial, nanocluster, nanochemistry, nanocolloids, nanoreactor and so on. A series of new journals are devoted particularly to this subject, monographs with the corresponding names have appeared, 'nano'-specialised institutes, chairs and laboratories have been founded; and numerous conferences are held. In most cases, new names were applied to long known objects or phenomena; however, new objects inaccessible for researchers some 20 years ago have also appeared. These include fullerenes, quantum dots, nanotubes, nanofilms and nanowires, *i.e.*, the objects with at least one nanometer (10^{-7} – 10^{-9} m) dimension.

The enhanced interest of the researchers in nanoobjects is due to the discovery of unusual physical and chemical properties of these objects, which is related to manifestation of so-called 'quantum size effects.' These arise in the case where the size of the system is commensurable with the de-Brogli wavelengths of the electrons, phonons or excitons propagating in them.

A key reason for the change in the physical and chemical properties of small particles as their size decreases is the increased fraction of the 'surface' atoms, which occur under conditions (coordination number, symmetry of the local environment, *etc.*) differing from those of the bulk atoms. From the energy standpoint, a decrease in the particle size results in an increase in the fraction of the surface energy in its chemical potential.

Currently, unique physical properties of nanoparticles are under intensive research.[1] A special place belongs to the magnetic properties in which the difference between a massive (bulk) material and a nanomaterial is especially pronounced. In particular, it was shown that magnetisation (per atom) and the magnetic anisotropy of nanoparticles can be much greater than those of a bulk specimen, while differences in the Curie (T_C) or Neel (T_N) temperatures, *i.e.*, the temperatures of spontaneous parallel or antiparallel orientation of spins, between nanoparticle and the corresponding microscopic phases reach hundreds of degrees. In addition, magnetic nanomaterials were found to possess a number of unusual properties — giant magnetoresistance, abnormally high magnetocaloric effect, and so on.

The magnetic properties of nanoparticles are determined by many factors, the key of these including the chemical composition, the type and the degree of defectiveness of the crystal lattice, the particle size and shape, the morphology (for structurally inhomogeneous particles†), the interaction of the particle with the surrounding matrix and the neighbouring particles. By changing the nanoparticle size, shape, composition and structure, one can control to an extent the magnetic characteristics of the material based on them. However, these factors cannot always be controlled during the synthesis of nanoparticles nearly equal in size and chemical composition; therefore, the properties of nanomaterials of the same type can be markedly different.

S P Gubin, G Yu Yurkov N S Kurnakov Institute of General and Inorganic Chemistry, Russian Academy of Sciences, Leninsky prosp. 31, 119991 Moscow, Russian Federation. Fax (7-095) 954 12 79, tel. (7-095) 954 71 36, e-mail: gubin@igic.ras.ru (S P Gubin), gy_yurkov@mail.ru (G Yu Yurkov)
Yu A Koksharov, G B Khomutov Department of Physics, M V Lomonosov Moscow State University, Leninskie Gory, 119992 Moscow, Russian Federation. Fax (7-095) 932 88 20, tel. (7-095) 939 29 73, e-mail: yua_koksharov@rambler.ru (Yu A Koksharov), tel. (7-095) 939 30 25, e-mail: gbk@mail.ru (G B Khomutov)

Received 9 January 2004
Uspekhi Khimii **74** (6) 539 – 574 (2005); translated by Z P Bobkoba

† Almost all particles are inhomogeneous because the properties of the surface and the interior of the particle are inevitably dissimilar. It can be stated with confidence that any nanoparticle has a 'shell' but not all of them have a clear-cut 'core'.

The last years have seen changes in the development of magnetic nanomaterials, which can be called revolutionary, to say the least. This is related both to the development of efficient methods for the preparation and stabilsation of nano-sized magnetic particles and to the progress in the physical methods for the investigation of such particles. For example, it became possible to prepare nanometre metal or oxide particles as not only ferromagnetic fluids (the preparation process was developed back in the 1960s)[2,3] but also as particles included into 'rigid' matrices (polymers, zeolites, *etc*.).

The magnetic characteristics of a material consisting of a non-magnetic solid dielectric matrix with magnetic nanoparticles (3–10 nm) distributed in the matrix were described in 1980.[4] The presence of nanoparticles‡ in these materials and their composition were established by small-angle X-ray scattering and Mössbauer spectroscopy.[5] More recently, these samples were investigated once again by modern methods , which largely confirmed the earlier results.[6]

Magnetic nanoparticles are abundant in nature and are found in many biological objects.[7] Magnetic nanomaterials are used in information recording and storage systems, in new permanent magnets, in magnetic cooling systems, as magnetic sensors, *etc*. All this accounts for the interest of various specialists in these systems.

Extensive literature is devoted to the applied aspects of the state-of-the-art technology of magnetic recording and its prospects.[8] Currently, powders with micron-size γ-Fe_2O_3, Co–γ-Fe_2O_3, Fe or Fe–Co grains are used most often in magnetic tapes or discs as media for magnetic recording. In this case, recording of one bit requires about 10^9 atoms,[9] whereas with the use of nanomaterials (particles 10 nm in diameter), not more than 10^5 atoms. Thus, transition to magnetic nanomaterials increases the information recording density by a factor of 10^3–10^4.

Among the magnetic materials that have found broad practical application in technology, ferromagnets deserve attention. An important characteristic of a ferromagnet is the coercive force (H_c), *i.e*., the magnetic field strength H corresponding to the point with $B = 0$ on the symmetric hysteresis loop $B(H)$ of the ferromagnet. Here B is the magnetic field induction in a ferromagnetic sample with zero demagnetising factor (for example, in a long cylinder whose axis is directed along the field). One more characteristic, apart from H_c, is the intrinsic coercive force (H_{ci}), defined as the magnetic field strength at the point $M = 0$ on the symmetric $M(H)$ hysteresis loop of the ferromagnet, where M is the magnetisation of a ferromagnetic sample with zero demagnetising factor. The coercive force and the intrinsic coercive force normally do not differ much in magnitude, but these are different physical quantities. When designing new magnetic materials, it is often a goal to attain the highest H_c. Modern magnetic materials have $H_c = 2$–3 kŒ (see Section IX).

In terms of the coercive force, ferromagnets are subdivided into soft magnetic ($H_c < 12.6$ Œ) and hard magnetic ($H_c > 126$ Œ) ones. The magnets with intermediate coercive force values are referred to as semi-hard. Table 1 presents data on the dependence of the magnetic properties of ferromagnets on the dimensions of the constituent particles. Apart from the dimensions, the magnetic properties of particles depend on the external conditions: temperature, pressure and, in some cases, the local environment, *i.e*., the medium in which the particle occurs, in particular, the crystalline or amorphous bulk matrix (for a particle), the local crystal environment (for a single atom) or the substrate (for a film).

In addition to ferromagnets in which the magnetic moments of the atoms are ordered, magnetic spin glasses — systems in which the competition of random magnetic interactions between magnetic moments results in a magnetic disordered state — also find application in technology.

‡ In those years, the term 'nanoparticle' did not yet exist and these objects were called 'ligand-free metal clusters' or just 'clusters.'

The purpose of this review is to survey the state-of-the-art views on the physics, the chemistry and the methods of preparation and stabilisation of magnetic nanoparticles used in nanotechnology for the design of new instruments and devices.

II. Nanoparticles and materials based on them (classification, definitions)

First of all, it is necessary to consider the general concepts related to the nano-sized objects.

A nano-object is a physical object differing appreciably in properties from the corresponding bulk material and having at least one nanometre dimension (not more than 100 nm).

Nanotechnology is the technology dealing with both single nano-objects and materials and devices based on them and with processes that take place in the nanometre range.

Nanomaterials are those materials whose key physical characteristics are dictated by the nano-objects they contain. Nanomaterials are classified into compact materials and nanodispersions. The first type includes so-called 'nanostructured' materials,[10] *i.e*., materials isotropic in the macroscopic composition and consisting of contacting nanometre-sized units as repeating structural elements.[11] Unlike nanostructured materials, nanodispersions include a homogeneous dispersion medium (vacuum, gas, liquid or solid) and nano-sized inclusions dispersed in this medium and isolated from each other. The distance between the nano-objects in these dispersions can vary over broad limits from tens of nanometres to fractions of a nanometre. In the latter case, we are dealing with nanopowders whose grains are separated by thin (often monoatomic) layers of light atoms, which prevent them from agglomeration.

A nanoparticle is a quasi-zero-dimensional (0D) nano-object in which all characteristic linear dimensions are of the same order of magnitude (not more than 100 nm). Nanoparticles can basically differ in their properties from larger particles, for example, from long- and well-known ultradispersed powders[12] with a grain size above 0.5 μm. As a rule, nanoparticles are shaped like spheroids. Nanoparticles with a clearly ordered arrangement of atoms (or ions) are called nanocrystallites. Nanoparticles with a clear-cut discontinuity of the system of electronic energy levels are often referred to as 'quantum dots' or 'artificial atoms' (most often, they have compositions of typical semiconductor materials).[13,14]

The term 'cluster', which has been widely used in chemical literature in former years, is currently used to designate small nanoparticles with sizes less than 1 nm. Thus, the term 'nanoclusters'[15] is excessive, because all known clusters have nanometre dimensions.

Nanorods and nanowires are quasi-one-dimensional (1D) nano-objects. In these systems, one dimension exceeds by an order of magnitude the other two dimensions, which are in the nano-range. This class includes, in particular, interesting nanostructures such as 'quantum wires'.[16]

The group of two-dimensional objects (2D) includes planar structures — nanodiscs, thin-film magnetic structures, magnetic nanoparticle layers, *etc*., in which two dimensions are an order of magnitude greater than the third dimension, which is in the nanometre range.

In this review we use the molecular approach outlined in a previous publication,[17] namely nanoparticles are considered as giant pseudomolecules having a core and a shell and often also external functional groups. The unique magnetic properties are usually inherent in the particles with a core size of 2–30 nm. For magnetic nanoparticles, this value coincides in the order of magnitude with the theoretical estimate for the smallest dimensions of a magnetic domain in most magnetic materials (see Table 1).

Table 1. Type of the change of the magnetic properties of a ferromagnet with a decrease in the substance dimensions from macroscopic to atomic.

Object	Characteristic size	Specific magnetic properties
Macroscopic (bulk) sample	$\geqslant 1$ μm	spontaneous magnetisation below T_C. The appearance of a nonzero magnetic moment is suppressed by the formation of a domain structure
Microscopic sample	50 – 1000 nm	magnetic characteristics strongly depend on the sample pre-history, preparation and processing method
Single-domain magnetic particles (small magnetic particles) in a diamagnetic matrix	1 – 30 nm	the presence of a blocking temperature [a] $T_b < T_C$ below which the magnetic moment of the particle retains orientation in space, while the particle ensemble demonstrates a magnetic hysteresis. At a temperature higher than T_b, the particle transfers into the superparamagnetic state. In the $T_b < T < T_C$ region, the particle has a spontaneous magnetisation and a nonzero total magnetic moment, which easily changes the orientation in the external field
Single atom (ion)	$\sim$0.2 nm	usual paramagnetic properties

[a] For isolated nanoparticles with sizes 1 – 30 nm, the temperature scale has one more characteristic point apart from the Curie and Neel temperatures, namely, the 'blocking' point $T_b < T_C(T_N)$.

III. Methods for the preparation of magnetic nanoparticles and nanomaterials

If the methods used to prepare nanoparticles are classified in terms of the type of the precursor and the features of its processing, the following key approaches to the formation of nanoparticles can be distinguished:

— preparation from macroscopic materials by dispersion;

— chemical synthesis, *i.e.*, targeted change in the substance composition with termination (in some way) of the nascent phase growth at the nano-size stage;

— transformations of nanoparticles with the change in the composition.

The last-mentioned route has found only a limited use as yet and is represented by a few examples.

A series of general methods for the nanoparticle synthesis have now been developed.[18] Most of them can also be used for the preparation of magnetic particles. An essential feature of their synthesis is the preparation of particles of specified size and shape (at least, the scatter of sizes should be small, 5% – 10%, and controllable). The shape control and the possibility of synthesis of anisotropic magnetic structures are especially important. In order to eliminate (or substantially decrease) the interparticle interactions, magnetic nanoparticles often need to be isolated from one another by immobilisation on a substrate surface or in the bulk of a stabilising inert matrix. It is important that the distance between the particles in the matrix should be controllable. Finally, the synthetic procedure should be relatively simple, inexpensive and reproducible.

The development of magnetic materials is often faced with the necessity of preparing nanoparticles of a complex composition, namely, ferrites, complex NdFeB or $SmCo_5$ alloys, *etc*. In these cases, the range of synthetic approaches substantially narrows down. For example, the thermal evaporation of compounds with a complex elemental composition is often accompanied by a violation of the stoichiometry in the vapour phase, resulting in the formation of other substances, while the atomic beam synthesis does not yield a homogeneous distribution of elements on the substrate. The mechanochemical methods of powder dispersion also violate (in some cases, substantially) the phase composition: in particular, ferrites do not retain the oxygen stoichiometry. Finally, the preparation of a target phase from heteroelement precursors may be associated with the difficulty of synthesis of the precursors. For example, no volatile compounds with a Sm atom bonded to five Co atoms are known; the maximum chemically attainable element ratio in $Sm[Co(CO)_4]_3$ is 1 : 3. It is even more difficult to propose a volatile stoichiometric precursor for the synthesis of NdFeB nanoparticles.

The physical characteristics of nanoparticles are known to be substantially dependent on their dimensions. Unfortunately, most of the currently known methods of synthesis afford nanoparticles with rather broad size distributions (dispersion $\sigma > 10\%$). The thorough control of reaction parameters (time, temperature, stirring velocity and concentrations of reactants and stabilising additives) does not always allow one to narrow down this distribution to the required range. Therefore, together with the development of methods for synthesis of nanoparticles with a narrow size distribution, the techniques of separation of nanoparticles into rather monodisperse fractions are perfected. This is done using controlled precipitation of particles from surfactant-stabilised solutions followed by centrifugation (the coarsest fraction is the first to be precipitated). After decantation, the precipitate can again be dissolved and subjected to precipitation/centrifugation. The process is repeated until nanoparticle fractions with specified sizes and dispersion degrees are obtained.

The methods of nanoparticle preparation cannot be detached from stabilisation methods. For 1 – 10 nm particles with a high surface energy, it is difficult to select a really inert medium,[17] because the surface of each nanoparticle bears the products of its chemical modification, which affect appreciably the nanomaterial properties. This is especially important for magnetic nanoparticles in which the modified surface layer may posses magnetic characteristics markedly differing from those of the particle core. Nevertheless, the general methods for nanoparticle synthesis not related directly to the stabilisation and the methods where the nanoparticle formation is accompanied by stabilisation (in matrices, by encapsulation, *etc*.) will be considered separately.

The methods of generation of magnetic nanoparticles in the gas or solid phase using high-energy treatment of the material are usually called physical, while the nanoparticle syntheses, which are often carried out in solutions at moderate temperatures are chemical methods. The chemical methods for the preparation of magnetic nanoparticles have developed most intensively in recent years; however, physical methods should not yet be considered as outworn.

1. Physical methods for the preparation of magnetic nanoparticles

a. Condensation methods

The method of nanoparticle synthesis from supersaturated metal vapours is based on the classical nucleation theory in which the nascent phase clusters are described by the spherical liquid drop model. Nanoparticles (clusters) are prepared using various ways of metal evaporation: laser vaporisation,[19, 20] thermal vaporisation,[21, 22] arc discharge, plasma vaporisation,[23] and solar energy-induced evaporation.[24] In each method, special installations are employed differing in engineering solutions of particular units.[25]

All the methods for metal evaporation listed above allow one to study both the physicochemical characteristics of nanoparticles in the gas phase (before the metal vapour deposition on the substrate) and the properties of films and powders obtained upon deposition. Since recently, the cryogenic method has been used to prepare nanoparticles. In this case, the condensation of metal atoms and metal compounds occurs at low temperatures in a cryogenic matrix, most often, in a liquid inert gas. This method allows the preparation of chemically highly pure nanoparticles uniform in composition and structure and having no pores or other morphological inhomogeneities.

In the classical thermal vaporisation method, a metal or alloy sample is heated in a tungsten boat in an argon or helium stream. The atoms of the vaporised metal lose kinetic energy upon collisions with inert gas atoms, gather in clusters and condense on a cooled substrate as a nanodispersed powder. By varying the evaporation rate, the substrate temperature and gas pressure and composition, one can control the particle size in the 3–100 nm range. Most often, prior to opening the installation and taking out the sample, nanoparticles are passivated by passing an inert gas/oxygen mixture for several minutes. In particular, this method was used to prepare heterometallic nanoparticles ($\sim$30 nm) with the composition Fe–M (M = Ni, Mn, Pt, Cr).[21] For the Fe–Cr system, it was shown that for a Cr content of 47.7 at.%, the metastable σ-phase with a tetragonal lattice detected in the 440–830 °C temperature range in the state diagram of the Fe–Cr alloy predominates in nanoparticles.[21,22]

Individual magnetic nanoparticles were first obtained by the molecular beam method.[26,27] In this case, metal evaporation takes place in vacuum in a diaphragm chamber. The evaporated particles pass through the diaphragm and form the molecular beam. The beam intensity determines the rate of condensation of the particles on the substrate. This method produces largely free (*i.e.*, ligand-free) clusters (nanoparticles); therefore, it can be used to determine the intrinsic magnetic properties of these particles without the distorting influence of the environment and to understand the fundamental grounds of the physics of magnetic clusters. Although unsurpassed in this respect, the molecular beam method has not found practical use for the preparation of magnetic nanomaterials.

The synthesis of nanoparticles by a hydrogen plasma metal reaction (HPMR) has been reported;[28,29] therefore, we do not consider this method here.

The preparation of nanoparticles by metal vapour spraying is a rather well-developed method in both practical and theoretical aspects. With thermal or laser vaporisation, this method allows the synthesis of gram amounts of nanoparticle powders. This method can be used for dispersing metals, alloys or oxides; however, the cost of nanomaterials obtained in this way remains rather high.

The low-energy cluster beam deposition (LECBD) method includes deposition of non-charged particles with a very low kinetic energy on a substrate.[30] In this case, the particles are not destroyed on getting on the substrate and can be inserted into various type of matrices, which are formed simultaneously by vaporisation of their components from another source. The size and composition of the deposited nanoparticles are controlled in the gas phase prior to deposition on the substrate using mass-analysing systems of various types.

b. Methods of nanodispersion of a compact material

The mechanochemical dispersion of a compact material in mills of various designs appears an attractive way to produce disperse systems. However, there exists a mechanical dispersion limit for solids,[31,32] which prevents in some cases the preparation of nanosized particles with a narrow dispersion. In addition, high energy impact on the material being ground result in intensive interaction of the nanoparticles formed with the dispersion medium. Some examples of successful use of mechanochemical dispersion for the preparation of magnetic nanoparticles are given in the following Sections.

Electrolytic erosion can also be used to disperse metals and alloys. In this case, spraying takes place inside a dielectric liquid and the liquid transformation products coat the surface of the nanoparticles formed. Depending on the process conditions, the metal nature, and the dispersion medium, the diameter of the nanoparticles formed is usually in the 2.5–20 nm range, but some particles can be as large as 100 nm.[33] Presumably, small particles are formed on quenching the metal vapour, while large ones are produced from molten drops. Using electrolytic erosion, nanoparticles with a complex composition for permanent magnets have been obtained.[34] However, in this case, too, the nanoparticles formed interact to a noticeable extent with the medium. For example, when organic solvents are used as the dielectric medium, product carbonisation takes place, while in the case of molten sulfur, sulfides are formed.[35]

Electrochemical generation is used as a method for the synthesis of substantial amounts of rather small (1–2 nm) nanoparticles with a narrow dispersion.[36] A standard electrochemical cell containing an alcohol solution of tetraalkylammonium halide was used to obtain cobalt particles. On passing the current, the cobalt anode dissolved to give Co nanoparticles near the cathode (glass carbon). The influence of electrolysis conditions on the magnetic characteristics of the resulting nanoparticles was studied using several examples.

The average size of a particle formed upon electrochemical dispersion is inversely proportional to the current density. The colloid solution of nanoparticles formed upon electrolysis can be stored under argon for several months. Evaporation of the solvent yields crystallites, which can be readily converted again into a colloid suspension.

The electrochemical process was used to obtain γ-Fe_2O_3 nanoparticles (3–8 nm), stable in organic solvents due to adsorption of cationic surfactants.[37]

2. Chemical synthesis of magnetic nanoparticles

Chemical methods for the synthesis of nanoparticles have been surveyed in a recent review;[38] therefore, we will mention only the latest publications illustrating the trends in the development of this approach.

Diverse metal-containing compounds (MCC) including metal carbonyls, organometallic compounds, metal carboxylates, *etc.*, are used as the precursors in the synthesis of magnetic nanoparticles. Most often, precursors decompose on heating or UV irradiation; other types of treatment of MCC, resulting in nanoparticles, have also been developed.

a. Thermolysis of metal-containing compounds

Thermal decomposition of metal-containing compounds has been studied in detail in relation to the development of the scientific grounds of the metal organic chemical vapour deposition (MOCVD) technique, which is used successfully to obtain nanoparticles. In a one-step CVD synthesis of nanodispersed Fe oxides, $[Fe(OBu^t)_3]_2$ has been proposed as the MCC.[39] When the reaction is carried out in a liquid medium in the presence of surfactants or polymers, it is possible to stabilise the resulting amorphous nanoparticles with diameters of up to 10 nm. An interesting example of two-stage thermolysis of $Fe(CO)_5$ has been reported.[40] First, an iron oleate complex is formed from $Fe(CO)_5$ and oleic acid at 100 °C; at 300 °C, the complex decomposes to give primary 'loose' nanoparticles (4–11 nm). After maintaining at 500 °C, these are converted, as shown by powder X-ray diffraction, into crystalline α-Fe nanoparticles. Laser photolysis of volatile MCC (most often, metal carbonyls) is also suitable for this purpose.[41]

b. Decomposition of metal-containing compounds on ultrasonic treatment

In this method, metal carbonyls and their derivatives are used as metal-containing compounds, although cases of successful use of

other organometallic compounds are also known. For example, Co nanoparticles were synthesised by ultrasound-induced decomposition of a solution of $Co_2(CO)_8$ in toluene.[42] In order to retain the monodispersity and prevent aggregation of the particles formed, sodium bis(2-ethylhexyl)sulfosuccinate was added to the solution. 'Amorphous' Co-containing nanoparticles were also obtained by ultrasonic treatment of a solution of $Co(CO)_3(NO)$ in decane in the presence of oleic acid.

For the synthesis of Fe-containing magnetic nanoparticles, $Fe(CO)_5$ is used most often.[43] Ultrasonic decomposition of iron pentacarbonyl in polyvinylpyrrolidine resulted in amorphous γ-Fe_2O_3 nanoparticles. Their dimensions were determined by the nature and concentration of the surfactants present in the solution.[44] It was shown experimentally that ultrasonic treatment of labile MCC is a convenient way of producing nanoparticles under mild conditions, which is important for the preparation of metastable aggregates. However, there are no methods for controlling their dimensions.

c. The reduction of metal-containing compounds

Magnetic metallic nanoparticles can be prepared from metal salts using strong reducing agents, namely, alkali metal dispersions in ethers or hydrocarbons, alkali metal complexes with organic electron acceptors (*e.g.*, naphthalene), $NaBH_4$ and other complex hydrides. By using $NaBH_4$ in aqueous solutions at room temperature, both homo- (Fe, Co, Ni) and heterometallic (Fe–Co, Fe–Cu, Co–Cu) nanoparticles were obtained as amorphous powders containing substantial amounts of boron (20 mass % or more). The reduction of $CoCl_2$ with $LiBEt_3H$ in the presence of trialkylphosphines yields nanoparticles of pure cobalt ε-phase with 2–11 nm size (depending on the alkyl chain length in trialkylphosphine).[45]

The general method for the preparation of metallic nanoparticles by reducing metal salts in aprotic solvents is documented.[46] High-boiling alcohols are often used as reducing agents. The reduction of cobalt acetate with dodecane-1,2-diol at 250 °C in oleic acid in the presence of trioctylphosphine gives 3–8 nm metal particles.[47] nickel-containing nanoparticles have been prepared in a similar way.[48]

Yet another method of synthesis is represented by radiation chemical reduction of metal ions in aqueous solutions. In particular, γ-irradiation of deaerated solutions of Co^{2+} and Ni^{2+} perchlorates in the presence of sodium formate and a stabiliser (surfactant) affords spherical nanoparticles (2–4 nm) of these metals with a narrow pore size distribution.[49]

d. Synthesis in reverse micelles

Recent years were marked by intensive development and wide use of the synthesis nanoparticles in nano-sized 'reactors' as the size of 'nanoreactors' can be controlled within certain limits. A micelle is an example of these nanoreactors. Reverse micelles are tiny drops of water stabilised in a hydrophobic liquid phase due to the formation of a surfactant monolayer on their surface. Owing to the exactly measured amount of MCC in each micelle (as the nanoparticle formation occurs without substance supply from the outside), it is possible not only to control the composition and the average size of the particles but also to obtain monodisperse samples with a narrow particle size distribution. Thus Co nanoparticles were synthesised by mixing two colloid solutions of reverse micelles with the same diameter (3 nm), one containing $CoCl_2$ and the other containing sodium tetrahydroborate of the same concentration.[50] Magnetic nanoparticles with an average diameter of 5.8 nm and a polydispersity of 11% were obtained in hexane as a colloid dispersion stable against aggregation and oxidation during a week. Syntheses of cobalt nanoparticles in reverse micelles are described in detail in the literature.[51–53]

e. Sol–gel method

The sol–gel method is widely used in a number of technologies.[54] In nanotechnology, it is used most often to obtain metal oxides but is also applicable to the synthesis of nanosized metals and fused bimetallic and heteroelement particles. For example, reduction of Ni^{2+} and Fe^{2+} ions inserted in silica gel in 3 : 1 ratio with hydrogen at 733–923 K resulted in Ni_3Fe nanoparticles (4–19 nm) within the SiO_2 matrix.[55]

e. Synthesis of magnetic nanoparticles at a gas–liquid interface

Nanoparticles can also be synthesised in the absence of solid substrates or matrices by redox reactions at an interface between two phases, one containing a metal compound (precursor) and the other, the reducing agent. This method was first implemented by Faraday back in 1857 to prepare a stable colloid solution of gold nanoparticles.[56] A new approach to the synthesis and self-assembly of nano-sized structures including magnetic ones in a fully anisotropic two-dimensional reaction system has been reported.[57–64] Nanoparticles were synthesised in a Langmuir monolayer of amphiphilic molecules,§ incorporating the precursor molecules at a gas–liquid interface. Decomposition of metal compounds in such a monolayer initiates the appearance and nucleation of active intermediates and the two-dimensional growth of nanoparticles on the liquid surface. The surfactant molecules of the monolayer can react with the nanoparticles formed and affect the growth processes, thus opening the way for effective control of the size and morphology of the structures formed. The growth and self-organisation of nanoparticles can also be affected by changing the chemical composition of the liquid or gas phase, *i.e.*, by adding compounds that react with nanoparticles on the liquid surface, by varying the temperature, by exposing the monolayer to electric or magnetic fields or various types of radiation (including light).

Two-dimensional diffusion and growth of nanoparticles depend on the thermodynamic state of the Langmuir monolayer. This can exist as so-called two-dimensional gas, two-dimensional liquid or a condensed two-dimensional phase (when the molecules are located close to one another). When the monolayer passes into the condensed state, the diffusion controlled processes stop and the system state settles down. This allows one to stop the nanoparticle growth and organisation at the specified moment and then to transfer the monolayer with the resulting nanoparticles and nanostructures on solid substrates and to study the resulting planar nanostructures by various methods.

The decomposition of the precursor molecule at the interface can be induced by electromagnetic radiation (in particular, light). This photochemical decomposition of iron pentacarbonyl in the Langmuir monolayer under contact with air gives nanoparticles and nanostructures of iron oxides, mainly γ-Fe_2O_3.[59] An external magnetic field has a substantial influence on the shape of the resulting anisotropic magnetic nanoparticles, their shape and orientation being dependent on the orientation of the applied field with respect to the interface.[59, 60, 62]

The influence of the applied fields on the two-dimensional growth of amorphous iron-containing magnetic nanoparticles by decomposition of iron pentacarbonyl on exposure to UV radiation in a mixed Langmuir monolayer at a gas–water interface with stearic acid as the surfactant has been studied.[57, 58, 60, 62] During the nanoparticle formation, the monolayer existed in the 'gas-like' state (the surface pressure was equal to zero).

The magnetic properties of multilayer Langmuir–Blodgett films containing nanoparticles were studied by EPR, which revealed ferromagnetic resonance signals and superparamagnetism.[60] Studies by scanning tunnelling microscopy (STM), atomic force microscopy (AFM) and transmission (tunnelling) electron microscopy (TEM) have shown that the size and shape of nanoparticles may change substantially during the growth from disc-like to oriented oblong under the action of an external magnetic field directed parallel to the monolayer plane.[59] When the mag-

§ Stearic or arachidic acid or other surfactants are normally used as amphiphilic molecules.

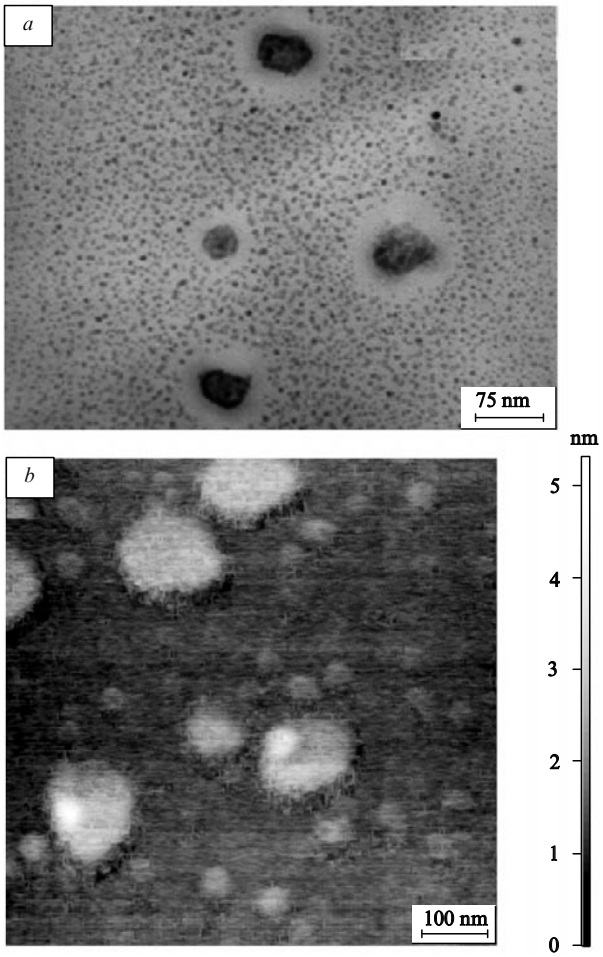


Figure 1. TEM (*a*) and ACM (*b*) micrographs of iron-containing nanoparticles synthesised in a Langmuir monolayer.[59]

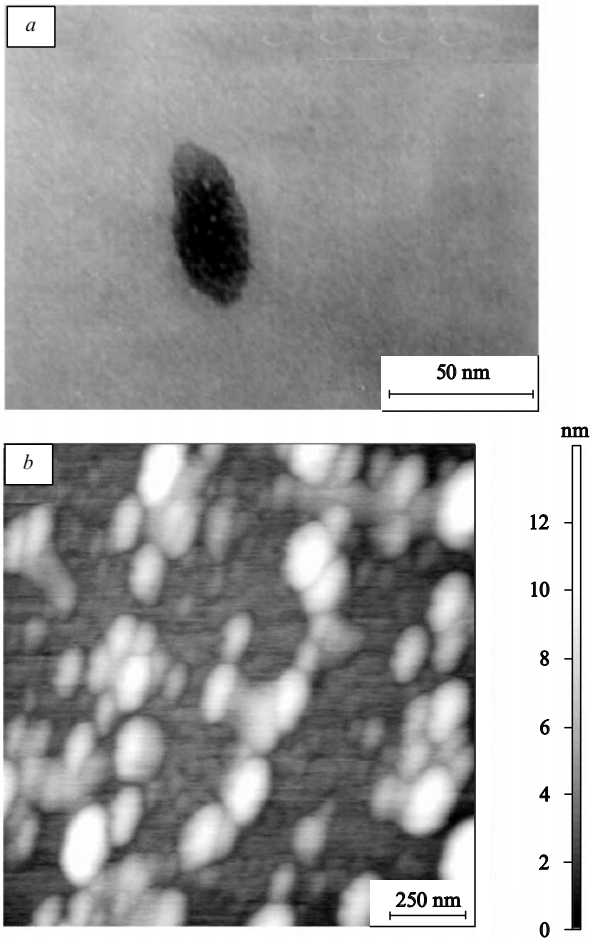


Figure 2. TEM (*a*) and ACM (*b*) micrographs of iron-containing nanoparticles synthesised in a Langmuir monolayer with application of a 2 kŒ external magnetic field directed parallel to the monolayer plane.[59]

netic field is perpendicular to the monolayer plane, the nanoparticles acquire an anisotropic shape symmetric relative to the axis that passes through the nanoparticle centre at right angle to the interface (Figs 1–3).

Figure 1 shows iron oxide nanoparticles synthesised in a Langmuir monolayer with the initial ratio $Fe(CO)_3 : C_{17}H_{35}CO_2H = 10 : 1$ under UV irradiation (4 min) at 21 °C and pH 5.6 in the absence of an external magnetic field. The resulting nanoparticles were planar and radially symmetric. Figure 2 shows the nanoparticles synthesised under analogous conditions but with an external magnetic field applied parallel to the monolayer plane. This gave anisotropic oblong nanoparticles whose longer axis coincided with the field direction.[59]

If the energy of the magnetic dipole–dipole interaction of nanoparticles exceeds the energy of thermal (Brownian) motion k_BT (k_B is the Boltzmann constant), the magnetic particles can be combined into chain structures. The formation of chain aggregates of magnetic particles is typical, in particular, of magnetic liquids. Figure 3 shows an organised chain ensembles of iron-containing magnetic nanoparticles synthesised in a Langmuir monolayer with an external magnetic field applied and with a short-term UV irradiation.[60]

Highly organised lamellar molecular structures obtained by the Langmuir–Blodgett method have been used as ordered matrices in the synthesis of various nanoparticles, including semiconductor particles, doped with magnetic metal ions (DMS).[65, 66] Thus CdS (3 nm) particles doped by Mn^{2+} ions were prepared by treatment with H_2S of a Langmuir–Blodgett film consisting of a mixture of cadmium and manganese salts of arachidic acid. Multilayer ordered structures have also been obtained by the Langmuir–Blodgett method *via* the formation of stable iron stearate monolayers on the aqueous phase surface.[67, 68]

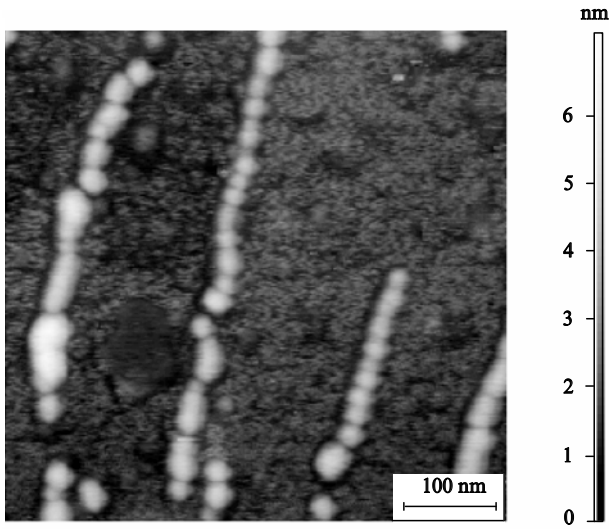


Figure 3. ACM micrographs of iron-containing nanoparticles synthesised in a Langmuir monolayer on a short-term (6 s) UV irradiation followed by dark incubation (4 min) with application of an external 2 kŒ magnetic field directed parallel to the monolayer plane.[60]

3. Specific methods for the preparation of particular types of magnetic nanoparticles

a. Heterometallic nanoparticles

As a rule, these particles are prepared by simultaneous thermal decomposition of two MCC of different compositions (hydrogen is used most often as the reducing agent). This method was used to prepare heterometallic nanoparticles, $Fe_{48}Pt_{52}$ and $Fe_{70}Pt_{30}$, from $Pt(acac)_2$ and $Fe(CO)_5$.[69] In the synthesis of Co–Pt particles, either $Pt(acac)_2$, or $Pt_2(dba)_3$ (dba is dibenzylideneacetone) was used as the source of Pt, while sources of Co included $Co_2(CO)_8$, $Co(CO)_3(NO)$ [70] and $Co(\eta^3\text{-}C_8H_{13})(\eta^4\text{-}C_8H_{12})$.[71]

Using the synthesis of $CoPt_3$ nanoparticles as an example, the mechanism of homogeneous nucleation has been studied. This allowed researchers [72] to deliberately and reproducibly obtain nanoparticles of the specified composition with a narrow size distribution in the 3–18 nm range. The synthesis of so-called 'shell' CoPt nanoparticles has been described.[73] The researchers first obtained Pt nanoparticles of diameter 2.5 nm and then coated them with a controlled amount of Co layers. This resulted in Co–Pt nanoparticles with a diameter of 7.6 nm.

In some cases, heterometallic particles are called 'alloys;' in our opinion, this is not always appropriate. For example, using the same initial compounds, $Co_2(CO)_8$ and $Pt(hfac)_2$, two types of Co–Pt nanoparticles with the same composition and different structures have been obtained,[74] namely, particles with a uniform distribution of Co and Pt atoms and particles with a cobalt core and a platinum shell, Pt@C. In the latter type of particles, mixing of the atoms of two metals is possible only at the interface.

It is also pertinent to consider the procedure for the synthesis of cobalt ferrite $CoFe_2O_4$ nanoparticles,[75] in which the first stage includes the preparation of the Fe–Co heterometallic particles and the second stage, their oxidation to $CoFe_2O_4$. Another route to analogous particle implies the use the heterometallic $(\eta^5\text{-}C_5H_5)CoFe_2(CO)_9$ cluster as the starting compound. The cobalt ferrite nanoparticles were also prepared by the microemulsion method [76] from a mixture of Co and Fe dodecylsulfates treated with an aqueous solution of methylamine.[77, 78]

b. Ferrites

Microcrystalline ferrites form the basis of materials currently used for magnetic information recording and storage. To increase the recorded information density, it seems reasonable to obtain nanocrystalline ferrites and to prepare magnetic carriers based on them. Grinding of microcrystalline ferrite powders to reach the nanosize of grains is inefficient, as this gives particles with a broad size distribution, the content of the fraction with the optimal particle size (30–50 nm) being relatively low.

The key method for the preparation of powders of magnetic hexagonal ferrites with a grain size of more than 1 μm includes heating of a mixture of the starting compounds at temperature above 1000 °C (so-called ceramic method). An attempt has been made [79] to use this method for the synthesis of barium ferrite nanoparticles. The initial components (barium carbonate and iron oxide) were ground for 48 h in a ball mill and the resulting powder was mixed for 1 h at a temperature somewhat below 1000 °C. This gave rather large particles (200 nm and greater) with a broad size distribution. Similar results have been obtained in the mechanochemical synthesis of barium ferrite from $BaCl_2$, $FeCl_3$ and alkali with subsequent oxidative annealing.[80]

Nanocrystalline ferrites are often prepared by the co-precipitation method. The $MnFe_2O_4$ spinel nanoparticles with a diameter of 40 nm are formed upon the addition of an aqueous solution of stoichiometric amounts of Mn^{2+} and Fe^{3+} chlorides to a vigorously stirred solution of alkali.[81] The $MgFe_2O_4$ (6–18 nm),[82] $Co_{0.2}Zn_{0.8}Fe_2O_4$ (2–45 nm) [83] and $BaFe_{12-2x}\cdot Sn_xZn_xO_{19}$ (~45 nm) [84] nanoparticles were obtained in a similar way. The $SrFe_{12}O_{19}$ nanoparticles (30–80 nm) were synthesised by co-precipitation of Sr and Fe citrates followed by annealing of the resulting precipitate.[85] Co-precipitation upon decomposition of a mixture of $Fe(CO)_5$ and $Ba(O_2C_7H_{15})_2$ under ultrasonic treatment has been successfully used [86] for the synthesis of barium ferrite nanoparticles (~50 nm).

Methods for the preparation of ferrite nanoparticles of different compositions in solutions at moderate temperatures have been developed. First, worth mentioning is the sol–gel method resulting in highly dispersed powders with required purity and homogeneity. Low annealing temperatures allow one to control crystallisation and to obtain single-domain magnetic ferrite nanoparticles with narrow size distributions and to easily dope the resulting particles with metal ions. This procedure was used to obtain Co- and Ti-doped barium ferrite nanoparticles (smaller than 100 nm) [87] and, Zn-, Ti- and Ir-doped strontium ferrite particles with a similar size.[88]

Smaller nanoparticles (15–25 nm) of cobalt ferrite were obtained in a hydrogel containing lecithin as the major component. Judging by the good magnetic characteristics, these particles possessed a substantial degree of crystallinity without any annealing.[89] The sol–gel method was successfully used to synthesise a Co ferrite nanowire 40 nm in diameter with a length of up to a micrometre.[90] This wire can also be obtained within carbon nanotubes.[91] For the synthesis of ferrite nanoparticles, oil-in-water type micelles [92] and reverse (water-in-oil) micelles [93] are also widely used.

The homogeneity of metal ion distribution in final products can be enhanced and the required stoichiometry can be attained by using pre-synthesis of heterometallic complexes of various composition. The thermal decomposition and annealing of the pre-synthesised $[GdFe(OPr^i)_6(HOPr^i)]_2$ complex give $GdFeO_3$ nanoparticles (~60 nm).[94] Virtually monodisperse nanoparticles (9 nm) of cobalt ferrite are formed [75] from $(\eta^5\text{-}C_5H_5)CoFe_2(CO)_9$. First, the Co–Fe nanoparticles are prepared and then they are oxidised during annealing.

c. Nanoparticles of rare earth elements

Six of the nine rare earth elements (REE) are ferromagnetic.¶ The magnetic nanomaterials based on these REE occupy a special place, as they can be used in magnetic cooling systems.[95] However, REE nanoparticles (of both metals and oxides) are still represented by only a few examples, most of all, due to the high chemical activity of highly dispersed REE. A synthesis of coarse (95 × 280 nm) spindle-shaped ferromagnetic EuO nanocrystals suitable for the design of optomagnetic materials has been reported.[96] The EuS nanocrystals were prepared by passing H_2S through a solution of europium in liquid ammonia.[97] The size of the EuS magnetic nanoparticles formed can be controlled (to within 20–36 nm) by varying the amount of pyridine added to the reaction medium.[97]

Gadolinium nanoparticles (12 nm) were prepared by reduction of gadolinium chloride by Na metal in THF. They proved to be extremely reactive and pyrophoric, which, however, did not prevent characterisation of these particles and measuring their magnetic parameters.[98] The Gd, Dy and Tb nanoparticles with an average size of 1.5–2.1 nm and an about 20% degree of dispersion were obtained in a titanium matrix by ion beam sputtering.[99, 100] At 4.5 K, the coercive forces for ~10 nm Tb and Gd nanoparticles were 22 and 1 kŒ, respectively. As the particle size decreases (< 10 nm), the H_c value rapidly diminished to zero, which is related, in the researchers' opinion,[100] to the decrease in the Curie temperature for small nanoparticles.

d. Magnetic nanoparticles of anisotropic shapes

The nanoparticles anisotropic in shape (non-spherical) are of special interest for magnetic recording purposes. A material containing oblong (needle-shaped) or flat (disc-shaped) particles is more easily susceptible to magnetic texturing, *i.e.*, ordering of the directions of the magnetic axes of the particles. This has long

¶ The atomic magnetic moments of rare earth elements are greater than that of Fe.

been used, for example, in audio recording tapes.[101] In addition, non-spherical particles possess an additional source of magnetic anisotropy, *i.e.*, the shape anisotropy. It was shown experimentally and substantiated theoretically[102] that planar ultrathin particles should be single-domain, irrespective of their in-plane dimensions. For these planar particles, the shape anisotropy is comparable in magnitude with the magnetic crystal anisotropy. The magnetic interaction between thin nanoparticles in plane is much lower than that between spherical nanoparticles in the bulk.

No theory of the synthesis of anisotropic particles has been developed due to the lack of methods of deliberate change of the nanoparticle shape in solutions. Although papers devoted to the synthesis of Co,[103] Fe[104] and Ni[105] anisotropic magnetic nanoparticles have been published, this still does not imply that the shape of magnetic nanoparticles is subject to reproducible control. Recently,[106] conditions for the preparation of highly anisotropic cobalt nanoparticles by the reduction of $Co(\eta^3\text{-}C_8H_{13})(\eta^4\text{-}C_8H_{12})$ with hydrogen have been found. By varying conditions of synthesis and the oleylamine to oleic acid ratio, the researchers selectively obtained spherical nanoparticles (4–10 nm), nanoneedles (40 nm long and 9 nm in diameter) and even nanowires.

Experimental data and theoretical calculations show that the interparticle anisotropic magnetic dipole–dipole interactions and kinetic factors can play a significant role in the magnetic nanoparticle growth induced by external fields. If at the moment of synthesis of iron oxide magnetic nanoparticles, the reaction medium is exposed to a magnetic field, the process yields anisotropic (oblong) particles. Apparently, this synthesis opens up the way for effective control of the morphology of magnetic nanomaterials.

Using the preparation of magnetic nanoparticles by ultrasound-induced decomposition of $Fe(CO)_5$ in a decalin solution as an example,[107] the effect of an external magnetic field on the growth processes has been studied. In an external magnetic field (7 kŒ), amorphous Fe_2O_3 nanoparticles were formed, of which 20%–30% had an anisotropic shape (50 nm long and 5 nm in diameter). In the absence of a magnetic field only quasi-isotropic nanoparticles with an average size of 25 nm were obtained. The electric arc decomposition of $Fe(CO)_5$ resulted in thread-like (10 to 100 nm in diameter) compounds also consisting of α-Fe and Fe_3C nanoparticles.[108]

The standard way of synthesis of nanothreads and nanowires composed of anisotropic Fe and Co nanoparticles includes the electrolysis of solutions of the metals at an aluminium cathode, which is pre-coated by an Al_2O_3 layer containing channels with a diameter of 18–35 nm and a depth of up to 500 nm.[109] During the electrolysis, these channels are filled by the reduced metal. After completion of the process, the matrix is dissolved in a mixture of acids to separate the nanoparticles. According to TEM, the nanoparticles have a length of up to 500 nm and an average diameter of 16 nm. Magnetic measurements have shown that the samples obtained have a coercive force of 2.7 kŒ for Fe (the highest value for pure α-Fe particles) and 1.4 kŒ for Co. By using an upgraded procedure, it is possible to prepare Fe nanowires ($d = 5$ nm) with a coercive force of 4.19 kŒ at 5 K.[110] Subsequently, column Co–Pt structures with a high magnetic anisotropy, promising for magnetic recording, have been obtained by this method.[111] An attempt has been made to control the magnetic anisotropy of Co–Pt nanoparticles.[112]

A peculiar procedure of thermal decomposition of carbonyls has been employed to prepare Fe and Co nanowires.[113] The particles were grown on the poles of a permanent magnet in the reaction area. This procedure allowed the preparation of 8–10 nm thick whiskers several millimetres long. The synthesis of monoatomic chains consisting of Co atoms has been reported.[114]

A simple method for the synthesis of heterometallic nanowires ($d \approx 30$ nm, more than 10 μm long) by heating a solution of platinum acetylacetonate and cobalt carbonyl in ethylenediamine at 200 °C for several days has been described.[115] The Fe–Pt, Ni–Pt and Cr–Pt nanowires were obtained in a similar way.

4. Methods for the synthesis of stoichiometrically inhomogeneous magnetic nanoparticles

The surface anisotropy markedly contributes to the total magnetic anisotropy of a nanoparticle; therefore, by controlling the surface composition, it is possible to control the magnetic properties of nanoparticles.

a. Oxidation of nanoparticles

No targeted research into the reactivity of oxidised nanoparticles or its comparison with the reactivity of the corresponding compact materials has been carried out; only a few publications considered the magnetic properties of the oxidised nanoparticles. For example, the magnetic properties of cobalt nanoparticles,† which were obtained by vacuum evaporation on the LiF substrate and then oxidised by exposure to air for a week, have been studied.[116] According to electron diffraction for two samples differing in the particle size (2.3 and 3.0 nm), the intensity of the HCP-Co reflections decreased after oxidation to become ~1/3 of the CoO-HCP line intensity. Hence, the researchers concluded that a small stable core of unoxidised cobalt atoms remains in all particles after oxidation. Comparative X-ray diffraction studies of the samples consisting of Co nanoparticles distributed in polyvinylpyridine stored under Ar and in air (the storage time was not indicated)[117] revealed no significant differences. Therefore, the authors considered a low degree of oxidation for cobalt.

In a more comprehensive study,[118] ^{57}Co-enriched cobalt nanoparticles were subjected to oxidation directly in a Mössbauer spectrometer. For this purpose, argon containing ~80 ppm of O_2 was passed through the sample at 300 K for 18 h. Analysis of the emission Mössbauer spectra showed that oxidation results in a fairly well-organised CoO layer on the surface of Co particles. Passing a pure oxygen stream through this gently oxidised sample for 1 h at 300 K did not induce any spectral changes. In the opinion of the researchers cited,[118] this is indicative of complete passivation of Co particles at the first oxidation stage.

It should be noted that the oxidation of magnetic metal nanoparticles during their synthesis cannot be avoided completely. Thorough mass-spectroscopic analysis of Fe nanoparticles obtained by laser vaporisation of the metal in a pure He medium showed that at least 5% of particles contain at least one oxygen atom.[20] If the deposition of oxygen present in the gas phase in trace amounts on the nanoparticle surface cannot be avoided even under these 'exceptional' conditions, it is evident that under 'usual' conditions, the nanoparticles of magnetic metals would always contain some amounts of oxides or suboxides of the elements on the surface. It can be plainly seen in the HRTEM micrograph (HRTEM is high-resolution tunnelling electron microscopy) of α-Fe nanoparticles (20 nm) synthesised by laser pyrolysis of $Fe(CO)_5$ under inert atmosphere that the particles are coated with a (3.5 nm) layer of iron oxide (the content of the chemically bound oxygen is 14.4 mass %).[119]

The data on the reactivity of Fe nanoparticles with respect to oxidation reported in the literature are contradictory. Thus rather large (~40 nm) nanoparticles of pure Fe obtained by thermal vaporisation contained less than 8 mass % of the oxide after exposure to air for three months.[120]

In some studies, the preparation of metal nanoparticles (especially Fe) was followed by their passivation, for example, by keeping for several hours in an atmosphere of oxygen-diluted argon.[121] This procedure prevented further spontaneous particle aggregation. The structure and the magnetic characteristics of such passivated nanoparticles (15–40 nm) have been described in detail.[122] The continuous oxide layers that coat the metallic

† Non-oxidised particles had a hexagonal close packing (HCP), while the oxidised ones, a face-centred cubic (FCC) lattice.

nanoparticle can be clearly seen in TEM images reported in this study. The interaction of the ferromagnetic core and the oxide shell, which resembles in the magnetic characteristics the interaction of magnetic moments in spin glass, was studied.

The oxidation of amorphous $Fe_{1-x}C_x$ nanoparticles obtained by thermal decomposition of $Fe(CO)_5$ in decalin in the presence of oleic acid for several weeks in air [123] has shown that the particles (6.9 nm) having a spherical shape and a very narrow size distribution consist of α- and γ-Fe_2O_3. However, passivation of nanocrystalline (~25 nm) Fe particles obtained by metal evaporation in a helium stream results in only a thin (1–2 nm) film of an antiferromagnetic oxide (apparently, FeO) forming on the surface.[124]

b. Chemisorption of small molecules on a nanoparticle surface

The interaction of α-Fe nanoparticles (2.4 nm) with small CO, H_2 and O_2 molecules has been studied.[125] It was noted that chemisorption of these molecules on a nanoparticle surface induces only minor changes in the parameters of the Mössbauer spectra. The reaction of α-Fe nanoparticles (2.3 nm) with nitrogen was studied *in situ* by Mössbauer spectroscopy.[126] It was shown that only the Fe atoms of the surface layer participate in the chemical binding of nitrogen (the process starts at 300 K). Note that the effect of the bound oxygen on the state of the metal surface atoms differs appreciably from that found for O_2 (see Ref. 127) and CO chemisorption.

c. Targeted modification of the surface of magnetic nanoparticles

The immobilisation of biological molecules (amino acids, DNA, simple peptides, polysaccharides, lipids) on the surface of magnetic nanoparticles is of certain interest for the design of magnetic markers used in biological and medical experiments. Physical sorption is often sufficient for such immobilisation; however, in some cases, chemical binding of the nanoparticle to the biomolecule is required. A seven-stage synthesis of γ-Fe_2O_3 nanoparticles (~20 nm) containing on the surface fragments of long organic molecules ending with reactive aldehyde groups has been described.[128] By the reaction of these aldehyde groups with enzyme amino groups, stable enzyme complexes with the magnetic γ-Fe_2O_3 nanoparticle were obtained. The heterogeneous catalytic activity of the enzyme immobilised in this way was found to be retained much longer than the activity of the same enzyme sorbed on a support surface.

IV. The most widely encountered magnetic nanoparticles

The fundamental characteristics of any nanoparticles, including magnetic ones, are the stoichiometry and the phase state. This Section considers the main types of magnetic nanoparticles and examples of their synthesis.

Fe. The preparation of nanoparticles consisting of pure iron is a complicated task, because they always contain oxides, carbides and other impurities.

BCC-Fe (α-Fe). The α-Fe nanoparticles with a body-centred cubic (BCC) lattice and an average size of ~10 nm were prepared by grinding a high-purity (99.999%) Fe powder for 32 h.[129]

A sample containing pure iron as nanoparticles (d_{aver} = 10.5 nm) can also be obtained by evaporation of the metal in an Ar atmosphere followed by deposition on a substrate.[121] When evaporation took place in a helium atmosphere, the particle size varied in the range of 10–20 nm.[130] Relatively small (100–500 atoms) Fe nanoparticles are formed in the gas phase on laser vaporisation of pure iron.[20]

FCC-Fe (γ-Fe). In the phase diagram of a bulk Fe sample, this phase exists at the ambient pressure in the temperature range of 1183–1663 K, *i.e.*, above the Curie point (1096 K). In some special alloys, this phase, which exhibits antiferromagnetic properties (the Neel temperature is in the 40–67 K range), was observed at room temperature.[131–133] However, a Mössbauer spectroscopy study [134] has shown that the FCC-Fe nanoparticles (40 nm) remain paramagnetic down to 4.2 K.

Some publications dealing with the synthesis of Fe nanoparticles present fairly weighty reasons indicating that these nanoparticles had an FCC structure. Apparently, the nanoparticles containing γ-Fe were first obtained by Majima *et al.*[135] These particles contained substantial amounts of carbon (up to 14 mass %) and had an austenite FCC structure analogous to γ-Fe. The researchers believed that the laser they used made it possible to reach a temperature of 1173–1423 K (the region of existence of γ-Fe in the phase diagram) in the reaction medium at the pulse instant, while the presence of reactive atomic carbon formed upon decomposition of CO and the short time of the laser pulse (100 nm) created the necessary conditions for fixing of the metastable structure. However, later, evidence for the existence of the γ-phase in the Fe nanoparticles that do not contain substantial amounts of carbon have been obtained. Nanoparticles (~8 nm) consisting, according to powder X-ray diffraction and Mossbauer spectroscopy, of γ-Fe (30 at.%), α-Fe (25 at.%) and iron oxides (45 at.%), were synthesised [136] by treatment of $Fe(CO)_5$ with a CO_2 laser radiation. The content of the γ-phase in the nanoparticles did not change for several years; the particles remain non-magnetic down to helium temperatures.

'Amorphous' Fe (metallic glass). The ultrasonic treatment of $Fe(CO)_5$ in the gas phase or of a solution of $Fe(CO)_5$ in decane at 0 °C under an inert atmosphere gave an X-ray amorphous powder as rather coarse (~30 nm) nanoparticles. The nanoparticles consisted of >96 mass % of Fe, <3 mass % of C and 1 mass % of O.[137] Differential thermal analysis (DTA) of the powder showed an exothermal transition around 585 K, which corresponded, in the authors' opinion, to crystallisation of the amorphous iron. Smaller Fe particles (8.5 nm) were obtained by thermal decomposition of $Fe(CO)_5$ in decalin (460 K) in the presence of surfactants.[138] The X-ray diffraction pattern of the powder formed did not display any sharp maxima, indicating the absence of a crystalline phase. It was assumed that amorphisation was due to the high content of carbon (>11 mass %) in the nanoparticles studied.

Fe_2O_3. Among several crystalline modifications of Fe_2O_3, there are two magnetic phases, namely, rhombohedral α-Fe_2O_3 (hematite) and cubic γ-Fe_2O_3 (maghemite) phases. In the α-Fe_2O_3 structure, all Fe^{3+} ions have an octahedral coordination, whereas in γ-Fe_2O_3 having the structure of a cation-deficient AB_2O_4 spinel, the metal atoms A and B occur in tetrahedral and octahedral environments, respectively.

The oxide α-Fe_2O_3 is antiferromagnetic at temperatures below 950 K, while above the Morin point (260 K) it exhibits so-called 'weak' ferromagnetism.

The α-Fe_2O_3 and FeOOH (goethite) nanoparticles are obtained by controlled hydrolysis of Fe^{3+} salts.[139] In order to avoid the formation of other phases, a solution of ammonia is added to a boiling aqueous solution of $Fe(NO_3)_3$ with intensive stirring. Boiling for 2.5 h and treatment of the precipitate with ammonium oxalate (to remove the impurities of other oxides) affords a red powder containing α-Fe_2O_3 nanoparticles (20 nm).[140] These nanoparticles are also formed on treatment of solutions of iron salts (Fe^{2+} : Fe^{3+} = 1 : 2) with an aqueous solution of ammonium hydroxide in air.[141] The synthesis of regularly arranged α-Fe_2O_3 nanowires with a diameter of 20–40 nm and a length of 2–5 μm has been described.[142]

A bulk γ-Fe_2O_3 sample is a ferrimagnet below 620 °C. The γ-Fe_2O_3 nanoparticles (4–16 nm) with a relatively narrow size distribution have been obtained [40] by mild oxidation (on treatment with Me_3NO) of pre-formed metallic nanoparticles. The same result can be attained by direct introduction of $Fe(CO)_5$ into a heated solution of Me_3NO. The oxidation with air oxygen is also used to prepare γ-Fe_2O_3 nanoparticles. For this purpose, the Fe_3O_4 nanoparticles (9 nm) are boiled in water at pH 12–13.[143] The kinetics of this process was studied.

The most popular route to γ-Fe_2O_3 nanoparticles is thermal decomposition of Fe^{3+} salts in various media. Rather exotic groups are used in some cases as anions. For example, good results have been obtained by using iron complexes with cupferron.[144] Special-purity γ-Fe_2O_3 is formed upon vaporisation of iron(III) oxide in a solar furnace with subsequent condensation.[145, 146] A mechanochemical synthesis of γ-Fe_2O_3 has been described.[147] An iron powder was milled in a planetary mill with water. During milling, the Fe atoms displace hydrogen from water and are converted into γ-Fe_2O_3. The researchers consider that this is a convenient one-stage synthesis of maghemite nanoparticles (15 nm).

Fe_3O_4 (magnetite). The cubic spinel Fe_3O_4 is ferrimagnetic at temperatures below 858 K. The route to these particles used most often involves treatment of a solution of a mixture of iron salts (Fe^{2+} and Fe^{3+}) with a base under an inert atmosphere. For example, the addition of an aqueous solution of ammonia to a solution of $FeCl_2$ and $FeCl_3$ (1 : 2) yields nanoparticles, which are transferred into a hexane solution by treatment with oleic acid.[148] The repeated selective precipitation gives Fe_3O_4 nanoparticles with a rather narrow size distribution. The synthesis can be performed starting only from $FeCl_2$, but in this case, a specified amount of an oxidant ($NaNO_2$) should be added to the aqueous solution apart from alkali. This method allows one to vary both the particle size (6.5 – 38 nm) and (to a certain extent) the particle shape.[149]

In some cases, thermal decomposition of compounds containing Fe^{3+} ions under oxygen-deficient conditions is accompanied by partial reduction of Fe^{3+} to Fe^{2+}. Thus thermolysis of $Fe(acac)_3$ in diphenyl ether in the presence of small amounts of hexadecane-1,2-diol (probable reducer of a part of Fe^{3+} ions to Fe^{2+}) gives very fine Fe_3O_4 nanoparticles (about 1 nm), which can be enlarged by adding excess $Fe(acac)_3$ into the reaction mixture.[150] For partial reduction of Fe^{3+} ions, hydrazine has been recommended.[151] The reaction of $Fe(acac)_3$ with hydrazine is carried out in the presence of a surfactant. This procedure resulted in superparamagnetic magnetite nanoparticles with controlled sizes, 8 and 11 nm.

Previously, Fe_3O_4 nanoparticles with an average size of 3.5 nm have been prepared by thermal decomposition of $Fe_2(C_2O_4)_3 \cdot 5H_2O$ at $T > 400$ °C.[152] The controlled reduction of ultradispersed α-Fe_2O_3 in a hydrogen stream at 723 K (15 min) is a more reliable method of synthesis of Fe_3O_4 nanoparticles. Particles with ~13 nm size were prepared in this way.[153]

FeO (wustite). Cubic Fe^{2+} oxide is antiferromagnetic (T_C = 185 K) in the bulk state. Joint milling of Fe and Fe_2O_3 powders taken in a definite ratio gave nanoparticles (5 – 10 nm) consisting of FeO and Fe.[154] On heating of these particles at temperatures of 250 – 400 °C, the metastable FeO phase disproportionates to Fe_3O_4 and Fe, while above 550 °C it is again converted into nanocrystalline FeO.[155, 156]

α-FeOOH (goethite). Among the known oxide hydroxides $Fe_2O_3 \cdot H_2O$, the orthorhombic α-FeOOH (goethite) is antiferromagnetic in the bulk state and has T_C = 393 K,[157] β-FeOOH (akagenite) is paramagnetic at 300 K,[158] γ-FeOOH (lipidocrokite) is paramagnetic at 300 K and δ-FeOOH (ferroxyhite) is ferrimagnetic.[159] Although the bulk α-FeOOH is antiferromagnetic, in the form of nanoparticles it has a nonzero magnetic moment due to the incomplete compensation of the magnetic moments of the sublattices. Goethite nanoparticles have been studied by Mössbauer spectroscopy.[160, 161] As a rule, α-FeOOH is present in iron nanoparticles as an admixture phase.

Fe_xC_y. Iron carbide is often present in Fe-containing nanoparticles. It is formed either upon decomposition of organic ligands present in the starting MCC or upon the reaction of Fe with the organic medium in which the synthesis is carried out. Data on the preparation of nanoparticles wholly consisting of iron carbide of one or another composition are few. It has been shown by Mössbauer spectroscopy[162] that thermal decomposition of $Fe(CO)_5$ (353 K) on a carbon support forms $Fe_{78}C_{22}$ nanoparticles (3.9 nm).

Ferrofluids or so-called magnetic liquids are suspensions of colloid magnetic particles stabilised by surfactants in liquid media.[2, 3] The magnetic phase in ferrofluids can be represented by magnetite,[163] ferrites[164] and Fe_xC_y particles resulting from the thermal decomposition of $Fe(CO)_5$.[165] Decalin or silicone oil are the usual liquid phases. The dimensions of magnetic particles are 5 – 10 nm. The commercial magnetic liquids most often contain magnetite.[2, 166, 167] Description of magnetic liquids with a Curie point below the boiling point has been reported.[164, 168, 169] The use of these composites is considered in a review.[170]

Apart from the 'classical' ferroliquids, ferrofluid emulsions in which oil drops containing a magnetic phase are dispersed in water by means of surfactants are also known.[171] The preparation of lyotropic ferronematics stable for several months with a high content (up to 1 vol.%) of the magnetic component, γ-Fe_2O_3 nanoparticles (~6 nm), based on a ferrofluid has been reported.[172]

Fe – Co alloys. The saturation magnetisation of Fe – Co alloys reaches a maximum at a Co content of 35 at.%; other magnetic characteristics of these metals also increase when they are mixed. Therefore, Fe_xCo_y nanoparticles attract considerable attention. Thus Fe, Co and Fe – Co (20 at.%, 40 at.%, 60 at.%, 80 at.%) nanoparticles (40 – 51 nm)[173] with a structure similar to the corresponding bulk phases have been prepared in a stream of hydrogen plasma. The Fe – Co particles reach a maximum saturation magnetisation (61 $cm^3\ g^{-1}$) at 40 at.% of Co and a maximum coercive force (860 Œ) is attained at 80 at.% of Co.

Fe – Ni. The bulk samples of the iron – nickel alloys are either nonmagnetic or are magnetically soft ferromagnets (for example, permalloys containing >30% of Ni and various doping additives). When the content of nickel is ~30%, their magnetic properties approach the properties of invar (36% of Ni, 64% of Fe, about 0.05% of C). The Fe – Ni nanoparticles have a much lower saturation magnetisation than the corresponding bulk samples over the whole concentration range.[174] An alloy containing 37% of Ni has a low T_C and a FCC structure. It consists of nanoparticles (12 – 80 nm) superparamagnetic over a broad temperature range.[175] Theoretical calculations predict a complex magnetic structure for these Fe – Ni particles (clusters).[176]

Fe – Pt. Nanoparticles of this composition have received much attention in recent years due to the prospects for a substantial increase in the information recording density for materials based on them.[69] The Fe – Pt nanoparticles (6 nm) with a narrow size distribution were prepared by joint thermolysis of $Fe(CO)_5$ and $Pt(acac)_2$ in the presence of oleic acid and oleylamine. Hexadecane-1,2-diol served as the reducing agent for Pt^{2+}. Further heating resulted in the formation of a protective film from the products of thermal decomposition of the surfactant on the nanoparticle surface, which does not change significantly the particle size. These particles can be arranged to form regular films and so-called 'colloid crystals'.[177] The reaction of FePt nanoparticles with Fe_3O_4 followed by heating of the samples at 650 °C in an Ar + 5% H_2 stream resulted in the FePt – Fe_3Pt nanocomposite with unusual magnetic characteristics.[178]

Co. Methods for the synthesis and magnetic properties of cobalt nanoparticles have been described in detail in a review;[18] therefore, we do not consider them here.

CoO. Cubic cobalt oxide is antiferromagnetic and has T_N = 291 K. Cobalt monoxide has played an important role in the discovery of the 'exchange shift' of the hysteresis curve,[179, 180] first found for samples consisting of oxidised Co nanoparticles.[181] Data on the dependence of T_N on the particle size were obtained in a study of CoO nanoparticles dispersed in a LiF matrix.[116] The particles obtained by vacuum deposition contained a small metal core, according to powder X-ray diffraction. As the particle size decreased from 3 to 2 nm, T_N decreased from 170 to 55 K, which can be explained satisfactorily in terms of the mean-field theory.[122] Apparently, the presence of an oxide layer on cobalt

nanoparticles can markedly increase the coercive force. For example, the coercive forces (at 5 K) of monodisperse 6 and 13 nm oxidised Co particles obtained by plasma gas condensation in an installation for the investigation of molecular beams were ~5 and 2.4 kŒ, respectively.[182] Unfortunately, the blocking temperature for 6 nm nanoparticles was lower than room temperature (~200 K); therefore, under normal conditions, their coercive force was equal to zero.

Co_3O_4. The Co_3O_4 nanoparticles (cubic spinel) with sizes of 15 to 19 nm dispersed in an amorphous silicon matrix exhibited ferrimagnetic‡ properties at temperatures below 33 K (for bulk samples, $T_N = 30$ K).[183] A method for controlled synthesis of Co_3O_4 cubic nanocrystallites (10–100 nm) has been developed.[184]

Ni. The number of publications devoted to the preparation of Ni nanoparticles is small, unlike Co and, the more so, Fe nanoparticles. In addition to the conventional metal evaporation methods,[150] thermal decomposition of organonickel compounds [$Ni(CO)_4$, $Ni(C_5H_5)_2$ (see Ref. 185) and $Ni(COD)_2$ (COD is cyclooctadiene) [186]] and the reduction of $NiBr_2$ in the presence of PPh_3 by treatment with potassium metal deserve attention.[187] In the latter case, Ni nanoparticles (~3 nm) coated by a thin oxide film are formed.

Materials for magnetic information recording. The following compositions are usually considered in the literature as media for magnetic information recording: α-Fe, γ-Fe_2O_3, Fe_2O_3–Fe_3O_4, Co–γ-Fe_2O_3, CrO_2, $BaFe_{12}O_{19}$. The compositions used in reality are much more complex, because they are doped by various additives that influence particular characteristics of the material. In recent years, nanocrystalline (5–10 nm) CoPr, FePt, CoPt, CoSm, SmFeSiC and SmFeAlC films are regarded as most promising.[188]

V. Methods of nanoparticle stabilisation

1. Encapsulation of nanoparticles and the preparation of magnetic nanoparticles in a shell

Nanoparticles of some metals are known to be pyrophoric, *i.e.*, they spontaneously ignite in air at room temperature; therefore, the creation of a protective shell on such nanoparticles (encapsulation) is a widely used protection and stabilisation method. Carbon is often used as the protective coating. The carbon layers formed on the metal surface are usually graphite-like and, hence, conductive. In those cases where an electrically insulating coating is required, boron nitride layers are used.[189]

Encapsulation of magnetic nanoparticles makes them stable against oxidation, corrosion and spontaneous aggregation, which allows them to retain the single-domain structure. The magnetic particles coated by a protective shell can find application as the information recording media, for example, as magnetic toners in xerography, magnetic ink, contrasting agents for magnetic resonance images, ferrofluids and so on. If the nano-sized magnetic particles are retained after compaction, the materials based on them can serve as excellent initial components for the preparation of permanent magnets.

The coating of metal particles by carbon (carbonisation) was first observed in the research of heterogeneous catalysis almost 50 years ago. Subsequently, this process (deleterious to oil refining and other industries) was comprehensively studied and, in recent years, it has been used deliberately to stabilise nanoparticles. The first structurally characterised carbon-encapsulated nanoparticles were obtained as side products in the electric arc synthesis of fullerenes. Subsequently, special studies have been carried out to identify the possibilities of using this method for the targeted synthesis of encapsulated nanoparticles, especially magnetic ones. These investigations have been surveyed.[190]

The original version of the arc method allowed one to prepare reliably only encapsulated nanoparticles of REE carbides. Subsequently, the yield of encapsulated nanoparticles has been increased due to a decrease in the amount of fullerenes formed. In this variant, the method became applicable for the synthesis of reasonable amounts of encapsulated magnetic nanoparticles (Fe–Co, Mn–Al). The encapsulated Fe and Co nanoparticles with a saturation magnetisation reaching 200 $cm^3\ g^{-1}$ were synthesised in this way. The perfection of the experimental technique allowed the researchers to eliminate completely the formation of pure carbon-containing products. This procedure was used to obtain Fe, Co and Ni nanoparticles (56, 40 and 37 nm, respectively) coated by 3 or 4 layers of graphitised carbon.[191] The authors emphasise that in none of the cases were metal carbide phases detected. However, the attempts to prepare encapsulated nanoparticles of hard magnetic materials, NdFeB or $SmCo_5$, proved unsuccessful — each element formed separate encapsulated particles.

Other methods for the synthesis of encapsulated magnetic nanoparticles are based on the use of high-temperature plasma, laser pyrolysis and thermal vaporisation. Thus the cobalt and carbon vapours formed upon an arc discharge in a helium atmosphere were condensed in the gas phase prior to deposition onto a cooled substrate.[192] This gave spherical particles with a radius of 10 to 100 nm consisting of a metallic core and a carbon shell, which contains up to 30 graphite-like carbon layers. Such a shell is considered to prevent oxidation of the metallic core.[193] Other compounds can also be used to form the protective shell. Thus treatment of a mixture of boron and cobalt powders with H_2 and NH_3 at 800 °C for 3 h furnished Co nanoparticles (20–60 nm) coated by a ~5-nm thick BN coating.[189] A CVD process for one-stage synthesis of γ-Fe_2O_3 nanoparticles (20–30 nm) coated by a SiO_2 layer with the same thickness has been developed.[194]

Due to the high temperature of carbon evaporation, the synthesis in radiofrequency plasma burners is considered to be most promising for obtaining large-scale amounts of encapsulated magnetic nanoparticles. Nanoparticles of metals, alloys, carbides and oxides can be prepared by this method. A drawback of this method is inhomogeneity of nanoparticles and differences in their composition.

Chemical methods are also used successfully for encapsulating magnetic nanoparticles. Thus stirring of a solution of tetraethoxysilane in alcohol with an aqueous suspension of α-Fe_2O_3 nanoparticles (24 h, 50 °C) gives Fe_2O_3 nanoparticles (4–5 nm) coated by amorphous SiO_2. The particles were found to retain the composition, the size and the shape after heating at 250 °C in an O_2 atmosphere.

Hydrolysis of Si, Ti and Zr alkoxides in the presence of metal nanoparticles is a general method for forming shells of the oxides of these elements on the particle surface. In some cases, the synthesis of oxides takes place simultaneously with the synthesis of the nanoparticles. This method was used to prepare[195] Co magnetic nanoparticles coated by SiO_2 layers. The starting compounds used were $Fe(acac)_3$ and $Si(OEt)_4$, the oxidative thermal decomposition of which in a flow reactor at 1000 °C gave the corresponding particles.

The coating of magnetic nanoparticles by a thin layer of a nonmagnetic metal is considered to be a promising method for their stabilisation. For example, the synthesis of Fe_3O_4 nanoparticles (5 nm) coated by metallic gold has been reported.[196] When determining the composition and the structure of these objects, the researchers faced serious difficulties. Much attention has been devoted in recent years to the methods for the formation of thin polymeric coatings (especially those based on biocompatible and readily biodegradable polymers) on the surface of magnetic nanoparticles.[197]

‡ Ferrimagnetism below T_N is typical of nanoparticles of all antiferromagnetic phases, because, unlike bulk samples, the magnetic moments of sublattices are not fully compensated. In particular, the arrangement of magnetic moments in the near-surface layer of nanoparticles differs appreciably from that in the bulk, which is specified by the type of crystal lattice and the type of exchange interactions.

2. Self-assembled monolayers on the nanoparticle surface

Self-assembled monolayers (SAM) on the nanoparticle surfaces are represented by monomolecular layers of amphiphilic molecules, which protect the particles from aggregation and simultaneously stabilise their suspensions (solutions) in certain solvents. In a typical example of the self-assembly of a monolayer of amphiphilic molecules of fatty acids on the Fe_3O_4 nanoparticle surface,[198] the freshly prepared nanoparticles (obtained by the standard procedure by treatment of a mixture of Fe^{2+} and Fe^{3+} chlorides with aqueous NH_3) were washed, separated into fractions by centrifuging and treated with an excess of lauric or decanoic acid, whose molecules were adsorbed on the surface of each particle. The protective role of amphiphilic molecules was manifested most clearly in the targeted synthesis of $Co-Pt_3$ nanoparticles of a strictly specified size (1.5–7.2 nm).[199] In the researchers' opinion, the success of the synthesis is related first of all to the use of a new stabilising agent, 1-adamantanecarboxylic acid.

The effect of cationoid (cetyltrimethylammonium bromide, CTAB) and anionoid (sodium didecylbenzenesulfonate, DBS) surfactants on the stabilisation of γ-Fe_2O_3 nanoparticles (4–5 nm) has been studied.[200] A nanoparticle having a large number of defects and dangling bonds on the surface is considered to interact with the surfactant rather strongly. This interaction has a pronounced influence on the electronic structure of the particle surface.[201]

Self-assembled monolayers are needed to create aqueous dispersions of magnetic nanoparticles.[202] Diverse magnetic colloid isotropic (magnetic emulsions [203] and vesicles [204–206]), anisotropic (steric and electrostatic ferrosmectics [207, 208]) and lyotropic ferronematics have been obtained on the basis of nanoparticles coated by a surfactant monolayer (see Section IV).[172]

VI. Types of materials containing magnetic nanoparticles

We discussed above 'free' nanoparticles as powders or suspensions (in the gas or liquid media). In practice, magnetic nanoparticles are normally used as films (2D systems) or compact materials (3D systems). The mere compacting of magnetic nanoparticles even those having a protective coating on the surface often results in the loss or substantial change in their unique physical characteristics. An optimal material should be a nonmagnetic dielectric matrix with single-domain magnetic nanoparticles with a narrow size distribution regularly arranged in the matrix.

1. Nanoparticles on a substrate surface

The methods for the preparation of magnetic nanoparticles on substrates have been described in detail in a review.[209] The same review presents comparison of the properties of these systems with the properties of free clusters.

The crystalline surface of the substrate exerts an 'organising' influence on the magnetic nanoparticles, thus promoting the growth of well-crystallised particles (replication effect), even when their dimensions do not exceed 3 nm. This was confirmed by the data of high-resolution tunnelling electron microscopy, which allows one to examine the atomic structure. The Co nanoparticles with dimensions not exceeding 3 nm were obtained by the LECBD method (see Section III) on a niobium foil; the structure of these particles was modelled by a truncated multiwall octahedron containing 1289 metal atoms.[30] Scanning tunnelling microscopy [210] has been used to study the formation of bimetallic Co–Pd nanoparticles by metal vapour deposition on an Al_2O_3 surface. Due to the substantial difference between the crystal structures of the two metals, their joint crystallisation and growth on the same substrate proceed according to different patterns, either the growth of a Pd layer on the Co base or the growth of a Co nanoparticle on the Pd base.

The influence of the nanoparticle size and the distance between them in the matrix on their magnetic characteristics has been studied by the LECBD technique.[211] Iron and cobalt nanoparticles containing about 300 atoms ($d \approx 1.5$ nm) have been prepared by laser vaporisation. Before getting on the substrate, the particle beam passes through a time-of-flight mass spectrometer. Magnetic, structural and electric studies of these films demonstrated that the effect of the matrix on the properties of nanoparticles is slight. The obtained dependences of the magnetic properties of the material on the particle concentration in the beam allowed the researchers to trace the system evolution from the superparamagnetic to ferromagnetic state following the enhancement of the interaction between the particles.

It was shown by powder X-ray diffraction and TEM that the ZrO_2 surface influences the morphology of the nanocrystallites of, for example, α-Fe and Fe_3O_4 formed thereon.[212] To prepare these, Fe was applied by the ion implantation process on a polished (100) face of cubic ZrO_2 stabilised by yttrium. The subsequent heat treatment of the samples on the surface gave (depending on the conditions) either α-Fe nanoparticles (10–20 nm) (1100 °C, Ar + 4%H_2) or Fe_3O_4 nanoparticles (3–9 nm) (milder conditions). To our knowledge, the formation of γ-Fe nanocrystallites (FCC phase) on the ZrO_2 surface was detected for the first time in the same study.

In another study,[213] an ordered ensemble of nanoparticles was formed using a hydroxide substrate (the composition of which was not indicated) pre-modified by a polyvinylpyrrolidone or polyethyleneimine monolayer. The modified substrate was immersed for a short period (30 s) into a solution of Fe–Pt nanoparticles stabilised by oleic acid and oleylamine. The molecules of the stabilising agents weakly linked to the nanoparticle surface were displaced by the polymer functional groups, which resulted in attachment of the particle to the substrate. Repeating this process many times gave regular three-dimensional structures of magnetic nanoparticles.

2. Nanoparticles in matrices

It has already been noted that stabilisation of nanoparticles is a necessary condition for the production of materials with reproducible properties. A highly promising method of stabilisation is the introduction of nanoparticles in different types of matrices.

a. Inorganic matrices

Zeolites and molecular sieves. The rigid matrices (zeolites) with fixed cavities and channels have long been used to prepare and stabilise nanoparticles. A frequently used matrix is faujasite, a NaX type zeolite with cavities having a diameter of 1.3 nm and connected by channels with a diameter of 0.8 nm. Before preparing nanoparticles in zeolite channels, water is removed from the channels at 673 K. The subsequent adsorption of $Fe(CO)_5$ on the faujasite surface at 77 K and its decomposition at 453 K in vacuum result in α-Fe nanoparticles (4 mass %) formed in the zeolite channels.[214] The X-ray diffraction data and the results of magnetic measurements do not rule out completely the possibility of formation of α-Fe nanoparticles also on the external surfaces of the zeolite grains. When the NaY zeolite is used as the matrix, the standard procedure for the preparation of nanomaterials includes dehydration (2 h, 500 °C) in an inert gas flow, filling of the cavities that have become vacant with $Co_2(CO)_8$, controlled thermal decomposition of the carbonyl inside the zeolite cavities at 200 °C and the removal of CO ligands with a hydrogen flow.[215] The ^{59}Co NMR data (spin echo method) led the researchers to the conclusion that the NaY cavities in the resulting material contained unoxidised cobalt particles with a 0.6–1.0 nm size.

The method for nanoparticle introduction into the LTA zeolite $Na_{12}Si_{12}Al_{12}O_{48} \cdot 27\,H_2O$ is basically different.[216] The method includes the introduction of 7.72 mass % of Fe^{3+} into ion channels by conventional ion exchange, zeolite dehydration in vacuum at 673 K and the reduction of iron ions with sodium metal vapour. The material thus obtained contained α-Fe nanoparticles

(1.1 nm) in the matrix cavities. In the synthesis[217] of Fe nanoparticles (4–6 nm) in X- and Y-zeolites, NaN_3, which gives highly reactive Na metal upon thermal decomposition, was used as the reducing agent.

Apart from zeolites, other porous matrices, for example, molecular sieves are also used to stabilise nanoparticles. A method for the introduction of γ-Fe_2O_3 nanoparticles (5.6 nm) into porous aluminosilicates synthesised simultaneously with nanoparticles has been developed.[218] The presence of nanometre-sized regular channels in the molecular sieves can be used to prepare magnetic nanostructures with anisotropic shapes inside the channels. In particular, the introduction of an aqueous solution of iron nitrate into a silicate molecular sieve (SBA-15) sample impregnated with a toluene solution of [(2-aminoethyl)amino]propyltrimethoxysilane (to modify the internal surface of the matrix) and the subsequent annealing of the sample at 600 °C in air gives α-Fe_2O_3 nanowire 6 nm in diameter in the matrix channels.[219] To take out the nanowire, the matrix was dissolved in alkali. The impregnation of a silicate molecular sieve powder of a different composition (MCM-41) with an aqueous solution of $CoCl_2$ followed by matrix annealing for 3 h in an oxygen flow at 750 °C gave[220] an antiferromagnetic material containing 6 mol.% of Co_3O_4 as nanoparticles (1.6 nm).

Glass. The conventional glass and its porous modifications are convenient matrices for nanoparticle stabilisation. A powder consisting of sodium glass ground to a grain size of several microns can exchange some Na^+ ions for Fe^{3+} ions in an aqueous solution. The subsequent reduction of Fe^{3+} with hydrogen at 823–923 K affords nanoparticles (5.5–8.5 nm) consisting of α-Fe and small amounts of FeO.[221] In another method, the $Fe(CO)_5$ vapour adsorbed by a porous glass (Porous Vycor Glass) with an average pore diameter of 10 nm was subjected to photolysis. The decomposition products filling the pores were 65% iron metal (in the researchers' opinion the rest were oxides).[222]

Xerogel and silica gel. The xerogel formed after drying (< 100 °C) of a silicic acid gel possesses good mechanical properties and a transparency comparable to that of glass. This makes this material an appropriate matrix for nanoparticle stabilisation. For example, γ-Fe_2O_3 nanoparticles ($\sim$10 nm) were prepared in a xerogel.[223] The shortest distances between the particles in the matrix were shown to be 50 nm, which may imply that they are magnetically isolated. The bulk samples containing magnetically oriented superparamagnetic maghemite γ-Fe_2O_3 nanoparticles introduced in the silica gel matrix exhibited an optical anisotropy in an external magnetic field induced by magnetooptical effects.[224]

Highly dispersed SiO_2 and Al_2O_3. The methods of synthesis of highly dispersed metallic catalysts supported on the SiO_2 and Al_2O_3 oxides are also applicable for the preparation of magnetic nanoparticles.[225] Thus ultrasonic treatment of solutions of $Fe(CO)_5$ and $Co(CO)_3NO$ in decane containing ultradisperse silica gel has given silica gel particles whose pores contained (TEM data) magnetic nanoparticles, Fe, Co or Fe–Co alloy [when both $Fe(CO)_5$ and $Co(CO)_3NO$ were used simultaneously].[226] A high catalytic activity of these particles for the reforming of hydrocarbons or catalytic hydrogenation of CO was demonstrated. The difficulties faced by identification of Co nanoparticles on the Al_2O_3 surface obtained by the reduction of Co aluminates have been discussed.[227]

Magnetic nanoparticles in non-magnetic metals. Magnetic metals can be dispersed in non-magnetic metals forming no alloys; this gives magnetic nanoparticles in a non-magnetic metal matrix. The mutual diffusion of the metal atoms in these samples is very limited. The non-magnetic matrices used most often are copper,[228] chromium and silver.[211] To prepare Co–Ag samples, a version of the LECBD method was used: a silver matrix was formed on a substrate simultaneously with deposition of Co nanoparticles (3–4 nm). A similar outcome can be attained by joint evaporation of Ag and Fe (or Co).[229] Cobalt nanoparticles ($\sim$3 nm) in a platinum matrix were synthesised in a similar way.[230]

To prepare samples containing Fe nanoparticles in mercury, 2 mass % of Na was first dissolved in mercury and the amalgam thus obtained was placed in an aqueous solution of an iron salt. After some period, iron reduced to the metallic state passed into mercury to give α-Fe nanoparticles (about 4000 atoms per particle).[231]

An interesting series of studies is devoted to the reaction of nanodispersed non-mixing metals. The joint condensation of Fe and Li vapours onto a liquid nitrogen-cooled substrate (pentane) gives α-Fe nanoparticles (3 nm) coated by a lithium metal layer.[232] The oxidation of these particles in air gave a powder of α-Fe nanoparticles coated by a Li_2CO_3 layer stable for several months. Iron nanoparticles coated by a Mg or MgF_2 layer were synthesised in a similar way.[233]

Dispersed carbon. The impregnation of dispersed carbon with an aqueous solution of cobalt nitrate containing ^{57}Co (10 μCu), subsequent drying (1 mass % Co) and reduction in an H_2 flow (573 K, 20 h) directly in the cell of a Mössbauer spectrometer resulted in the formation of Co particles with a size from 2 to 5 nm.[118,234]

b. Organic polymer matrices

The stabilisation of nanoparticles in polymer matrices is the first method for the production of magnetic nanomaterials.[235,236] The monograph[41] devoted to the synthesis of metal nanoparticles in polymers includes a small chapter describing the preparation of magnetic materials. In recent years, a number of new interesting publications on this topic have appeared.

Ion exchange resins. A widely used method for the production of nanoparticles is based on the ability of ion exchange resins to absorb substantial amounts of metal ions. Further reduction or, more rarely, oxidation gave nanoparticles of the required composition inside the matrix.[237] Thus treatment of a resin preliminarily saturated with Co^{2+} ions with excess $NaBH_4$ yielded Co–B-containing nanoparticles with a broad size distribution (3–30 nm).[238] The resin saturation with Fe^{2+} and Fe^{3+} ions and the subsequent treatment with alkali at 65 °C afforded Fe_3O_4 nanoparticles with sizes of 4–15 nm.[239] In the case of resin impregnation with only iron(II) ions, these were partially oxidised by heating the resin at 70 °C in an aqueous solution containing a mixture of potassium nitrate and hydroxide. The magnetite nanoparticles formed inside the resin had an average diameter of 17 nm.[240] Using the standard Dowex resin, well characterised γ-Fe_2O_3 nanoparticles (8.5 nm) with a narrow size distribution were obtained.[241]

Soluble polymers. If a MCC is decomposed in a polymer-containing solution, the new phase nuclei formed, after having reached a size of several nanometres, would be built into the polymer matrix due to the high surface energy. When the polymer contains heteroatoms or functional groups capable of coordination, the process is more efficient. For example, a sol of γ-Fe_2O_3 nanoparticles is easily incorporated into polyvinyl alcohol to give a dispersion with an average particle size of 6.4 nm.[242] A method for the preparation of Co nanoparticles in polyvinylpyrrolidone has been reported.[117,243] In this case, decomposition of $Co(\eta^3\text{-}C_8H_{13})(\eta^4\text{-}C_8H_{12})$ is carried out in the presence of a polymer in a THF solution at 60 °C in a hydrogen flow (10 h). The black powder thus formed is purified by reprecipitation from THF or CH_2Cl_2. A similar procedure starting from the corresponding organometallic compounds[244] gave small (2 nm) heterometallic nanoparticles, Co–Rh and Co–Ru, in polyvinylpyrrolidone. The use of a simpler method (treatment of the polyvinylpyridine–Co^{2+} complex with alkali)[245] gives large nanoparticles (50 nm) containing both CoO and $CoCl_2$.

For the synthesis of Fe containing particles, $Fe(CO)_5$ is used most often. A large series of polymers containing Fe nanoparticles (7–16 nm)[246] have been obtained by heating solutions of polymers and $Fe(CO)_5$ in decalin under argon (130–160 °C, 16 h). The polymers used included polybutadiene, polystyrene and styrene copolymers with butadiene, 4-vinylpyridine, *N*-vinylpyr-

rolidone, phenylvinylketoxime. The magnetic properties of the samples, which contained, according to the researchers' statement,[247] Co nanoparticles in polystyrene, were described.

Carbochain polymers without heteroatoms and functional groups. The possibility of using polymers containing no functional groups or heteroatoms as matrices for stabilisation of magnetic nanoparticles seems quite attractive, as these polymers (*e.g.*, polyethylene and polypropylene) are good dielectrics; they are stable, inexpensive and easily processable into articles of any shape. The advantages of magnetic materials obtained using these polymers are low specific gravity, high homogeneity of nanoparticle distribution and, what is the most important, isolated arrangement of the nanoparticles at distances much greater than their dimensions. However, the lack of solubility (or poor solubility) of most polymers of this type in organic solvents appreciably restricts the possibilities of introduction and homogeneous distribution of magnetic nanoparticles with a narrow size distribution in these polymers.

The mechanochemical dispersion process, *i.e.*, long-term grinding (up to 200 h) of an iron powder with polyethylene grains under Ar, proved to be inefficient for the preparation of a Fe–polyethylene nanocomposite.[248] The minimum size of the obtained particles was 10 nm (based on X-ray reflection broadening), the size distribution was broad and the distribution of particles in the matrix was nonuniform. The well developed method for forming nanoparticles (2–8 nm) in a solution (melt) of polymers in mineral oil is more promising. This method is versatile as regards both the composition of the resulting magnetic nanoparticles (Fe, Co, Ni, Fe–Co, Fe–Mo, Fe–Pt, Fe–Nd, Fe–Sm, Fe_2O_3, Fe_3O_4, ferrites) and type of polymer (low- and high-density polyethylene, polypropylene, polyamides). The content of nanoparticles in the sample can reach 60 mass %. The synthesis of magnetic nanomaterials as washers (25×5 mm) and thick (3 mm) films possessing good magnetic characteristics has been reported.[5, 6, 249]

The introduction of nanoparticles into a practically versatile carbochain polymer, namely, polytetrafluoroethylene, has been a difficult task until recently. However, recently [250, 251] a method for immobilisation of magnetic (Fe, Co, Ni) nanoparticles (6–12 nm) on the surface of ultradisperse polytetrafluoroethylene nanograins (150–200 nm) has been developed. Using this method, a readily magnetised sample was obtained.

Polymers containing heteroatoms. The polymers containing coordinating atoms can act as macromolecular ligands with respect to both metal ions and nanoparticles. In particular, they are able to replace other ligands. The introduction of Co, Fe, Fe–Pt and Co–Pt nanoparticles stabilised by oleic acid and oleylamine into a solution of polyvinylpyrrolidone or polyethyleneimine in CH_2Cl_2 resulted in a soluble polymer containing the above-listed nanoparticles. This method was used to create polymer films with a regular arrangement of nanoparticles.

Polyvinylpyrrolidone was used [252] to stabilise Ni nanoparticles (3–4 nm) synthesised by the reduction of $Ni(COD)_2$ with hydrogen at room temperature, while polyacrylamide was used to produce Ni nanoparticles on γ-irradiation.[253]

Polyimines. An original method for the introduction of nanoparticles into polyimines [254] that present interest from the applied standpoint consists of saturation of the polymer by magnetic metal ions (Fe^{2+}, Co^{2+}) followed by air exposure of the material. The spontaneous hydrolysis of the Fe^{2+} and Co^{2+} salts in the polymer after the removal of water from it (during drying of the sample) yields Fe_2O_3 and CoO nanoparticles, respectively.

Implantation of high-energy Fe^+ ions (40 keV) into ~1 μm-thick polymer films has been used [255] to prepare Fe nanoparticles (mainly, α-Fe).

Block copolymers. Block copolymers contain regular cavities with a lamellar, cylindrical or spherical shape, which can serve as nanoreactors for the synthesis of nanoparticles.[256] The synthesis of films of the $[NORCOOH]_{30}[MTD]_{300}$ block copolymers (NORCOOH is 2-norbornerne-5,6-dicarboxylic acid, MTD is methyltetracyclododecene) containing γ-Fe_2O_3 nanoparticles (5 nm) has been described.[257]

VII. Magnetic nanoparticles in biological objects

Long before the first magnetic nanoparticles have been synthesised, they were detected in natural biological complexes. It was found that magnetic nanoparticles play an important role in the metabolism and functioning of living organism. The magnetic nanoparticles found most often in living organisms are magnetite and ferrihydrite (the mineral core of ferritin).

Magnetite-containing magnetosomes are rather abundant and have been repeatedly observed by TEM.[258] Highly ordered quasi-one-dimensional chain ensembles of magnetic nanoparticles of iron oxides (Fe_3O_4 with a γ-Fe_2O_3 impurity) are present in the magnetic bacteria *Magnetotactic spirillum* and play an important functional role by ensuring the orientation of bacteria in the Earth's magnetic field.[7] The formation of inorganic nanostructures in biological systems occurs spontaneously on contact with a highly organised molecular matrix; it is highly reproducible as regards the particle shape and composition and takes place at nearly ambient temperatures (much below 100 °C) and in the aqueous phase. These processes include a set of complex and not fully understandable reactions that substantially depend on the supramolecular organisation of particles and the structure of the organic matrix, which influences the nanoparticle nucleation and growth. For example, the bacterial protein *Listeria innocua*, having an inner cavity with a diameter of 5 nm, has been used to prepare the γ-Fe_2O_3 nanoparticles with a narrow size distribution (9.3 ± 0.2 nm).[259] Elucidation of the mechanism of biomineralisation and their use for the development of new methods for the synthesis of nanoparticles and the effective control of their composition, structure, size and morphology can form a rather promising approach in nanobiotechnology and in the development of new nanomaterials.

The magnetic nanoparticles are found not only in bacteria but also in the cells of higher living organisms. It is considered that the anisotropic magnetite nanoparticles present in cells can interact with the Earth's magnetic pole and transfer information to other bioreceptors of the organism. Presumably, the stable space sense of many higher living organisms (for example, in the seasonal migration of birds and fishes) is related to their ability to locate themselves with respect to the Earth's magnetic field at each particular instant.

Ferritin is the most abundant form of non-haem iron in living organisms and plants.[260] Its major role is to preserve the biological reserve of iron.[261] This water-soluble protein consists of an inorganic core with a diameter of ~7 nm and a protein shell with ~6 nm thickness. The core contains ~4500 Fe^{3+} ions [262] as a hydrated oxide close in composition to FeOOH [263] and has H_2PO_3 groups on the external surface.[264, 265] In terms of the type of magnetic structure, ferritin is an antiferromagnet; however, due to the incomplete compensation of magnetic moments of the two sublattices, the ferritin core has a nonzero magnetic moment, like other magnetic nanoparticles of similar sizes. Ferritin itself exhibits superparamagnetic properties. Horse spleen ferritin is commercially available and has been comprehensively studied.[266]

Since natural ferritin mainly contains antiferromagnetic ferrihydrate with a relatively low magnetic moment as the core, modified magnetoferritin in which the ferrohydrate core has been replaced by a magnetite or maghemite core with a higher magnetisation is used more often for applied purposes (Fig. 4).[267, 268] The protein shell ensures the biocompatibility of ferritin and magnetoferritin particles.

The synthetic polymer colloids containing magnetic nanoparticles were first obtained in the mid-1970s. They have found application in biochemical experiments on the targeted interaction with cells and biologically active compounds, gene transfer and DNA extraction.[269] Of considerable interest is the synthesis of inorganic magnetic nanoparticles using organised molecular

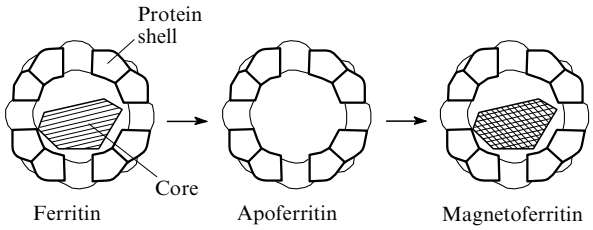


Figure 4. Scheme of the change in the magnetic core of ferritin.

structures analogous to biological systems. In particular, inclusion of magnetic nanoparticles into multilayer polyelectrolyte shells of latex particles containing glucose oxidase allowed the efficiency of these particles as nanobioreactors to be markedly increased due to the effective stirring of their colloid solution in the alternating magnetic field.[270]

Organised polymer systems and even single macromolecules are now widely used in nanotechnology for the formation of ordered ensembles of nanoparticles and nanostructures. The preparation of new organised planar complexes of amphiphilic polycations with DNA formed in a monolayer on the aqueous surface has been described.[271] In addition to individual quasilinear DNA molecules, DNA complexes with a toroidal structure and complexes with planar, extended, and net-like structures were found on the monolayer surface. The monolayer and multilayer films formed on the basis of these complexes were used as nanoreactors for the synthesis of inorganic nanostructures. First, binding of Fe^{3+} cations from the aqueous phase took place followed by the formation of the inorganic phase in the presence of a reducing agent ($NaBH_4$ or ascorbic acid) at pH 9–10 in air. This gave superthin stable polymeric nanocomposite films incorporating DNA molecules and assembled quasilinear ensembles of 2–4 nm iron oxide nanoparticles (magnetite and maghemite) as structural units.[272–274]

The introduction of iron oxide nanoparticles into DNA complexes can be used to elucidate the role of iron ions in the change in the composition and magnetic properties of nucleoproteid DNA complexes at certain stages of the cell cycle. It has been reported [275] that the magnetite nanoparticles formed upon mixing of Fe^{2+} and Fe^{3+} ions in the presence of DNA practically did not react with DNA. The corresponding DNA complexes with magnetite nanoparticles have been prepared by reduction (increase in the pH) of pre-synthesised DNA complexes with Fe^{2+} and Fe^{3+} ions.

Magnetic nanoparticles can be used in the systems of targeted transfer of biologically active compounds and drugs (in particular, for the cancer therapy using the hyperthermic effect caused by magnetic heating [269, 276, 277]), in the detection, isolation, immobilisation and modification of biologically active compounds, cells and cell organelles, and as contrasting materials in magnetic resonance tomography.[258] Of particular interest is the synthesis of so-called biocompatible magnetic nanoparticles, which is attained by modification and structurisation of their surface.[278] A serious problem that can restrict the application of magnetic nanoparticles is their potential toxicity.[279]

VIII. Physical methods for determination of the composition and dimensions of nanoparticles

Nanomaterials represent a relatively new object for studies by physical methods. There is no unique method for determination of the nanoparticle composition and dimensions; as a rule, a set of methods including powder X-ray diffraction, TEM, EXAFS, *etc.*, are used. Detailed analysis of the potential of these methods is beyond the scope of our review. We only outline, using a number of examples, the problems faced by researchers in determination of the nanomaterial structures and the ways for solving these problems.

X-Ray diffraction analysis of nanomaterials seldom produces diffraction patterns with a set of narrow reflections adequate for identification of the composition of the particles they contain. Some X-ray diffraction patterns exhibit only two or three broadened peaks of the whole set of reflections typical of the given phase. First of all, this is the case for freshly prepared samples containing nanoparticles with dimensions of several nanometres. To obtain more reliable information on the composition of these samples, they are 'hardened' on heating, which makes the X-ray diffraction pattern more informative.

In the case of larger particles (provided that high-quality X-ray diffraction patterns can be obtained), it is often possible not only to determine the phase composition but also to estimate, based on the reflection width, the size of coherent X-ray scattering areas, corresponding to the average crystallite (nanoparticle) size. This is usually done by the Scherer formula

$$d = \frac{0.9\lambda(54.7)}{b\cos\theta},$$

where λ is the X-ray wavelength, b is the width at half-height of the reflection after correction for the instrumental broadening, deg, and 2θ is the diffraction angle.

In some cases, it is possible to identify fine structural effects, for example, phase transitions in Co metal particles. In most cases, the synthesis of cobalt nanoparticles at moderate temperatures gives the high-temperature FCC β-Co phase [116] whose heating and cooling (down to 28 K) do not result in phase transformations. In a special study [280] devoted to the preparation of nanoparticles of the Co metal with a hexagonal close packing, the possible reasons for the stability of Co nanoparticles as the β-phase and the driving forces and the mechanism of the $\beta \rightarrow \alpha$ transition are discussed. It was found that long-term (for more than a week) keeping of samples containing β-Co nanoparticles in air did not cause any significant changes in their X-ray diffraction patterns. It was shown that even in thin Co films alternating with thicker Cu layers, the FCC structure of the β-phase is retained.

The modern possibilities of the use of synchrotron radiation for determination of the structures of magnetic materials have been discussed.[281]

The nanoparticle dimensions are determined most often using TEM, which directly shows the presence of nanoparticles in the material under examination and their arrangement relative to one another (Fig. 5). The phase composition of nanoparticles can be derived from electron diffraction patterns recorded for the same sample during the investigation. Note that in some cases, TEM investigations of dynamic processes are also possible. For example, the development of dislocations and disclinations in the

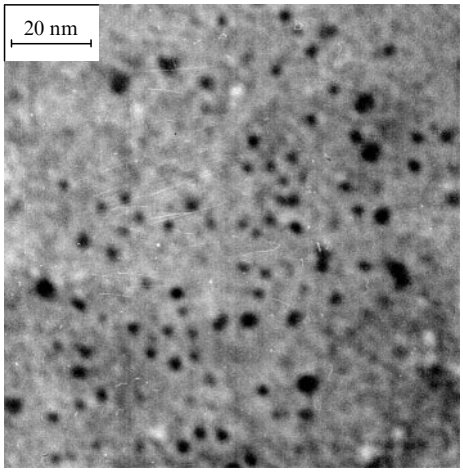


Figure 5. Micrograph of a sample containing Co nanoparticles in a polyethylene matrix.

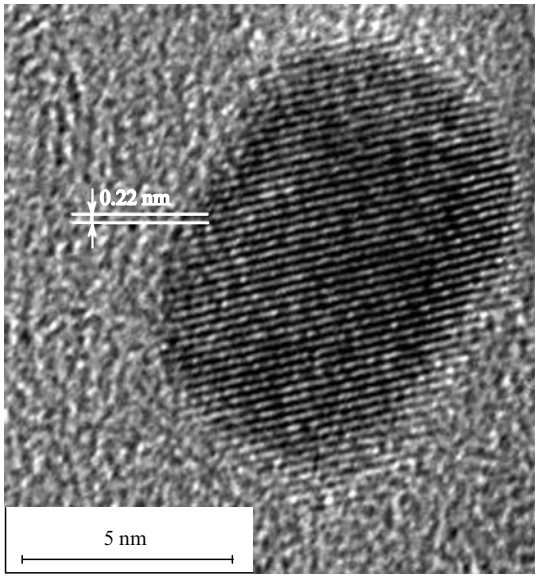


Figure 6. Typical HRTEM micrograph of a cobalt nanoparticle in a LDPE matrix.

nanocrystalline BCC-Fe during the mechanochemical treatment has been observed.[282]

More comprehensive information is provided by high-resolution transmission electron microscopy, which allows one to study the structure of both the core and the shell of a nanoparticle with atomic resolution, and in some cases, even to determine their stoichiometric composition. Figure 6 shows a typical HRTEM image of a cobalt nanoparticle in a polyethylene matrix, which allows one to determine the particle shape and dimensions, the type of crystal lattice, the distance between the layers and the presence of a shell.

The structures of non-crystalline samples are often studied by EXAFS spectroscopy. An important advantage of this methods is its selectivity, because it provides the radial distribution (RDA) curve for the atoms of the local environment of the chosen chemical element in the sample. The interatomic distances (R) and coordination numbers (N) obtained by EXAFS are then compared with the known values for the particular phase. Thus using this method, two types of cobalt atoms were detected in the Co nanoparticles formed on laser vaporisation, namely, the internal atoms with a shortest Co–Co distance of 2.50 Å (comparable with that observed in the Co metal) and the surface atoms with a Co–Co distance of 2.80 Å.[211] The total number of Co–Co bonds for a Co atom, *i.e.*, its coordination number N, was equal to 11 according to EXAFS (for the bulk FCC-Co, $N = 12$). The decrease in the coordination number was attributed to the presence of a large portion of surface atoms with low coordination numbers. This was used to estimate the average Co particle size (3–4 nm). These data are in good agreement with the results obtained by TEM and small-angle X-ray scattering (SAXS) for these samples.

Mössbauer spectroscopy provides data on the phase composition of nanoparticles, especially, magnetic phases. The method is widely used to determine the structure of Fe-containing nanoparticles.[283–285] For example, Mössbauer spectroscopy has been used to establish the composition of magnetic particles formed upon thermal decomposition of $Fe(CO)_5$ in a polyethylene matrix.[6] It was shown that the particles consist of α-Fe, γ-Fe_2O_3 and iron carbides in ratios depending on the nanoparticle concentration in the matrix.

Other physical methods are used more rarely to study the nanoparticle structures. Integrated research makes it possible to determine rather reliably the structures of simple nanoparticles; however, determination of the structures of nanoparticles composed of a core and a shell of different compositions are often faced with difficulties.

The structural studies of nanoparticles should result ultimately in the construction of structural models. Unfortunately, this is not always done. Meanwhile, the results obtained by EXAFS are difficult to interpret without model construction. For example, the construction of models for the spherical Co nanoparticles ($d = 1.6–2.6$ nm) with HCP, FCC, BCC and mixed types of packing and comparison of the RDA curves calculated for them with experimental curves indicate that the inner and surface areas of the particle have different structures.[117] The arrangement of atoms in the core corresponded to a BCC lattice with short Co–Co distances, while on the particle surface the arrangement of the cobalt atoms was less ordered, the relationship of distances rather resembling the HCP structure. However, the Co–Co distances inside the particle and on the surface determined experimentally differed from each other by a greater value than the corresponding postulated distances, which was not quite consistent with the model proposed.

The nanoparticle shell always contains light atoms (O, C, B, *etc*.). The problem of identification of these atoms, determination of their number and the mode of interaction with the core metal remain most challenging. The 'cluster' model of a nanoparticle accounts for a number of structural features of its surface layer in which the metal crystal lattice is 'diluted' with light atoms (O, C) according to a pattern well-known in the cluster chemistry.[286] According to this model, the surface layer of a particle has three types of binding between light atoms and metal polyhedra (*i.e.*, with fragments of the metal packing), namely, terminal, bridging and intrapolyhedral.

A typical example of the construction of models of these nanoparticles has been reported.[50] The reduction of $CoCl_2$ with $NaBH_4$ is accompanied by insertion of the boron atoms into the Co particle, especially, the surface layers. The comparison of the calculated dependences of the electron density for a number of model nanoparticles (neat Co; B_2O_3-coated cobalt or cobalt boride) with the experimental dependences obtained by SAXS showed that none of these models corresponds to the experimental data. It was suggested that the Co nanoparticles formed are either devoid of the ligand shell or are surrounded by a monoatomic layer, which cannot be detected by SAXS.

A number of models of the structure of nanoparticles with complex compositions are discussed in the literature. A study of iron-containing nanoparticles in the ethylene–tetrafluoroethylene (FT-40) copolymer matrix by Mössbauer and X-ray emission spectroscopy has shown [287] that the particle is composed of α-Fe and iron carbide and fluoride (the fluoride results from defluorination of the matrix). For interpreting the results, the researchers proposed so-called 'onion' model for the structure of the nanoparticle with an α-Fe core coated by iron fluoride and carbide shells. Figure 7 shows a version of this model describing the

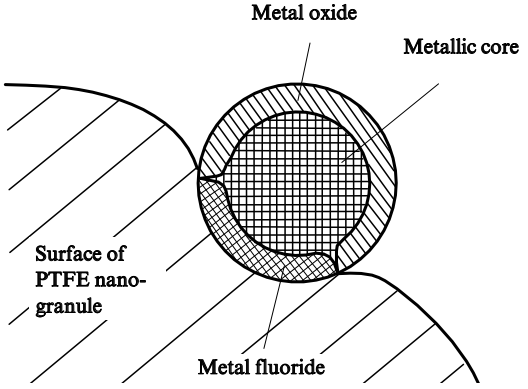


Figure 7. Model of the structure of a metallic nanoparticle stabilised by a PTFE grain.

structure of a nanoparticle located on the surface of a super-dispersed polytetrafluoroethylene (PTFE) nanograin.

IX. Characteristic features of the nanoparticle magnetism (theory)

It will not be an exaggeration to say that the intensive studies of nanoparticles as a special class of objects started from the discovery of unusual magnetic properties. In 1930, Frenkel and Dorfman showed on the basis of energy considerations that particles of a sufficiently small size should be single-domain. In the mid-20th century, the theory of single-domain particles started to be actively developed [288–299] and the related phenomena were studied experimentally.[300–309] These studies identified a substantial increase in the coercive force of a ferromagnet on passing from a multidomain to the single-domain structure, which is important for the creation of permanent magnets. The results of calculation of the characteristic particle size (for different magnetic materials) where the particle becomes single-domain are presented in Table 2.

Table 2. Critical diameter (for room temperature) of a single-domain spherical particle with the axial magnetic anisotropy.

Material	Critical diameter /nm		
	from Ref. 310	from Ref. 311	from Ref. 312
Co	70	70	68
Ni	–	55	32
Fe	30 (see [a])	14	12
$BaFe_{12}O_{19}$	–	–	580
Fe_3O_4	–	128	–
γ-Fe_2O_3	–	166	–
Nd–Fe–B	200	–	214
$SmCo_5$	1500	–	1528

[a] A similar value (26 nm) is reported in another publication.[313]

The critical diameter values corresponding to particle transition from the multidomain to the single-domain state presented in the Table were calculated for spherical particles with an axial magnetic anisotropy. For other types of anisotropy (cubic, hexagonal, *etc*.) and other particle shapes, the numerical estimation of the critical diameter for the single-domain character changes. In particular, the particle can be transferred into the single-domain state without decreasing the volume if it has a shape other than a sphere, for example, an oblong ellipsoid. Experimental determination of the critical diameter above which a single-domain particle becomes multidomain is a complicated task, although now it has become possible to observe this transition directly through a magnetic force microscope [314, 315] or a quantum magnetic interferometer (μ-SQUID).[316–318] For a 20 nm-thick disc-like cobalt particle, a study by a magnetic force microscope gave a critical diameter for the single-domain state of 200 nm. Elliptical particles with the same thickness became single-domain at sizes less than 150×450 nm. These values are markedly greater than the calculated ones (see Table 2).

To put it more exactly, the term 'single-domain' does not require a necessary uniform magnetisation throughout the whole particle bulk but only implies the absence of domain walls. In addition, a single-domain particle is not necessarily a 'small' particle (as opposed to a 'bulk' particle) as regards specific magnetic characteristics. Data of a publication [319] and their analysis [320] demonstrate that a rather large particle can be single-domain but still possessing the physical properties of a bulk material. Thus, the specific properties of nanoparticles start to be manifested at sizes much smaller than the 'single-domain limit'.

It is considered that significant changes in the main physical characteristics of a bulk material appear when the dimensions of its particles decrease to an extent where the ratio of the number of surface atoms N_s to the total number N of atoms in the particle approaches 0.5.[17] An interesting formulation of this criterion as applied to magnetic nanoparticles has been proposed. Assuming that in a surface layer of thickness Δr (defectiveness parameter), the number of exchange bonds is twice as low as that in the particle bulk and that the Curie temperature is directly proportional to the bulk density of exchange bonds, Nikolaev and Shipilin [320] have analysed the dependence of T_C on the magnetite particle size obtained earlier.[319] The defectiveness parameter Δr was found to depend on the particle radius r. In particular, for magnetite $\Delta r \to 0$ for $r \geqslant 20$ nm (the radius for the single-domain state of magnetite is ~ 70 nm, see Table 2). As the particle radius decreases, the parameter Δr substantially increases and for $r = 2.5$ nm, it amounts to 0.5 nm. Thus, the smaller the magnetic particle size, the greater the effective depth to which the violation of the regular structure extends.

One more remarkable property of the nanoparticles, which allowed their experimental discovery in the mid-20th century, is the superparamagnetism. The higher the particle magnetic moment, the lower the magnetic field H_s that is required to observe the magnetisation saturation phenomenon. In a rough approximation, the H_s value (saturation field) can be estimated from the formula

$$\mu_{ef} H_s \approx k_B T,$$

where μ_{ef} is the effective magnetic moment of the particle. For paramagnetic $Gd(SO_4)_3 \cdot H_2O$, the effective magnetic moment of the Gd^{3+} ion is $7\,\mu_B$. Thus, the H_s value for this paramagnet at room temperature would be $H_s \approx 300\,k_B/7 \approx 10^6$ Œ. For a particle with an effective magnetic moment of $10^4\,\mu_B$, the saturation field would decrease to 10^3 Œ. The phenomenon of saturation of the magnetisation curve in low (for a usual laboratory) fields of ~ 1 kŒ has been called 'superparamagnetism,' while a material exhibiting such properties is called a 'superparamagnetic'.§

The model of an ideal superparamagnetic was mainly worked out by the early 1960s,[321] but now it continues to develop.[312, 322] The simplest variant of this model considers a system of N non-interacting identical particles with the magnetic moment μ_{ef}. Since the magnetic moment of the particle is assumed to be large, its interaction with the magnetic field H is calculated without taking the quantum effects into account. In the case of isotropic particles, the equilibrium magnetisation of the $\langle M \rangle$ system is described by the Langevin equation

$$\langle M \rangle = N\mu_{ef}\left[\mathrm{cth}\left(\frac{\mu_{ef}H}{k_B T}\right) - \frac{k_B T}{\mu_{ef}H}\right]. \quad (1)$$

Equation (1) has been derived with the assumption that single particles are magnetically isotropic, *i.e*., all directions for their magnetic moments are energetically equivalent, but this condition is hardly ever fulfilled. If the particles are magnetically anisotropic, the calculation of the equilibrium magnetisation becomes more complicated. According to the nature of factors giving rise to the non-equivalence of the directions of magnetic moments, one can distinguish the magnetically crystalline anisotropy; the shape anisotropy; anisotropy associated with the internal stress and external impact; exchange anisotropy, and so on.[323]

For nanoparticles, the surface magnetic anisotropy plays a special role. Unlike other kinds of magnetic anisotropy, the surface anisotropy is proportional to the surface area of the particle S rather than to its volume V. The surface anisotropy

§ Typical features of a superparamagnetic include also the absence of a magnetic hysteresis and the presence of thermal fluctuations of the magnetic moment of a nanoparticle (similar to the thermal fluctuations in a conventional paramagnetic).

appears due to the violation of the symmetry of the local environment and the change in the crystal field, which acts on magnetic ions located on the surface. Uniaxial anisotropy is the simplest type of magnetic anisotropy as regards the symmetry properties.¶ In the general case, the equation for the energy of the uniaxial magnetic anisotropy is written as the sum of two contributions:

$$E(\theta) = (K_V V + K_S S)\sin^2\theta, \quad (2)$$

where K_V is the volume anisotropy constant, V is the particle volume, K_S is the surface anisotropy constant, θ is the angle between the vector of the particle magnetic moment $\boldsymbol{m}$ and the anisotropy axis.

When the surface makes no contribution to the anisotropy, the angular dependence of the particle energy has the form

$$E(\theta) = K_V V \sin^2\theta\,.$$

If no external magnetic field or surface anisotropy are present, the minimum energy of the particle is attained at the orientation of the magnetic moment $\boldsymbol{m}$ along the anisotropy axis. In this case, two neighbouring minima are separated by a barrier with height $K_V V$. In an external magnetic field H applied at the angle ψ to the anisotropy axis, the particle energy is equal to

$$E(\theta) = K_V V \sin^2\theta - M_s V H \cos(\theta - \psi). \quad (3)$$

(The particle is assumed to be uniformly magnetised to saturation, its magnetic moment being $m = M_s V$.) The dependence of the particle energy on the angle θ for different angles ψ is shown in Fig. 8 for $K_V = 4.5\times10^5$ J m^{-3}, $V = 10^3$ nm^3, $M_s = 1.4\times10^6$ A m^{-1}, $H = 10^5$ A m^{-1}. It can be seen that in the vicinity of $\theta = 0$, π and 2π, there are three energy minima separated by non-equivalent barriers [in the case of $\psi = 0$ and π (curves *1* and *5*), the barriers are equivalent].

In the general case, in the presence of an external magnetic field, rotation of the magnetic moment of the particle to reach the orientation corresponding to an energy minimum requires overcoming an energy barrier, $\Delta E \approx K_V V$. The relation for the characteristic time of thermal fluctuations of the magnetic moment of a single-domain particle with a uniaxial anisotropy provided that $\Delta E/k_B T \geqslant 1$ was obtained by Neel [295]

$$\tau = \tau_0 \exp\left(\frac{\Delta E}{k_B T}\right). \quad (4)$$

Later, relation (4) was extended by Brown [296–299] to the cubic anisotropy case.†

The pre-exponential factor τ_0 depends on many parameters including temperature, gyromagnetic ratios, saturation magnetisation, anisotropy constants, the height of energy barrier, and so on.[324, 325] However, for the sake of simplicity τ_0 is often considered to be a constant in the range of 10^{-9}–10^{-13} s.[311]

Relation (4) determines the characteristic time needed for the thermal equilibrium in a system of non-interacting single-domain magnetic particles to establish. At higher temperatures, $\Delta E/k_B T \ll 1$; the time required for system transition into a state with the minimum energy is short compared to the characteristic time of measurements τ_{meas}, and the system is not expected to show a magnetic hysteresis. In the case where $\Delta E/k_B T \gg 1$, the system transition into an equilibrium state may take a very long time depending appreciably on the particle. For $\tau_0 = 10^{-9}$ s, $K_V = 10^5$ J m^{-3} and $T = 300$ K for a magnetically anisotropic spherical particle 11.4 nm in diameter, we get $\tau = 10^{-1}$ s and for a particle with a diameter of 14.6 nm, $\tau = 10^8$ s.[311]

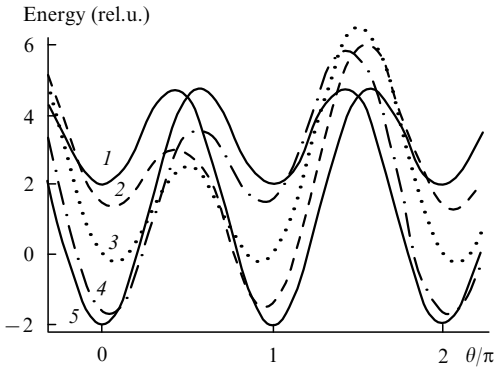


Figure 8. Angular dependence of the energy of a uniaxial magnetic particle $E(\theta)$ at different orientations of the external magnetic field H. ψ = 180 (*1*), 135 (*2*), 90 (*3*), 35 (*4*), 0 (*5*).

If $\tau_{meas} \gg \tau$, the system occurs in the superparamagnetic state and rapidly reaches an equilibrium magnetisation on changing the temperature or the external field. Otherwise ($\tau_{meas} \ll \tau$), after a change in the external magnetic field, the system does not arrive to a new equilibrium state over the time τ_{meas} and its magnetisation does not change. The case $\tau = \tau_{meas}$ in relation (4) corresponds to the blocking temperature T_b. If $\tau_{meas} = 100$ s (characteristic time for the static magnetic measurements) and $\tau_0 = 10^{-9}$ s, the condition $\tau_{meas} = \tau$ in relation (4) gives $K_V V \approx 25.3\, k_B T$. Hence,

$$T_b = \frac{K_V V}{25 k_B}\,. \quad (5)$$

It is noteworthy that relation (5) specifies the blocking temperature for a zero magnetic field. As the external magnetic field is enhanced, the blocking temperature decreases by a power law

$$T_b(H) = T_b(0)\left(1 - \frac{H}{H_c}\right)^{\kappa}, \quad (6)$$

where $\kappa = 2$ (for low fields [326]) and 2/3 (for high fields [327]), $H_c = 2K/M_s$.

The experimental data obtained for magnetite nanoparticles show that upon an increase in the field from zero to 700 Œ, the blocking temperature decreases from 140 to 75 K, relation (6) being fulfilled rather accurately below 50 Œ with $\kappa = 2$, and for fields from 50 to 700 Œ, with $\kappa = 2/3$.[328]

When investigating the magnetic properties of the samples containing nanoparticles, the magnetisation curve is usually measured up to saturation magnetisation (Fig. 9).[329] To deter-

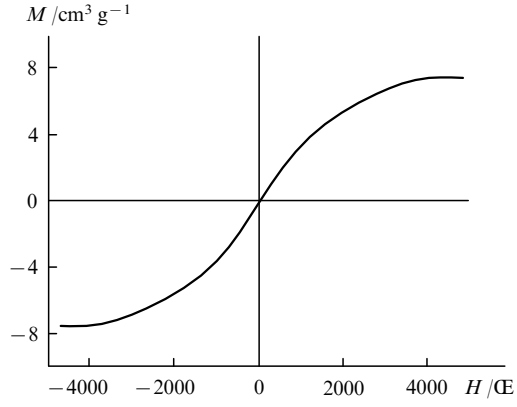


Figure 9. Magnetisation *vs.* magnetic field value (at 295 K) for a sample containing γ-Fe_2O_3 nanoparticles in a polyethylene matrix.[329]

¶ The anisotropy is called uniaxial if the magnet has only one axis of easy magnetisation. The easy magnetisation axis in a magnetically anisotropic medium corresponds to a direction of the magnetisation vector relative to the crystal lattice of the magnet such that the energy of the magnetically anisotropic medium is minimum.

† In the case of cubic anisotropy, there are three mutually perpendicular easy magnetisation axes.

mine the temperature dependence of the magnetic moment m, two types of measurements are carried out, namely, zero-field cooling (ZFC) and field cooling (FC). According to the ZFC procedure, the sample is cooled (usually down to the liquid helium temperature) in the absence of a magnetic field and then a moderate measuring field is applied (1–100 Œ) and the temperature is gradually raised, the magnetic moment m_{ZFC} values being recorded. The FC procedure differs from ZFC only by the fact that the sample is cooled in a nonzero magnetic field. For magnetic nanoparticles, the $m_{FC}(T)$ and $m_{ZFC}(T)$ curves usually coincide at relatively high temperatures but start to differ below a certain temperature T_{ir} (irreversibility temperature). The $m_{ZFC}(T)$ curve has a maximum at some temperature T_{max}, and the $m_{FC}(T)$ curve, most often, ascends monotonically to very low temperatures (Fig. 10). The dependence of magnetisation on the applied field at various temperatures is often additionally measured (Fig. 11).[330] Electron magnetic resonance and Mössbauer spectroscopy data are also used for analysis of the magnetic properties.

For an idealised system containing identical nanoparticles with uniaxial anisotropy and a random orientation of easy magnetisation axes, the difference between the temperature dependences of m_{FC} and m_{ZFC} at a qualitative level follows from Eqn (3) and Fig. 8. In the case of a zero field, on cooling below the blocking temperature, the magnetic moments of particles are oriented along their easy magnetisation axes [$\theta = \psi = 0$ in Eqn (3)], the total magnetic moment of the system being equal to zero both at the beginning and at the end of cooling. After the external field H has been switched on, the magnetic moments for which $\theta - \psi < 90^\circ$ [see Eqn (3)] do not need to overcome an energy barrier and they rotate to the minimum-energy position, thus creating a non-zero magnetisation. For example, for the curve $\psi = 35^\circ$ in Fig. 8, the rotation angle will be 29°. Conversely, the magnetic moments for which $\theta - \psi > 90^\circ$ on switching on the magnetic field are separated from the energy minimum by a potential barrier which they can overcome only over a long period of time [see Eqn (4)]. Therefore, in the case of ZFC measurements for $T < T_b$, the system gets into a metastable state with a relatively low total magnetic moment $M_s^2 H/3K_V$, which does not depend on the temperature.[331] When $T = T_b$, the system passes *via* a jump ‡ into a stable superparamagnetic state with the magnetic moment

$$m_{ZFC} = \frac{M_s^2 VH}{3k_B T}. \qquad (7)$$

For $M_s VH \ll k_B T$ and a random orientation of the axes of easy magnetisation of particles, relation (7) holds also for $T > T_b$.[310]

In the FC measurements, cooling of the sample takes place in a nonzero magnetic field; at any temperature above T_b, magnetisation is determined by Eqn (7). When $T < T_b$, the system magnetisation can no longer change over the time of measurements. Therefore, the magnetic moment in the FC procedure at $T < T_b$ is equal to

$$m_{FC} \approx \frac{M_s^2 VH}{3k_B T} = \text{const}.$$

For a system consisting of single-domain nanoparticles with a size, shape, *etc*. dispersions, the $m_{ZFC}(T)$ and $m_{FC}(T)$ curves are not separated at $T = T_b$, but are separated at a higher temperature $T_{ir} > T_b$, which is called the irreversibility point.[332] Another characteristic point in the $m_{ZFC}(T)$ curve is the temperature T_{max}, which is often identified as the average temperature of system blocking $\langle T_b \rangle$. For a temperature below $\langle T_b \rangle$, an increase in $m_{FC}(T)$ is observed, which is then replaced by a 'saturation' section and in some cases, by a maximum.[310] The T_{ir} value can be identified with the blocking temperature for the largest particles, and T_{max}, with the blocking temperature for the smallest particles. However, it should be borne in mind that all these characteristic temperatures (and their relationship with the volume distribution of particles) can depend on the rate of sample cooling and subsequent heating[333] and on the intensity of the interparticle interactions. If the rate of sample heating is much lower than the cooling rate, the $m_{FC}(T)$ may have a maximum at $T < \langle T_b \rangle$.[310] In the case of strong interparticle interactions, the energy distribution of particles ΔE [see Eqn (2)] may narrow down (in relative units σ/μ, where σ is the dispersion, μ is the average value) with respect to the volume distribution.[310] In this case, a more accurate calculation of the local magnetic field acting on a single particle is required.

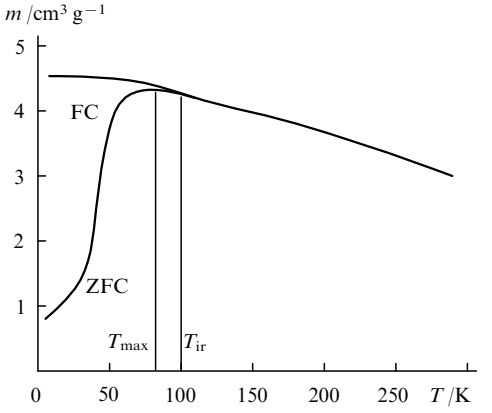


Figure 10. Temperature dependences of the magnetic moment (ZFC and FC measurements) for a sample containing γ-Fe_2O_3 nanoparticles in a polyethylene matrix.

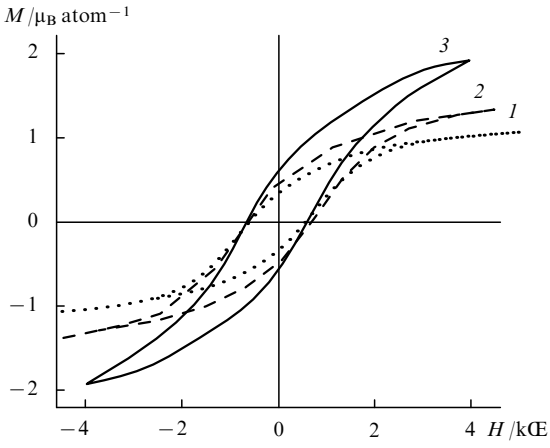


Figure 11. Magnetisation *vs*. the magnetic field at 295 (*1*), 77 (*2*) and 4.2 K (*3*) for a sample containing Co nanoparticles (4 mass %) in a polyethylene matrix.[330]

‡ In experimental studies at $T = T_b$, sharp changes in magnetisation are never observed, because a size spread (and, generally, other types of spread) always exists for the particles. Small particles pass into the superparamagnetic state at a lower temperature than large particles and the magnetisation jump is smeared. The temperature corresponding to the maximum in the $m_{ZFC}(T)$ curve roughly coincides with the average temperature of particle transition into the superparamagnetic state, which corresponds to the maximum distribution of all particles over the volume V. In addition, even for absolutely identical particles, the relaxation time increases smoothly rather than by a jump, although rapidly. It follows from relation (4) that

$$\frac{d\tau}{\tau} = -\left(\frac{dT}{T}\right)\left(\frac{\Delta E}{k_B T}\right) \approx -25\left(\frac{dT}{T}\right),$$

i.e., near T_b the relative change in the relaxation time is 25 times as fast as the relative change in the temperature.

Note that the $m_{ZFC}(T)$ and $m_{FC}(T)$ curves differ not only for the systems of magnetic nanoparticles but also for macroscopic magnets with disorder elements (exchange coupling frustration, topological disorder, structural defects) and even in ordered ferromagnets with a substantial magnetic anisotropy.[334]

The difficulty of the theoretical investigation of the magnetic hysteresis in nanoparticles lies in the fact that this non-linear, non-equilibrium and non-local phenomenon caused by the existence of energy minima (resulting from the magnetic anisotropy) and the barriers separating them depends, in a complex manner, on the external magnetic field. The results of theoretical studies using relatively simple models seldom provide a plausible description for real magnetic nanomaterials as they do not take into account their microstructure, in particular, the effect of boundaries and defects on the local magnetisation.[317]

An important role of the microstructure in the formation of magnetic characteristics is indicated by the studies of nanocomposite materials (for example, Nd–Fe–B/α-Fe[335] and FePt–Fe_3Pt[178] systems), which represent a magnetically soft medium with nano-sized grains distributed therein (< 100 nm).[336] In these materials, the magnetically hard phase ensures a high coercive force, while the magnetically soft phase provides a high saturation magnetisation. In addition, the substantial exchange interaction between the grains ensures a relative residual magnetisation higher than 0.7.[335,336] Therefore, materials of this type are called exchange-coupled magnets.

In recent years attempts have been undertaken to study the effect of the internal structure (microstructure) of a nanoparticle on the magnetic characteristics of real nanomaterials.[312] Most successful was the use of numerical calculations within the framework of the micromagnetism theory (so-called 'computer micromagnetism').[337–340] Even when a nanoparticle has a defect-free crystal structure, the different local environments of atoms at the particle boundary and inside the particle result in a nonuniform magnetisation in the particle and distortion of the perfect collinear magnetic structure.[341,342] The calculations show that at the final temperature, magnetisation decreases along the direction from the particle centre toward the boundary,[343] and the magnetic moment of each particular surface atom can be greater than that of the bulk atoms.[344] The decrease in the magnetisation on the particle surface compared to that in the bulk is due a lower energy of the surface spin wave excitations,[322] in other words, more pronounced action of the thermal fluctuations on the surface. The increase in the magnetic moment of surface atoms can be attributed, within the framework of the band theory, to the decrease in the coordination number, and, as a consequence, to narrowing the corresponding energy band and an increase in the density of states. Apparently, this also accounts for the rare cases of magnetic order appearing in metal nanoparticles whose bulk analogues are non-magnetic.[345–348]

The qualitative isothermal dependence of the coercive force H_c on the characteristic size of magnetic particles is shown in Fig. 12 *a*. The increase in H_c upon a decrease in the particle size follows from the Stoner–Wohlfarth theory according to which the spins of atoms forming a nanoparticle rotate coherently, *i.e.*, concertedly. It is known from experiments that the coercive force in real magnetic materials (including nanomaterials) is much lower§ than the limiting values predicted by the theory even at very low temperatures. One reason is that under the action of an external magnetic field, the spins of the atoms forming the nanoparticle can rotate not only coherently but also in a more complex manner to form spin modes: 'swirls' (Fig. 13), 'fans', *etc*.[312] The appearance of non-coherent spin modes is facilitated if nanoparticles form agglomerates (for example, chains). The coherent

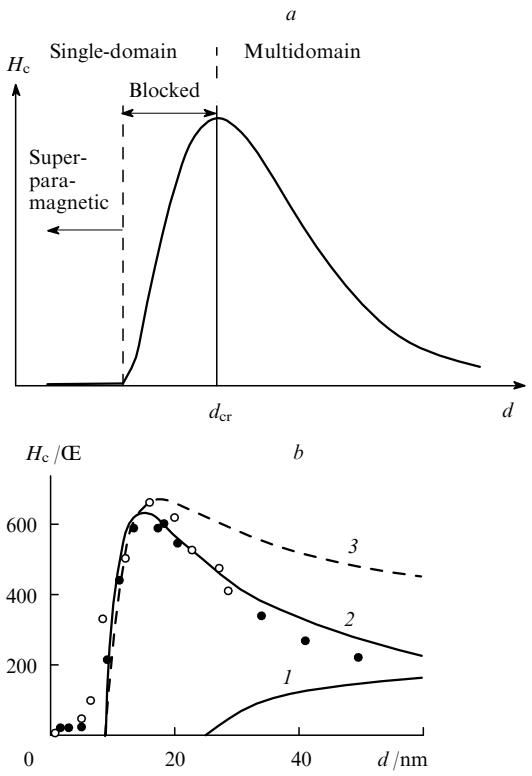


Figure 12. Qualitative (*a*) and quantitative (*b*) dependences of the coercive force H_c on the particle diameter.[318]
(*a*) Qualitative dependence that follows from the simple model of single-domain particle; (*b*) experimental (dots) and calculated (curves *1*–*3*) dependences for iron nanoparticles. The experimental values were obtained for iron particles in oxide Al_2O_3 (light dots) and SiO_2 (dark dots) matrices. The calculation was carried out with the assumption that $K_S = 4 \times 10^{-4}$ J m^{-2} and $K_V = 5 \times 10^4$ J m^{-3}; (*1*) cubic bulk anisotropy, (*2*) axial surface anisotropy, (*3*) simultaneous account for the axial surface anisotropy and bulk anisotropy.

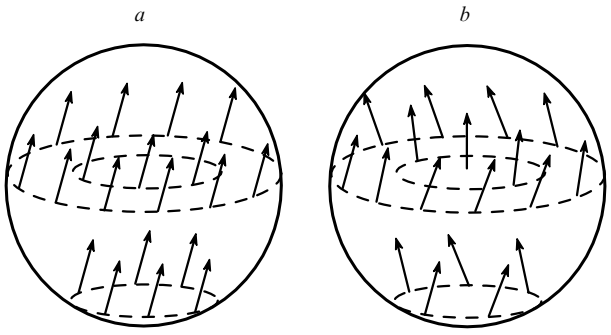


Figure 13. Simplest spin modes formed upon magnetisation reversal in a single-domain particle: (*a*) coherent rotation, (*b*) eddy mode.[312]

rotation can, apparently, take place only in absolutely defect-free uniform particles with a zero surface anisotropy.

It is evident by intuition that the coercive force should be the lower the greater the number of options (mechanisms) for spin rotation in the direction opposite to the initial one. In a multidomain particle, this rotation can be additionally associated with the displacement of domain boundaries.[349] As the particle size decreases, the number of domains decreases, and the role of interdomain boundaries in magnetisation reversal becomes less pronounced. Therefore, up to the critical particle size (d_{cr}, see Fig. 12 *a*), the coercive force increases with a decrease in *d*. However, further decrease in the particle size and transition to

§ According to the Stoner–Wohlfarth model, the anisotropy field $H_A = 2K_V/M_s$ is the upper limit for H_c. According to a publication,[312] the H_c value in real materials varies in the range of $(0.2–0.4)\,H_A$.

single-domain particles entails an increase in the role of thermal fluctuations. This explains a decrease in H_c at $d < d_{cr}$ (see Fig. 12 *a*, *b*).

Important information on the magnetic properties of nanoparticles and material based on them can be derived from measurements of slow relaxation processes.[310, 322, 328, 350] In the simplest cases, for a system of identical magnetic nanoparticles, the equilibrium magnetisation upon the change in the magnetic field (for example, quick switching off) is described by the equation

$$M(t) = M_0 \exp\left(-\frac{t}{\tau}\right), \quad (8)$$

where the relaxation time τ is determined by relation (4).

For low-temperature measurements of the residual magnetisation of systems containing magnetic nanoparticles which can exist in the blocked state, three types of experimental procedures are used ¶ (see Ref. 351). During the measurements of isothermal residual magnetisation (IRM), the sample is cooled in a zero magnetic field; after that, the field H is first applied and then switched off at a constant temperature T. In this case, the residual magnetisation of M_{IRM} depends on the H and T values. In the measurements of the thermal residual magnetisation M_{TRM}, the sample is placed in a constant magnetic field H at a high temperature (when all particles are superparamagnetic) and then cooled to low temperature and the field is switched off. Finally, the DC demagnetisation is measured in the same way as M_{IRM}, but the sample is first magnetised to saturation at low temperature, then the field H is switched on in the opposite direction and then switched off. In the absence of interparticle interactions [328]

$$M_{DCD}(H) = M_{IRM}(\infty) - 2M_{IRM}(H). \quad (9)$$

The non-observance of this rule is considered to indicate the presence of interaction between the particles,[352] although for a particle with mixed anisotropy (for example, uniaxial + cubic), this conclusion should be used with caution.[353]

For real systems, the function f(E) of particle distribution over the heights of the energy barrier always has a finite width, which is associated with the size, shape, morphology and composition differences between the particles. In this case, the relaxation properties of a system cannot be described using one parameter. For a rectangular distribution f(E), the simple equation (8) should be replaced by the following relation [311]

$$M(t) = M_0 - S\ln\left(\frac{t}{\tau_0}\right), \quad (10)$$

where S is the magnetic viscosity coefficient.

If the applied external magnetic field H varies at a constant temperature, the maximum magnetic viscosity coefficient is attained at $H = H_c$. The logarithmic law (10) is usually confirmed experimentally only for relatively short observation periods.[310] The deviations from the logarithmic law can provide information on the symmetry of magnetic anisotropy, size distribution of particles, and so on.

Taking account of magnetic interactions between nanoparticles is a complicated theoretical task. In a recent discussion [310, 354, 355] dealing with the effect of interparticle interactions on the blocking temperature, two models were proposed, one predicting an increase in T_b,[345] whereas the other, conversely, a decrease in T_b [310] following an enhancement of the interparticle interactions. The interactions change the height of the energy barrier separating two states of a particle with the opposite directions of the magnetic moment. If the barrier grows, T_b increases and *vice versa*. The influence of the change in the distances between the maghemite nanoparticles with a diameter of 6–7 nm on the blocking temperature has been studied experimentally.[356] The distances between the particles were changed by compacting the sample. The maximum increase in the sample density was 55%; simultaneously, T_b [corresponding to the maximum in the curve $m_{ZFC}(T)$] increased from 50 to 80 K. Assuming that for noncharged nanoparticles, the predominant magnetic dipole–dipole interactions are inversely proportional to the cubed distance between the particles, one can expect a linear dependence of T_b on the sample density. This is in good agreement with a publication.[356]

In the presence of interparticle interactions, the qualitative picture of the behaviour of a system of magnetic nanoparticles following a decrease in temperature may become more complicated than the mere transition to the blocked state.[357] The possible transitions are shown in Fig. 14.[310] If the particles are arranged irregularly in space, the interparticle interactions should transfer the system into the 'spin glass' type state at some temperature T_g.[357] Which of the temperatures, either T_g or the average blocking temperature $\langle T_b \rangle$ would be higher for the given type of particles depends on the particle size and on the average distance between them. Since the temperature dependences of the magnetic moment (ZFC – FC) for a system of non-interacting particles and for a 'spin glass' are similar,[358] determination of the nature of the transition is a non-trivial task.

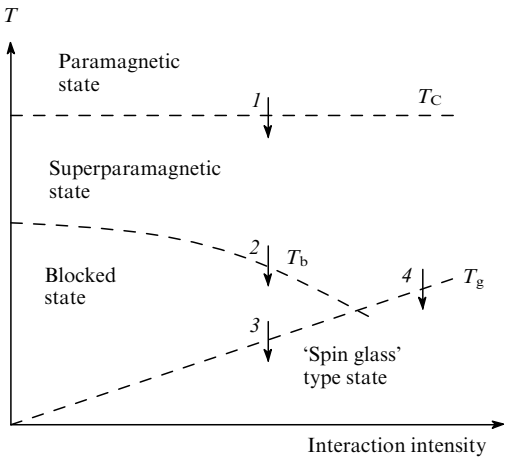


Figure 14. Scheme of the possible transitions in a system of magnetic nanoparticles arranged randomly in space taking into account interparticle interactions.[310]
(*1*) Transition from the paramagnetic to superparamagnetic state within single particles; (*2*) transition from the superparamagnetic into 'blocked' state; (*3*) transition from the 'blocked' state into a 'spin glass' type state; (*4*) transition from the superparamagnetic state to a 'spin glass' type state.

To choose theoretically between these states, one first has to know the way of estimating the interacting force in the nanoparticle system. Often, it is assumed that the interparticle interactions can be neglected if the particle concentration in the matrix is low and, hence, the average distance between them is rather high (1.5 times higher than the average particle diameter).[351] This assumption can be proved by verifying experimentally the fulfillment of relation (9).

Recently,[359] an interesting approach to taking account of the effect of interparticle interactions on the magnetisation curves of nanoparticles has been proposed. On the basis of the monotonic decrease in μ_{ef} with a decrease in temperature observed experimentally, the researchers cited introduced phenomenological corrections into relation (1). It was assumed [359] that the magnetic dipole–dipole interactions, which predominate in the systems under consideration, act as a random factor and prevent magnetisation (ordering) of the system, *i.e.*, function in the same way as the temperature. It is worth noting that, although the proposed

¶ These measurements are carried out at relatively low temperatures so that the particles (or their substantial portion) passed into the blocked state.

approach [359] is strictly applicable only to equilibrium systems, it describes satisfactorily the magnetisation curves at any temperatures, including those below the blocking temperature T_b [in this case, the average value over two branches of the hysteresis loop should be taken as $M(H)$]. The applicability of this model for $T < T_b$ is apparently due to the predominance of interparticle interactions over one-particle effects for all the samples studied.[359]

X. Magnetic characteristics of nanoparticles (experimental data)

The first experimental data on the properties of magnetic nanoparticles were obtained in experiments with cluster beams.[26,27] Despite the difficulty of interpretation, these experiments provided the unique possibility of determining the dependence of magnetic parameters on the number of atoms in the nanoparticle. Thus isothermal dependences of the average atomic magnetic moment $\langle\mu_{ef}\rangle$ on the number of atoms n in Fe, Co, Ni nanoparticles demonstrated for the first time that the specific magnetic moment of a nanoparticle increases with a decrease in the particle size. This trend is the most pronounced for Ni, which may be due to a higher density of the valence electrons.[26] The Co nanoparticles with a number of atoms n of 56 to 215 are superparamagnetic at 97 K having $\langle\mu_{ef}\rangle = 2.24\,\mu_B$. This value is greater than the μ values for macroscopic samples of cobalt.[26,27]

Thus, the experimental data imply that the effective magnetic moment of atoms in 3d-metal nanoparticles can be greater than its magnetic moment in a bulk metal. This may be attributed to the fact that the magnetic moment of an atom on the cluster surface should be regarded as localised, while in the bulk metal with band magnetism, as a delocalised (this delocalisation results in a decrease in the average magnetic moment of the atom in the bulk metal). It is noteworthy that for the smallest Ni nanoparticles, the magnetic moment barely changes with temperature over the whole temperature range studied, due to the large number of surface atoms.[26] For larger clusters, a non-zero contribution of surface atoms into the magnetic moment is retained even at temperatures above 631 K (the Curie temperature of the bulk phase). For $Ni_{550-600}$ nanoparticles, the magnetic moment at 631 K amounts to 25% of the low-temperature value $0.6\,\mu_B$.

Thus, it follows from experiments with molecular beams that the magnetic order is retained in nanoparticles at higher temperatures than in the bulk samples,[26,27] which is manifested as an increase in the Curie temperature with respect to bulk phases. For cobalt ($T_C \approx 1400$ K), the atomic magnetic moment in nanoparticles with the numbers of atoms $n = 50-600$ changes only slightly with an increase in the temperature to ~ 1000 K and always remains greater than the bulk value. The temperature dependences of the average magnetic moment for iron nanoparticles follow a more complex pattern. A possible reason is in the specific features of the iron phase diagram and structural transitions, which complicate the pattern of magnetic behaviour. No transitions to the conventional paramagnetic state were detected up to the highest temperatures (~ 1000 K).

The properties of REE clusters, namely, Gd [26] and Tb [360] clusters, are even more peculiar. Whereas 3d-metal nanoparticles behave in molecular beam experiments as either superparamagnetic particles or particles with a 'frozen' magnetic moment, Gd_n clusters exhibit a dual behaviour.[27] Two types of clusters with the same mass but different properties have always been observed in experiments,[361] namely, those having properties of superparamagnetic particles and those with the properties of 'frozen' moment particles. It is yet unclear whether this is related to the existence of structural or magnetic isomers of the same Gd_n cluster.

Among the gadolinium clusters studied with numbers of atoms from 11 to 92, superparamagnetic properties were found for Gd_{22}, Gd_{30} and Gd_{33} (even at low temperatures).[26,27,361] Conversely, the Gd_{11-16}, Gd_{19-21}, Gd_{23-26}, Gd_{53}, Gd_{54} and some other clusters clearly exhibit 'frozen' magnetic moments at 100 K. As the temperature increases to room temperature, some of these clusters become superparamagnetic (for example, Gd_{17}), whereas some other (Gd_{12-16}, Gd_{19-21}, Gd_{23}, Gd_{26}, Gd_{55}) remain 'frozen'. At 800 ± 200 K, all the gadolinium clusters studied become superparamagnetic, the atom magnetic moments in the clusters remaining ordered, *i.e.*, the Curie temperature for gadolinium clusters is much higher than for the bulk phase (293 K). It should be noted that the effective magnetic moment per atom in all Gd_n clusters is at least twice lower than the bulk value equal to $7\,\mu_B$.

Terbium clusters behave similarly to gadolinium clusters.[360] At room temperature, the vast majority of terbium clusters are superparamagnetic. At low temperatures, many of them pass to a state characterised by a 'frozen' magnetic moment but some remain superparamagnetic. Using the Tb_n clusters as examples, the influence of the addition of oxygen to a metal cluster was studied. It was found that the addition of oxygen to Tb_n clusters, except for Tb_{22}, does not change their magnetic properties. The magnetic moment of the superparamagnetic Tb_{22} cluster 'freezes' at ~ 250 K upon the addition of oxygen.

Clusters of some other elements: chromium ($n = 9 \pm 31$), palladium ($n = 100 \pm 120$) and vanadium ($n = 8 \pm 99$) have also been studied using cluster beams.[26] They all proved to be paramagnetic.†

The interest in magnetic nanoparticles inserted into various matrices is due, first of all, to their potential practical use. In addition to traditional catalysis,[363] magnetic nanoparticles can be used for superhigh-density information recording,[364–366] for solving some medical problems (for example, as drug carriers) [367,368] and for creation of heavy-duty magnets,[335,369,370] 'spin' electronics elements [281,371–374] and various sensors,[371,375] including biomolecular ones.[376]

The last 10 years were marked by impressive progress in the development of materials for high-density magnetic recording. In 1992, the highest density of magnetic recording in commercial hard discs was about 10 Mbit in^{-2}. With this recording density, the dimensions of one bit in the plane of a round-shaped magnetic medium equals 800×64 nm^2. This corresponds to 40 000 bpi along the track and 25 000 tpi (see ‡) in the radial direction.

In 2001, a magnetic recording density of 100 Gbit in^{-2} was attained,[366] which corresponds to a bit dimensions of 300×15 nm^2. In view of the fact that one storage bit now forms up to 1000 separate grains (this is due to the need to maintain the signal-to-noise ratio at a plausible level), to reach a recording density of 100 Gbit in^{-2}, the size of one particle in the radial direction should be about 0.3 nm, *i.e.*, 2–4 atoms. Further increase in the density suggests both a decrease in the particle size and modification of the record format.

Owing to the magnetic nanomaterials, the amount of the stored information has been increased by 4 orders of magnitude during the last 20 years. The size of the hard discs of home personal computers has increased from 10 Mbyte (in the mid-1980s) to 300–500 Gbyte (currently). These achievements in the magnetic recording became possible, first of all, due to the decrease in the size of the transition region § between the neighbouring bits and a decrease in the distance between the recording head and the surface of the magnetic medium.[377]

† The magnetism of the nanoparticles of non-magnetic metals is beyond the scope of this review; therefore, we refer only to the most significant publications.[345,346,362]

‡ The plane of the round-shaped magnetic medium is divided into concentric tracks.

§ The width of the transition region for a continuous magnetic medium equals the minimum distance between the regions with opposite directions of magnetisation. For a discrete medium containing magnetic particles in a non-magnetic matrix, the width of the transition layer is equal to the average distance between the particles.

The existence of the transition region between the neighbouring 'bits' with a parallel orientation of magnetic moments (lying in the plane of the magnetic layer) is due to their 'demagnetising' fields and also the scattered field of the recording head. The width of the transition region a can be estimated from the formula

$$a \approx \frac{dM_R D}{H_c}, \quad (11)$$

where d is the distance between the recording head and the magnetic medium surface, M_R is the residual magnetisation, D is the magnetic layer thickness.[377] It can be seen from relation (11) that the greater the coercive force and the smaller the $M_R D$ product, the thinner the transition layer. Thus, these two parameters are the most important characteristics of a material for magnetic recording.

Although an increase in H_c results in a higher recording density, the coercive force should not be too high, because in this case, the recording head would require creation of strong magnetic fields for magnetisation reversal.¶ The characteristic H_c values for modern materials used in magnetic recording amount to $\sim$2500 Œ (for floppy discs)[365] and $\sim$3500 Œ (for hard discs).[378, 379] The recording heads with a higher coercive force should be fabricated from materials with a high saturation magnetisation, for example, $Fe_{65}Co_{35}$.[366] According to forecasts, the use of these heads would make it possible to reach a 500 Gbit in^{-2} density of the vertical recording for a medium containing 5 nm nanoparticles with $H_c \approx 16\,000$ Œ.[366] Among the known magnets, this coercive force is demonstrated only by Nd–Fe–B (14 000 Œ) and Sm_2Co_{17}–$SmCo_5$ (9000 Œ) produced by sintering.[312, 380]

For α-Fe, the record-breaking H_c value at room temperature ($\sim$2700 Œ) was observed for large cylindrical nanoparticles with a length of 250–500 nm and a diameter of 16 nm obtained in a porous aluminium matrix.[109] At low temperatures ($\sim$10 K), the values $H_c \approx 2400$–2600 Œ were found for much smaller particles (3–5 nm).[121] The particles formed were virtually unoxidised on the surface and their forced oxidation resulted in lowering of H_c to 2100 Œ. The coating of α-Fe nanoparticles by rare earth oxides resulted in a decrease of H_c to 1750–1950 Œ.[381] In the researchers' opinion,[382] the reversal of magnetisation of these nanoparticles is a coherent rotation, *i.e.*, it corresponds to the classical Stoner–Wohlfarth model.

The coercive force of a ferromagnetic material is generally described by the formula [381]

$$H_c = \frac{2\alpha K_V}{M_s} - N_{ef} M_s, \quad (12)$$

where α and N_{ef} are the 'microstructure defectiveness' parameter of the material.† The first term in Eqn (12) corresponds to the contribution of the crystalline magnetic anisotropy and the second one is due to the shape anisotropy. For an isolated particle, N_{ef} means the demagnetising factor; in this case, $\alpha = 1$. The theoretical limit for the coercive force is often estimated from the formula $(H_c)_{max} = 2\,K_V/M_s$, which corresponds to a single-domain spherical particle with coherent magnetisation rotation. For iron, nickel and cobalt nanoparticles, the calculated $(H_c)_{max}$ values are $\sim$600, $\sim$200 and $\sim$7500 Œ, respectively.[312] Note that owing to the shape anisotropy [the second term in relation (12)], coercive force values of $\sim$14, $\sim$11 and $\sim$4 kŒ can be obtained for single-domain iron, cobalt and nickel particles,[383] which is markedly greater than $(H_c)_{max}$. Unfortunately, the experimental values of H_c for magnetic materials (including those containing nanocrystallites, nanoparticles or nanograins) rarely exceed 25%–30% of $(H_c)_{max}$ (so-called Brown paradox).[382, 384]

The up-to-date permanent magnets can be assigned to nanocrystalline materials, as they consist of separate magnetic grains usually compacted by either of two methods, by sintering or from a melt. The former method yields multidomain grains with characteristic sizes of 1–20 μm and the latter one furnishes single-domain grains with a size of 10–200 nm.[381] The materials for magnetic recording are also granulated. The use of a single grain as an information bit can be taken as a natural limit to the increase in the magnetic recording density.[378]

For reliable information storage, the magnetic moment of a particle should not change under the action of thermal fluctuations for a long period of time. To this end, the particle size should satisfy the 'superparamagnetic limit' condition according to which the particle should be in the blocked state at room temperature. At $K_V V/300k_B = 40$, the lifetime of a one-particle information bit is $\sim$10 years, while at $K_V V/300k_B = 60$, it is 10^9 years.[378] Thus, a decrease in the particle size requires an increase in their magnetic anisotropy.

It has already been noted that the magnetic anisotropy of nanoparticles includes a number of constituents: crystalline magnetic anisotropy, shape anisotropy, surface anisotropy and other (see Section IX).[310] The crystalline magnetic anisotropy, which makes the major contribution to the magnetic anisotropy, depends on the chemical composition and the crystal structure of the compound. Now the record values for the crystalline magnetic anisotropy‡ (in J m^{-3}) were found for $SmCo_5$ (17.0×10^6), Sm_2Fe_4B (12.0×10^6), $Sm_2Fe_{17}N_3$ (8.9×10^6), PtFe (6.6×10^6), $Pr_2Fe_{14}B$ (5.6×10^6), YCo_5 (5.2×10^6), $Nd_2Fe_{14}B$ (5.0×10^6), CoPt (4.9×10^6), $Sm(Fe_{11}Ti)$ (4.9×10^6) and Sm_2Co_{17} (3.3×10^6).[312]

In the modern hard discs, the CoPt alloy with Cr, Ta, B, Mn additives needed to reduce the interaction between single grains, are used as the magnetic layer. This decreases the length of the transition region, and, as a consequence, leads to a higher recording density. The possibility of using compounds with a higher anisotropy, in particular, compounds of magnetic 3d metals with rare earth metals for magnetic recording is currently under investigation.[335]

Figure 12 *b* shows the dependences of the coercive force of iron nanoparticles on their diameter d at room temperature.[313] Nanoparticles were obtained by radiofrequency sputtering of iron under argon (at a low pressure) followed by annealing in a vacuum. It can be seen that H_c reaches a maximum at $d = 18$ nm, which approximately corresponds to the single-domain structure limit for α-Fe. For $d > 18$ nm, the coercive force decreases according to the law $\sim 1/d$. To interpret the obtained dependence, Chen *et al.*[313] had to assume the presence of the effective surface magnetic anisotropy K_{ef} in a particle

$$K_{ef} = \frac{6K_S}{d}. \quad (13)$$

The parameter K_S found in the study cited [313] was 4×10^{-4} J m^{-2}. In an earlier work [127] in which relation (13) was first proposed, the value $K_S \approx 10^4$ J m^{-2} was found to explain the presence of giant magnetic resonance in α-Fe nanoparticles on a carbon (soot) surface. From the symmetry considerations, the parameter K_S for perfect spherical nanoparticles should be equal to zero;[322] therefore, it can apparently be used to estimate the deviation of the nanoparticle shape from spherical.[127]

Note that the surface anisotropy can serve as a resource for increasing the coercive force of the nanoparticle. Calculation of the influence of the surface anisotropy on H_c for the ellipsoidal maghemite nanoparticles with a longer axis of $\sim$300 nm has shown that for $K_S \approx 2 \times 10^{-2}$ J m^{-2} the coercive force ($\sim$2 kŒ) is twice as great as that for $K_S = 0$.[385] The reasons for the difference between the magnetic properties of nanoparticles

¶ This can be avoided by heating the writable region by a laser beam, which would induce a temporary decrease in the coercive force.

† The microstructure defectiveness means any deviation from the perfect crystal structure inherent in single crystals.[382]

‡ All anisotropy values refer to room temperature.

formed by this class of compound with similar sizes and chemical composition have been discussed.[386]

The temperature dependence of the saturation magnetisation of the α-Fe nanoparticles § coated by a Mg or MgF_2 shell has been studied.[223] Particles with a size of 3–18 nm were prepared by condensation in pentane at 77 K in evacuated quartz tubes. The magnetic moment was measured at a field strength of up to 55 kŒ. The saturation magnetisation for iron nanoparticles with sizes of <7 nm was much lower than that for the bulk iron (~ 220 s cm^3 g^{-1}).¶ The temperature dependence of the magnetisation for all the particles studied corresponded approximately to the law

$$M_s(T) = M_0[1 - BT^b], \tag{14}$$

where B and b are a constant and the Bloch factor, respectively. For the bulk ferromagnets, $b = 1.5$, *i.e.*, the '3/2 law' holds. However, in the study cited,[223] this rule is valid only for particles with the characteristic size $d > 7$ nm, whereas for smaller particles, the parameter b is much lower (thus for the Fe@MgF_2 nanoparticles with $d = 3$ nm, $b = 0.37$). However, for 2–3 nm iron nanoparticles in a SiO_2 matrix, the parameter b was 3/2,[387] while for $MnFe_2O_4$ particles (5–15 nm), $b = 1.5–1.9$ were found.[388] A similar value ($b = 1.9$) was found for the Fe_xC_y nanoparticles ($d = 3.1$ nm).[389] The Bloch constant B for both types of nanoparticles is several orders of magnitude higher than the value for the bulk material. For the Fe@MgF_2 particle with $d < 4$ nm, the B value is an order of magnitude greater than for Fe@Mg. Thus, the magnetic properties of nanoparticles (magnetisation and its temperature variation) depend more crucially on the state of the particle surface than on the particle volume.

A similar conclusion can be drawn from the results of another publication [390] in which three types of samples containing iron nanoparticles were studied. The average diameter of particles obtained by the reduction of oxides was about 20 nm in all samples, but the thickness of the oxide shell surrounding the metallic core was different in different samples. The saturation magnetisation M_s was $\sim 970–1300$ kA m^{-1} at $T = 1.5$ K and decreased as the oxide shell became thicker. Since the magnetisation of iron oxides is lower than that of α-Fe, the decrease in M_s can be attributed to an increase in the proportion of the oxide phase in the particle volume. The different magnetisation levels can also be observed for the same phase with different levels of defectiveness.[386]

The smaller the particles, the more pronounced the effect of the surface layer on the magnetic properties. Figure 15 shows the temperature dependences of the coercive force of iron nanoparticles in the amorphous matrix of aluminium oxide obtained by laser vaporisation in a high vacuum.[391] It can be seen in HRTEM images that the particles are well isolated: the distance between separate elliptical nanoparticles is about 2.5–3.7 nm. The blocking temperatures [determined from the maximum in the $m_{ZFC}(T)$ curve] and the coercive force (at 10 K) depend on the particle diameter.

d /nm	T_b /K	H_c /Œ
4.5–4.7	60	150
7.0–7.8	280	350

For the largest particles, the dependence $H_c(T)$ is described by the relation

$$H_c(T) = H_c(0)\left(1 - \frac{T}{T_b}\right)^{0.5}, \tag{15}$$

derived [321] with the assumption of uniform magnetisation of the nanoparticle (this cannot be the case when a substantial surface layer is present). For smaller particles, the role of the surface is more pronounced and the temperature dependence of the coercive force has a more complicated pattern (see Fig. 15). Similar changes in the course of the $H_c(T)$ curve were observed for nanoparticles (6–8 nm) depending on the oxidation state of the surface.[392]

The estimate of the particle size from the T_b values using the magnetic anisotropy parameter $K_V = 4.8 \times 10^4$ J m^{-3} for the 'bulk' α-Fe almost coincided with the TEM data. The magnetic anisotropy values of α-Fe particles ranged from 8.4×10^4 to 1.6×10^5 J m^{-3}, the K_V value decreased with an increase in the shell thickness. Approximately the same values of magnetic anisotropy for iron nanoparticles were reported in other publications.[121, 221, 392]

The dependence of the coercive force on the temperature provides one more way for the determination of the blocking temperature.[248, 330, 393] Figure 16 shows the temperature dependences of the saturation magnetisation M_s and the coercive force H_c for iron nanoparticles with a diameter of 5–10 nm in a silicon nitride matrix.[393] It can be seen that at low temperatures, the coercive force is well described by relation (15), whereas near T_b (at 100 K), determined by extrapolating $H_c(T^{0.5})$ to zero, the experimental H_c values markedly deviate from those calculated using relation (15). This may be due to the size spread of the particles or with strong interparticle interactions.[248] Note that the dependence of the saturation magnetisation M_s of these particles on temperature is well described by relation (14) [393] over the whole temperature range because inside a nanoparticle, the magnetic order is retained even at $T \gg T_b$. This method for determination of the blocking temperature from the $H_c(T)$ dependence is especially convenient in the case where T_b is much higher than room temperature. This was demonstrated [330] using a cobalt nanoparticle in the polyethylene matrix.

The influence of modification of nanoparticles on their magnetic properties was also studied for 'layered' particles obtained by the reverse micelle method.[394] In the Fe–Au particles consisting of a ferromagnetic iron core (8–10 nm) and an Au shell, a shell thickness of 2–3 nm did not influence the blocking temperature (~ 50 K) or coercive force (~ 400 Œ) to within the

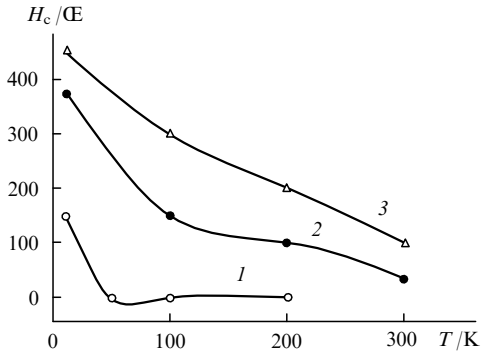


Figure 15. Coercive force H_c *vs.* temperature T for the iron nanoparticles in the Al_2O_3 matrix.[391] Average particle size /nm: 4.5 (*1*), 7.0 (*2*), 9.0 (*3*).

§ The crystal structure of the particles and almost complete absence of oxide phase were proved by powder X-ray diffraction.

¶ The decrease in the saturation magnetisation of ferro-, ferri- and antiferromagnetic nanoparticles with respect to bulk samples, which is observed in experiments almost in all cases, is usually attributed to off-orientation of the atomic magnetic moments in the particle.[121, 386] For iron nanoparticles, the decrease in magnetisation is often correlated with an increase in their oxidation state. The magnetisation of α-Fe nanoparticles was found [119] to be 95 S cm^3 g^{-1} and the magnetisation of Fe_3C nanoparticles obtained in the same way (thermal decomposition of OMC) was 132 S cm^3 g^{-1}. For bulk samples, an opposite relationship between the magnetisations is observed (220 for α-iron and 14 s cm^3 g^{-1} for iron carbide). This inversion was attributed [119] to different susceptibilities of these two types of nanoparticles to oxidation (the α-Fe particles are more oxidised at the surface).

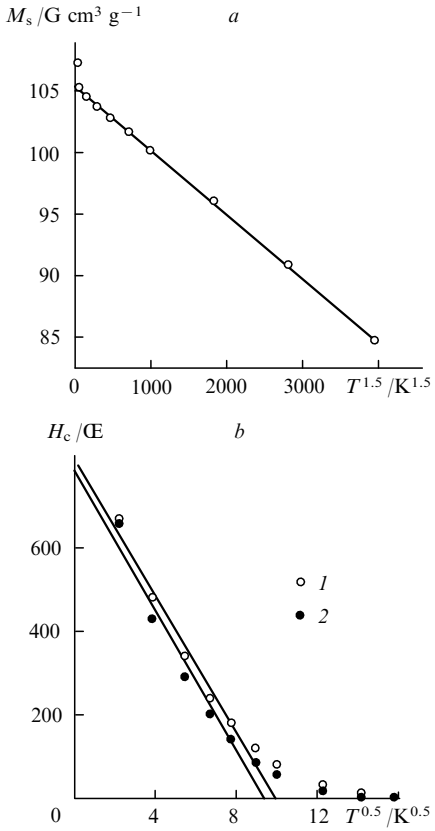


Figure 16. Temperature dependences of the saturation magnetisation M_s (*a*) and coercive force H_c (*b*) for iron nanoparticles (with a diameter of $\sim 5-10$ nm) in the silicon nitride matrix.[393]
The dots show the experimental data and the lines correspond to calculations in terms of the simple spin wave model; dots *1* and *2* correspond to two samples obtained under roughly the same conditions (given for evaluation of reproducibility of the results).

error of measurements. Approximately equal values of T_b and H_c were observed for nano-sized 'onion' particles consisting of an Au core and a Fe shell, which is in turn coated by gold[394] (Fig. 17). On the basis of these data, it was concluded that the contact with gold does not have any noticeable influence on the magnetic properties of Fe nanoparticles.[394] Note that nickel particles (~ 700 nm) coated by palladium (~ 10 nm) demonstrate, conversely, a marked (approximately twofold) growth of the coercive force compared to that of Ni particle devoid of this shell.[395] This might be due to the polarising magnetic effect of palladium atoms with respect to the ferromagnetic matrix.[349]

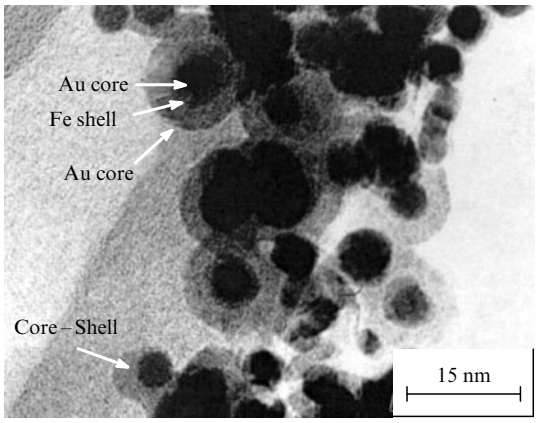


Figure 17. Micrograph of nanoparticles having the 'onion' nanostructure.[394]

XI. Further prospects for the study of magnetic nanoparticles

The fields considered above do not exhaust all possible aspects for the use of magnetic nanoparticles and nanomaterials. In particular, further development of electronics will be largely related to the use of magnetic nanoparticles. This is indicated by numerous works on spinotronics — a new field of electronics dealing with charges and spins.[371, 372, 396] In recent years, considerable attention has been devoted to nanostructures based on magnetic semiconductors.[397] This is due to the prospects opened by the use of not only the charge of the current carriers (electrons and holes) in electronic semiconductor materials but also the magnetic moments directly related to the spin. Spin–orbit coupling may become an important tool for the control of magnetic characteristics in nanostructures.[398] It is expected that the use of the magnetic moment of the charge carrier would markedly extend the scope of the design of new electronic devices,[399] in particular, this would help to solve the problem of non-volative superdense magnetic memory (MRAM — Magnetic Random Access Memory) which is not subject to wear on recording and reading operations.[400, 401]

Several groups of currently studied physical phenomena that may find application in spinotronics can be distinguished:

— dependence of the electrical conductivity of a uniform material on an external magnetic field: anisotropic magnetoresistance (AMR) in thin ferromagnetic films (for example, in permalloy), giant magnetoresistance (CMR) in manganites;

— giant magnetoresistance (GMR) in structures with alternating layers of ferromagnetic and paramagnetic (or antiferromagnetic) metals and granulated structures;

— tunnelling magnetoresistance (Spin Depending Tunnelling) in layered structures containing a paramagnetic (or antiferromagnetic) dielectric between layers of the ferromagnetic metal;

— injection of spin-polarised current carriers from a ferromagnetic material into a non-magnetic one;

— mutual influence of the magnetism and the density of various charge carriers in ferromagnetic semiconductors.

Many magnetoelectronic effects can be interpreted using the Mott–Campbell–Fert model according to which electrons with opposite spins are not mixed in scattering processes in a ferromagnet (two-current model). Since the density of the electron states depends appreciably on the spin, the probability of transition of a conduction electron between regions in a ferromagnet can be varied by changing their magnetisation. Thus the probability of transition between regions with a parallel orientation of the magnetisation vectors is higher (the electrical resistance is, correspondingly, lower) than that for the antiparallel orientation.

Study of the mutual influence of the magnetism and the electrical conductivity in ferromagnetic semiconductors (for example, ZnO–Mn) is a more complicated task. In these systems, the charge carriers are simultaneously mediators of the magnetic interaction between the localised magnetic moments of transition metal ions. By changing the concentration of the charge carriers (for example, by injection), one can control the strength of the magnetic interactions and, hence, the magnetic properties of the material, for example, magnetisation, which can affect the conductor resistivity.

Although the calculations show that the p-type magnetic semiconductors based on ZnO or GaN with 5% Mn and a charge carrier density of 3.5×10^{20} cm^{-3} can form the basis of a material with $T_C > 300$ K,[397] no ferromagnetic semiconductors with a Curie temperature higher than room temperature have been obtained as yet.[402] Numerous accounts concerning overcoming this barrier for various compounds have not been reliably substantiated. The recognised record in this field now belongs to the

GaMnAs semiconductor with $T_C = 110$ K.[403] Ferromagnetism above room temperature was discovered in the Co–ZnO, Fe, Cu–ZnO, V–ZnO and Co–TiO_2 samples (films or bulk samples); however, the obtained data are not perfectly reproducible.[402] The GaMnN, ZnO–Mn and Co–TiO_2 systems and other oxide semiconductors have also been mentioned as promising materials.[403, 404] For nanoparticles of this class, optical studies have been mainly carried out,[405, 406] while their magnetic properties have not been adequately studied.

Yet another problem of spintronics is the appearance of barriers at the boundaries between the layers with different magnetic or electric properties, which prevent realisation of spin–polarisation effects.

Some of the phenomena listed above have already been implemented in the GMR sensors (used, in particular, in the read heads of hard discs)[371] and in the first MRAM chips.[407] However, most of the enormous number of the proposed magnetoelectronic devices (spin filters, diodes, transistors) have not been implemented even on a laboratory scale (for example, Datta-Das spin-field-effect transistor). Some other (for example, the SPICE transistor) have been implemented as laboratory specimens, but not brought to a level of practical application as yet.[408]

The magnetic properties of nanoparticles can also prove quite useful for the design of quantum computers.[409, 410]

A revolutionary achievement is the design of MRAM chips.[401] This type of memory appears to be universal, because it surpasses the existing types of memory (SRAM, DRAM, FLASH, FRAM) in all important characteristics. The MRAM devices are able to compete successfully with hard discs, because at a comparable (in the future) recording density they do not contain moving parts. An especially attractive feature of the MRAM is non-volatility and wear resistance (infinite number of recording and reading events). Currently existing MRAM specimens with a 4 Mbit capacity are based on 0.18 μm CMOS technology with a recording and reading time of 25 ns[411] and magnetic cells based on a magnetic tunnelling transition (MTJ).

To increase the recording density and decrease the current, it is most expedient to use ring magnetic cells.[412, 413] Their advantage over particles of other shapes is in the higher stability of the magnetic eddy configuration due to the absence of boundary distortions of the magnetic structure. This, in particular, can result in a decrease in the superparamagnetic limit, which would allow the use of particles of the minimum possible size. A method for the formation of ring cells on the silicon surface by means of electron lithography and subsequent molecular-beam epitaxy has been proposed.[413] The minimum inner diameter of particles obtained by this technique was 100 nm. A decrease in the particle size to 10 nm can increase the recording density to 400 Gbyte in^{-2}, which is comparable with the recording density limit predicted for hard discs.[412]

Thus, by changing the morphology of nanoparticles (size, shape, composition, core–shell relationship, particle arrangement in the matrix), one can influence their magnetic characteristics. The crystal structure of the core and shell of the particle can be changed by heat treatment (annealing) or other methods of targeted change of nanoparticle properties. Complex particles have been obtained with regions responsible for different properties (for example, the magnetic nucleus and the biologically active shell) clearly separated in space and particles with extremal spatial characteristics (hyperplanar and ultrafine particles — nanowires). In some cases, valuable characteristics appear due to the lucky combination of the properties of particles and the matrix containing them (elastic exchange magnets, see Section IX).[381, 414]

However, the science of magnetic nanoparticles still has a broad spectrum of unsolved theoretical and practical problems. We would like to mention some of them.

A quantitative theory for the internal magnetic structure of nanoparticles is still lacking. The experience of using the simple theory of single-domain particles developed in the main in the mid-20 century by Neel and Brown shows that the model of uniform (collinear) magnetisation of a nanoparticle without splitting into domains does not necessarily correspond to the real situation.[312] Since the solution of the static problem of distribution of magnetic moments in a nanoparticle is rather complicated, it is not surprising that a more complex dynamic task on nanoparticle magnetisation reversal is far from being solved.

One more practical problem which remains unsolved and thus holds up approaching the natural limit of the magnetic memory density is the insufficiently large (much lower than the theoretical value) coercive force of the nanoparticles suitable for the use in hard discs for technological reasons. Apparently, this is due to the complex internal magnetic structure of real nanoparticles.

The design of new highly ordered functional nanostructured composite materials with enhanced properties requires the development of effective methods for nanoparticle organisation. The future research will be aimed at development of the approaches to the synthesis of composite nanoparticles characterised by a set of practically valuable properties (magnetic, electrical, optical). Undoubtedly, magnetic nanoparticles would also find application in other fields, of which nanobiotechnology is expected to become most important. The possible use in biology and medicine, for example, as magnetic biomarkers, anticancer drugs, *etc.*[269, 276, 277]

XII. Conclusion

Magnetic nanoparticles play an important role in the rapidly developing branches of science specialising in the study of objects (existing in nature or, more often, artificially produced) with nano-sized structural blocks. Despite the fact that the extensive use of magnetic nanoparticles (especially for biological applications[415]) and nanomaterials containing them is delayed by the difficulty of producing materials with a narrow size distribution of particles and stable reproducible characteristics and the high cost of their large-scale production,[416] such nanoparticles are used more and more often in the everyday practice. Some companies have already arranged the manufacture of the first samples of nanomaterials. In our opinion, it is time for extensive search for the ways of practical use magnetic nanoparticle.

This reviews was written with the financial support Russian Foundation for Basic Research (Project Nos 02-03-33158, 03-04-48981, 04-03-32090, 04-03-32311, 04-03-32597 and 05-03-32083), the INTAS (Grants 99-1086, 01-483), the International Science and Technology Centre (Project No. 1991), the Russian Science Support Foundation and the programs of the fundamental research of the RAS 'the Fundamental Problems of the Physics and Chemistry of Nanosized Systems and Materials' and 'The Targeted Synthesis of Inorganic Substances with Specified Properties and the Design of Functional Materials Based on Them.'

References

1. M I Baraton *Synthesis, Functionalization, and Surface Treatment of Nanoparticles* (Los-Angeles, CA: Am. Sci. Publ., 2002)
2. R Rosensweig *Ferrohydrodynamics* (Cambridge: Cambridge University Press, 1985)
3. S Taketomi, S Chikazumi *Magnetic Fluids-principle and Application* (Tokio: Nokkan Kogyo Shinbun, 1988)
4. V P Piskorskii, G A Petrakovskii, S P Gubin, I D Kosobudskii *Fiz. Tv. Tela* **22** 1507 (1980)[a]
5. S P Gubin, I D Kosobudskii *Usp. Khim.* **52** 1350 (1983) [*Russ. Chem. Rev.* **52** 766 (1983)]
6. S P Gubin, Yu I Spichkin, G Yu Yurkov, A M Tishin *Russ. J. Inorg. Chem.* **47** (Suppl. 1) 32 (2002)
7. R B Frankel, R P Blakemore, R S Wolfe *Science* **203** 1355 (1979)
8. K O'Grady, R L White, P J Grundy *J. Magn. Magn. Mater.* **177–181** 886 (1998)
9. J P Bucher, L A Bloomfield *Int. J. Mod. Phys. B* **7** 1079 (1993)
10. P Moriarty *Rep. Prog. Phys.* **64** 297 (2001)
11. A I Gusev, A A Rampel' *Nanokristallicheskie Materialy* (Nanocrystalline Materials) (Moscow: Fizmatlit, 2001)

12. I D Morokhov, L I Trusov, S P Chizhik *Ul'tradispersnye Metallicheskie Sredy* (Ultradispersed Metal Media) (Moscow: Atomizdat, 1977)
13. R Turton *The Quantum Dot* (Oxford: Spectrum, 2000)
14. K L Wang, A A Balandin, in *Quantum Dots: Physics and Applications in Optics of Nanostructured Materials* (Eds V A Markel, T F George) (New York: Wiley, 2001) p. 515
15. I P Suzdalev, P I Suzdalev *Usp. Khim.* **70** 203 (2001) [*Russ. Chem. Rev.* **70** 177 (2001)]
16. J Hu, T W Odom, C M Lieber *Acc. Chem. Res.* **32** 435 (1999)
17. S P Gubin *Ros. Khim. Zh.* **44** (6) 23 (2000) [b]
18. S P Gubin, Yu A Koksharov *Neorg. Mater.* **38** 1287 (2002) [c]
19. D M Cox, D J Tevor, R L Whetten, E A Rohlfing, A Kaldor *Phys. Rev. B* **32** 7290 (1985)
20. W A de Heer, P Milani, A Chatelain *Phys. Rev. Lett.* **65** 488 (1990)
21. Yu I Petrov E A Shafranovskii, Yu F Krupyanskii, S V Esin *Dokl. Akad. Nauk* **379** 357 (2001) [d]
22. X G Li, A Chiba, S Takahashi, K Ohsaki *J. Magn. Magn. Mater.* **173** 101 (1997)
23. F Fendrych, L Kraus, O Chayka, P Lobotka, I Vavra, J Tous, V Studnicka, Z Frait *Monatsh. Chem.* **133** 773 (2002)
24. B Martinez, A Roig, X Obradors, E Molins *J. Appl. Phys.* **79** 2580 (1996)
25. Yu I Petrov, E A Shafranovskii *Izv. Akad. Nauk, Ser. Fiz.* **64** 1548 (2000)
26. I M L Billas, A Châtelain, W A de Heer *J. Magn. Magn. Mater.* **168** 64 (1997)
27. I M L Billas, A Châtelain, W A de Heer *Surf. Rev. Lett.* **3** 429 (1996)
28. L B Lueck *Magn. Media Intern. Newslett.* **12** 43 (1991)
29. S M C Borgers *IEEE Trans. Cons. Electr.* CE-34 597 (1988)
30. M Jamet, W Wernsdorfer, C Thirion, D Mailly, V Dupuis, P M'elinon, A P'erez *Phys. Rev. Lett.* **86** 4676 (2001)
31. V A Kuznetsov, A G Lipson, D M Sakov *Zh. Fiz. Khim.* **67** 782 (1993) [e]
32. C Suryanarayana *Prog. Mater. Sci.* **46** 1 (2001)
33. A E Berkowitz, J L Walter *J. Magn. Magn. Mater.* **39** 75 (1983)
34. M F Hansen, K S Vecchio, F T Parker, F E Spada, A E Berkowitz *Appl. Phys. Lett.* **82** 1574 (2003)
35. U A Asanov, S K Sulaimankulova, I E Sakavov, S A Adylov *Sul'fidoobrazovanie v Usloviyakh Elektroerozii Metallov* (Sulfide-formation under Conditions of Metal Electroerosion) (Frunze: Ilim, 1989)
36. J A Becker, R Schafer, J R Festag, J H Wendorff, F Hensel, J Pebler, S A Quaiser, W Helbug, M T Reetz *Surf. Rev. Lett.* **3** 1121 (1996)
37. C Pascal, J L Pascal, F Favier, M L E Moubtassim, C Payen *Chem. Mater.* **11** 141 (1999)
38. T Hyeon *Chem. Commun.* **10** 927 (2003)
39. S Mathur, M Veith, V Sivakov, H Shen, V Huch, U Hartmann, H B Gao *Chem. Vap. Deposition* **8** 277 (2002)
40. T Hyeon, S S Lee, J Park, Y Chung, H B Na *J. Am. Chem. Soc.* **123** 12 798 (2001)
41. A D Pomogailo, A S Rozenberg, I E Uflyand *Nanochastitsy Metallov v Polimerakh* (Metal Nanoparticles in Polymers) (Moscow: Khimiya, 2000)
42. J S Yin, Z L Wang *Nanostruct. Mater.* **10** 845 (1999)
43. K S Suslick, M Fang, T Hyeon *J. Am. Chem. Soc.* **118** 11 960 (1996)
44. T Prozorov, G Kataby, R Prozorov, A Gedanken *Thin Solid Films* **340** 189 (1999)
45. S Sun, C B Murray *J. Appl. Phys.* **85** 4325 (1999)
46. K-L Tsai, J L Dye *J. Am. Chem. Soc.* **113** 1650 (1991)
47. C B Murray, S Sun, W Gaschler, H Doyle, T A Betley, C R Kagan *IBM J. Res. Dev.* **45** 47 (2001)
48. C B Murray, S Sun, H Doyle T A Betley *MRS Bull.* **26** 985 (2001)
49. B G Ershov *Ros. Khim. Zh.* **45** (3) 20 (2001) [b]
50. C Petit, M P Pileni *Appl. Surf. Sci.* **162 – 163** 519 (2000)
51. M P Pileni *Langmuir* **13** 3266 (1997)
52. J P Chen, C M Sorensen, K J Klabunde, G C Hadjipanayis *J. Appl. Phys.* **76** 6316 (1994)
53. C Petit, A Taleb, M P Pileni *J. Phys. Chem. B* **103** 1805 (1999)
54. D R Uhlmann, G Teowee, J Boulton *J. Sol-Gel Sci. Technol.* **8** 1083 (1997)
55. P Bose, S Bid, S K Pradhan, M Pal, D Chakravorty *J. Alloys Compd.* **343** 192 (2002)
56. M Faraday *Philos. Trans. R. Soc. London* **147** 145 (1857)
57. G B Khomutov, S P Gubin, Yu A Koksharov, V V Khanin, A Yu Obidenov, E S Soldatov, A S Trifonov *Mater. Res. Soc. Symp. Proc.* **577** 427 (1999)
58. G B Khomutov, A Yu Obydenov, S A Yakovenko, E S Soldatov, A S Trifonov, V V Khanin, S P Gubin *Mater. Sci. Eng., C* **8 – 9** 309 (1999)
59. G B Khomutov *Colloids Surf., A* **202** 243 (2002)
60. G B Khomutov, S P Gubin, V V Khanin, Yu A Koksharov, A Yu Obydenov, V V Shorokhov, E S Soldatov, A S Trifonov *Colloids Surf., A* **198 – 200** 593 (2002)
61. G B Khomutov, S P Gubin *Mater. Sci. Eng., C* **22** 141 (2002)
62. G B Khomutov, V V Kislov, S A Pavlov, R V Gainutdinov, S P Gubin, A Yu Obydenov, A N Sergeev-Cherenkov, V V Shorokhov, E S Soldatov, A L Tolstikhina, A S Trifonov *Surf. Sci.* **532 – 535** 287 (2003)
63. G B Khomutov *Adv. Colloid Interface Sci.* **111** 79 (2004)
64. G B Khomutov, R V Gainutdinov, S P Gubin, V V Kislov, A A Rakhnyanskaya, A N Sergeev-Cherenkov, A L Tolstikhina *Surf. Sci.* **566 – 568** 396 (2004)
65. T Yamaki, T Yamada, K Asai, K Ishigure *Thin Solid Films* **327 – 329** 586 (1998)
66. T Yamaki, T Yamada, K Asai, K Ishigure, H Shibata *Thin Solid Films* **327 – 329** 581 (1998)
67. X Peng, Y Zhang, J Yang, B Zou, L Xiao, T Li *J. Phys. Chem.* **96** 3412 (1992)
68. Y S Kang, D K Lee, C S Lee, P Stroeve *J. Phys. Chem. B* **106** 9341 (2002)
69. S Sun, C B Murray, D Weller, L Folks, A Moser *Science* **287** 1989 (2000)
70. M Chen, D E Nikles *J. Appl. Phys.* **91** 8477 (2002)
71. T O Ely, C Pan, C Amiens, B Chaudret, F Dassenoy, P Lecante, M J Casanove, A Mosset, M Respaud, J -M Broto *J. Phys. Chem. B* **104** 695 (2000)
72. E V Shevchenko, D V Talapin, H Schnablegger, A Kornowski, O Festin, P Svedlindh, M Haase, H Weller *J. Am. Chem. Soc.* **125** 9090 (2003)
73. N S Sobal, U Ebels, H Möhwald, M Giersig *J. Phys. Chem. B* **107** 7351 (2003)
74. J-I Park, J Cheon *J. Am. Chem. Soc.* **123** 5743 (2001)
75. T Hyeon, Y Chung, J Park, S S Lee, Y W Kim, B H Park *J. Phys. Chem. B* **106** 6831 (2002)
76. J P Chen, K L Lee, C M Sorensen, K J Klabunde, G C Hajipanayis *J. Appl. Phys.* **75** 5876 (1994)
77. N Moumen, M P Pileni *Chem. Mater.* **8** 1128 (1996)
78. N Moumen, M P Pileni *J. Phys. Chem.* **100** 1867 (1996)
79. G Benito, M P Morales, J Requena, V Raposo, M Vazquez, J S Moya *J. Magn. Magn. Mater.* **234** 65 (2001)
80. J Ding, T Tsuzuki, P G McCormick *J. Magn. Magn. Mater.* **177 – 181** 931 (1998)
81. Z J Zhang, Z L Wang, B C Chakoumakos, J S Yin *J. Am. Chem. Soc.* **120** 1800 (1998)
82. Q Chen, Z J Zhang *Appl. Phys. Lett.* **73** 3156 (1998)
83. S Dey, A Roy, J Ghose *J. Appl. Phys.* **90** 4138 (2001)
84. H C Fang, Z Yang, C K Ong, Y Li, C S Wang *J. Magn. Magn. Mater.* **187** 129 (1998)
85. A Vijayalakshimi, N S Gajbhiye *J. Appl. Phys.* **83** 400 (1998)
86. K V P M Shafi, A Gedanken *Nanostruct. Mater.* **12** 29 (1999)
87. G Mendoza-Suarez, J C Corral-Huacuz, M E Contreras-Garcia, H Juarez-Medina *J. Magn. Magn. Mater.* **234** 73 (2001)
88. Q Fang, Y Liu, P Yin, X Li *J. Magn. Magn. Mater.* **234** 366 (2001)
89. S Li, V T John, S H Rachakonda, G C Irvin, G L McPherson, C J O'Connor *J. Appl. Phys.* **85** 5178 (1999)
90. G Ji, S Tang, B Xu, B Gu, Y Du *Chem. Phys. Lett.* **379** 484 (2003)
91. C Pham-Huu, N Keller, C Estournes, G Ehret, J M Greneche, M J Ledoux *Phys. Chem. Chem. Phys.* **5** 3716 (2003)
92. C Liu, A J Rondinone, Z J Zhang *Pure Appl. Chem.* **72** 37 (2000)

93. C J O'Connor, Y S L Buisson, S Li, S Banerjee, R Premchandran, T Baumgartner, V T John, G L McPherson, J A Akkara, D L Kaplan *J. Appl. Phys.* **81** 4741 (1997)
94. S Mathur, H Shen, N Lecerf, A Kjekshus, H Fjellvåg, G F Goya *Adv. Mater.* **14** 1405 (2002)
95. A M Tishin, Yu I Spichkin *The Magnetocaloric Effect and its Applications* (Bristol, Philadelphia: Institute of Physics Publ., 2003)
96. S Thongchant, Y Hasegawa, Y Wada, S Yanagia *Chem. Lett.* **30** 1274 (2001)
97. S Thongchant, Y Hasegawa, Y Wada, S Yanagida *Chem. Lett.* **32** 706 (2003)
98. J A Nelson, L H Bennet, M J Wagner *J. Am. Chem. Soc.* **124** 2979 (2002)
99. D Johnson, P Perera, M J O'Shea *J. Appl. Phys.* **79** 5299 (1996)
100. M J O'Shea, P Perera *J. Appl. Phys.* **85** 4322 (1999)
101. R J Veitch, A Ilmer, W Lenz, V Richter *J. Magn. Magn. Mater.* **193** 279 (1999)
102. F Marty, A Vaterlaus, V Welch, C Stamm, U Maier, D Pescia *J. Appl. Phys.* **85** 6166 (1999)
103. V F Puntes, D Zanchet, C K Erdonmez, A P Alivisatos *J. Am. Chem. Soc.* **124** 12874 (2002)
104. S -J Park, S Kim, S Lee, Z G Khim, K Char, T Hyeon. *J. Am. Chem. Soc.* **122** 8581 (2000)
105. N Cordente, M Respaud, F Senocq, M-J Casanove, C Amiens, B Chaudret *Nano Lett.* **1** 565 (2001)
106. F Dumestre, B Chaudret, C Amiens, M-C Fromen, M-J Casanove, P Renaud, P Zurcher *Angew. Chem., Int. Ed.* **41** 4286 (2002)
107. T Prozorov, R Prozorov, Yu Koltypin, I Felner, A Gedanken *J. Phys. Chem. B* **102** 10165 (1998)
108. A V Okotrub, V L Kuznetsov, A Sharaya, Yu V Butenko, A L Chuvilin, Yu V Shubin, V A Varnek, O Klein, H Pascard *Khim. Inter. Ustoich. Razvit.* **10** 781 (2002) [f]
109. X Bao, F Li, R M Metzger *J. Appl. Phys.* **79** 4866 (1996)
110. X Y Zhang, G H Wen,Y F Chan, R K Zheng, X X Zhang, N Wang *Appl. Phys. Lett.* **83** 3341 (2003)
111. N Yasui, A Imada, T Den *Appl. Phys. Lett.* **83** 3347 (2003)
112. I J Jeon, D-W Kong, D-E Kim, D-H Kim, S-B Choe, S C Shin *Adv. Mater.* **14** 1116 (2002)
113. G H Lee, S H Huh, J W Park, H-C Ri, J W Jeong *J. Phys. Chem. B* **106** 2123 (2002)
114. P Gambardella, A Dallmeyer, K Maiti, M C Malagoli, W Eberhardt, K Kern, C Carbonek *Nature (London)* **416** 301 (2002)
115. Z Zhang, D A Blom, Z Gai, J R Thompson, J Shen, S Dai *J. Am. Chem. Soc.* **125** 7528 (2003)
116. S Sako, K Ohshima, M Sakai, S Bandow *Surf. Rev. Lett.* **3** 109 (1996)
117. M Respaud, J M Broto, H Rakoto, A R Fert, L Thomas, B Barbara, M Verelst, E Snoeck, P Lecante, A Mosset, J Osuna, T Ould Ely, C Amiens, B Chaudret *Phys. Rev. B* **57** 2925 (1998)
118. F Bødker, S Mørup, S W Charles, S Linderoth *J. Magn. Magn. Mater.* **196 – 197** 18 (1999)
119. X Q Zhao, Y Liang, Z Q Hu, B X Liu *J.Appl. Phys.* **80** 5857 (1996)
120. H Y Bai, J L Luo, D Jin, J R Sun *J. Appl. Phys.* **79** 361 (1996)
121. S Gangopadhyay, G C Hadjipanayis, B Dale, C M Sorensen, K J Klabunde, V Papaefthymiou, A Kostikas *Phys. Rev. B* **45** 9778 (1992)
122. L Del Bianco, A Hernando, M Multigner, C Prados, J C Sanchez-Lopez, A Fernandez, C F Conde, A Conde *J. Appl. Phys.* **84** 2189 (1998)
123. M D Bentzon, J van Wonterghem, S Mørup, A Thölen, C J W Koch *Philos. Mag. B* **60** 169 (1989)
124. C Prados, M Multigner, A Hernando, J C Sanchez, A Fernandez, C F Conde, A Conde *J. Appl. Phys.* **85** 6118 (1999)
125. F Bødker, S Mørup, S Linderoth *J. Magn. Magn. Mater.* **140 – 144** 373 (1995)
126. F Bødker, I Chorkendorff, S Mørup *Z. Phys. D.* **40** 152 (1997)
127. F Bødker, S Mørup, S Linderoth *Phys. Rev. Lett.* **72** 282 (1994)
128. A Dyal, K Loos, M Noto, S W Chang, C Spagnoli, K V P M Shafi, A Ulman, M Cowman, R A Gross *J. Am. Chem. Soc.* **125** 1684 (2003)
129. L Del Bianco, A Hernando, E Bonetti, E Navarro *Phys. Rev. B* **56** 8894 (1997)
130. J F Löffler, J P Meier, B Doudin, J-P Ansermet, W Wagner *Phys. Rev. B* **57** 2915 (1998)
131. U Gonser, C J Meechan, A H Muir, H Wiedersich *J. Appl. Phys.* **34** 2373 (1963)
132. S C Abrahams, L Guttman, J S Kasper *Phys. Rev.* **127** 2052 (1962)
133. U Gonser, H G Wagner *Hyperfine Interact.* **24 – 26** 769 (1985)
134. N Saegusa, M Kusunoki *Jpn. J. Appl. Phys.* **29** 876 (1990)
135. T Majima, T Ishii, Y Matsumoto, M Takami *J. Am. Chem. Soc.* **111** 2417 (1989)
136. K Haneda, Z X Zhou, A H Morrish, T Majima, T Miyahara *Phys. Rev. B* **46** 13832 (1992)
137. M W Grinstaff, M B Salamon, K S Suslick *Phys. Rev. B* **48** 269 (1993)
138. J van Wonterghem, S Mørup, S W Charles, S Wells, J Villadsen *Phys. Rev. Lett.* **55** 410 (1985)
139. U Schwertmann, E Murad *Clays Clay Miner.* **31** 277 (1983)
140. M F Hansen, C B Koch, S Mørup *Phys. Rev. B* **62** 1124 (2000)
141. L Zhang, G C Papaefthymiou, J Y Ying *J. Appl. Phys.* **81** 6892 (1997)
142. Y Y Fu, R M Wang, J Xu, J Chen, Y Yan, A V Narlikar, H Zhang *Chem. Phys. Lett.* **379** 373 (2003)
143. J Tang, M Myers, K A Bosnick, L E Brus *J. Phys. Chem. B* **107** 7501 (2003)
144. J Rockenberger, E C Scher, A P Alivisatos *J. Am. Chem. Soc.* **121** 11595 (1999)
145. B Martinez, X Obradors, L Balcells, A Rouanet, C Monty *Phys. Rev. Lett.* **80** 181 (1998)
146. A Rouanet, H Solmon, G Pichelin, C Roucau, F Sibieude, C Monty *Nanostruct. Mater.* **6** 283 (1995)
147. R Janot, D Guerard *J. Alloys Compd.* **333** 302 (2002)
148. T Fried, G Shemer, G Markovich *Adv. Mater.* **13** 1158 (2001)
149. I Nedkov, T Merodiiska, S Kolev, K Krezhov, D Niarchos, E Moraitakis, Y Kusano, J Takada *Monatsh. Chem.* **133** 823 (2002)
150. S Sun, H Zeng *J. Am. Chem. Soc.* **124** 8204 (2002)
151. Y Hou, J Yu, S Gao *J. Mater. Chem.* **13** 1983 (2003)
152. Yu F Krupyanskii, I P Suzdalev *Zh. Eksp. Teor. Fiz.* **67** 736 (1974) [g]
153. R N Panda, N S Gajbhiye, G Balaji *J. Alloys Compd.* **326** 50 (2001)
154. J Ding, W F Miao, E Pirault, R Street, P G McCormick *J. Alloys Compd.* **267** 199 (1998)
155. L Minervini, R W Grimes *J. Phys. Chem. Solids* **60** 235 (1999)
156. K Tokumitsu, T Nasu *Scr. Metall.* **44** 1421 (2001)
157. C J W Koch, M B Madsenm S Mørup *Hyperfine Interact.* **28** 549 (1986)
158. S Mørup, T M Meaz, C B Koch, H C B Hansen *Z. Phys. D* **40** 167 (1997)
159. T Meaz, C B Koch, S Mørup, in *Proceedings of the Conference ICAME-95, Bologna, 1996* Vol. 50, p. 525
160. M B Madsen, S Mørup *Hyperfine Interact.* **42** 1059 (1988)
161. I P Suzdalev *Dinamicheskie Effekty v Gamma-rezonansnoi Spektroskopii* (Dynamical Effects in Mössbauer Spectroscopy) (Moscow: Atomizdat, 1979)
162. J van Wonterghem, S Mørup *J. Phys. Chem.* **92** 1013 (1988)
163. V I Nikolaev, A M Shipilin, E N Shkolnikov, I N Zaharova *J. Appl. Phys.* **86** 576 (1999)
164. T Upadhyay, R V Upadhyay, R V Mehta, V K Aswal, P S Goyal *Phys. Rev. B* **55** 5585 (1997)
165. J van Wonterghem, S Mørup, S W Charles, S Wells *J.Colloid Interface Sci.* **121** 558 (1988)
166. R Rosensweig *Ann. Rev. Fluid Mech.* **19** 437 (1987)
167. K Raj, R F Moskowitz *IEEE Trans. Magn.* MAG-16 358 (1980)
168. H Matsuki, K Murakami *J. Magn. Magn. Mater.* **65** 363 (1987)
169. K Nakatsuka, Y Hama, J Takahashi *J. Magn. Magn. Mater.* **85** 207 (1990)

170. H E Horng, C-Y Hong, S Y Yang, H C Yang *J. Phys. Chem. Solids* **62** 1749 (2001)
171. J Liu, E M Lawrence, A Wu, M L Ivey, G A Flores, K Javier, J Bibette, J Richard *Phys. Rev. Lett.* **74** 2828 (1995)
172. V Berejnov, Yu Raikher, V Cabuil, J-C Bacri, R Perzynski *J. Colloid Interface Sci.* **199** 215 (1998)
173. X G Li, T Murai, T Saito, S Takahashi *J. Magn. Magn. Mater.* **190** 277 (1998)
174. X G Li, A Chiba, S Takahashi *J. Magn. Magn. Mater.* **170** 339 (1997)
175. A M Afanas'ev, I P Suzdalev, M Ya Gen, V I Gol'danskii, V P Korneev, E A Manykin *Zh. Eksp. Teor. Fiz.* **58** 115 (1970) [g]
176. B K Rao, S R de Debiaggi, P Jena *Phys. Rev. B* **64** 024418 (2001)
177. E Shevchenko, D Talapin, A Kornowski, F Wiekhorst, J Kltzler, M Haase, A Rogach, H Weller *Adv. Mater.* **14** 287 (2002)
178. H Zeng, J Li, J P Liu, Z L Wang, S Sun *Nature (London)* **420** 395 (2002)
179. M Kiwi *J. Magn. Magn. Mater.* **234** 584 (2001)
180. A E Berkowitz, K Takano *J. Magn. Magn. Mater.* **200** 552 (1999)
181. W H Meiklejohn, C P Bean *Phys. Rev. B* **102** 1413 (1956)
182. D L Peng, K Sumiyama, T Hihara, S Yamamuro, T J Konno *Phys. Rev. B* **61** 3103 (2000)
183. M Sato, S Kohiki, Y Hayakawa, Y Sonda, T Babasaki, H Deguchi, M Mitome *J. Appl. Phys.* **88** 2771 (2000)
184. J Feng, H C Zeng *Chem. Mater.* **15** 2829 (2003)
185. S R Hoon, M Kilner, G J Russel, B K Tanner *J. Magn. Magn. Mater.* **39** 107 (1983)
186. D deCaro, J S Bradley *Langmuir* **13** 3067 (1997)
187. K-L Tsai, J-L Dye *Chem. Mater.* **5** 540 (1993)
188. D J Sellmyer, M Yu, R D Kirby *Nanostruct. Mater.* **12** 1021 (1999)
189. H Kitahara, T Oku, T Hirano, K Suganuma *Diamond Relat. Mater.* **10** 1210 (2001)
190. M E McHenry, S Subramoney, in *Fullerenes. Chemistry, Physics, and Technology* (New York: Wiley-Interscience, 2000) p. 839
191. J Jiao, S Seraphin, X Wang, J C Withers *J. Appl. Phys.* **80** 103 (1996)
192. Y Saito, J Ma, J Nakashima, M Masuda *Z. Phys. D* **40** 170 (1997)
193. E M Brunsman, R Sutton, E Bortz, S Kirkpatrick, K Midelfort, J Williams, P Smith, M E McHenry, S A Majetich, J O Artman, M DeGraef, S W Staley *J. Appl. Phys.* **75** 5882 (1994)
194. J -H Yu, C -W Lee, S -S Im, J -S Lee *Rev. Adv. Mater. Sci.* **4** 55 (2003)
195. Y Kobayashi, M Horie, M Konno, B Rodriguez-Gonzalez, L M Liz-Marzan *J. Phys. Chem. B* **107** 7420 (2003)
196. T Kinoshita, S Seino, K Okitsu, T Nakayama, T Nakagawa, T A Yamamoto *J. Alloys Compd.* **359** 46 (2003)
197. K Landfester, L P Ramirez *J. Phys.: Condens. Matter* **15** 1345 (2003)
198. L Fu, V P Dravid, D L Johnson *J. Appl. Surf. Sci.* **181** 173 (2001)
199. E V Shevchenko, D V Talapin, A L Rogach, A Kornowski, M Haase, H Weller *J. Am. Chem. Soc.* **124** 11480 (2002)
200. L Guo, Z Wu, T Liu, S Yang *Physica E (Amsterdam)* **8** 199 (2000)
201. T Liu, L Guo, Y Tao, T D Hu, Y N Xie, J Zhang *Nanostruct. Mater.* **11** 1329 (1999)
202. J-C Bacri, R Perzynski, D Salin, V Cabuil, R Massart *J. Magn. Magn. Mater.* **85** 27 (1990)
203. F L Calderon, T Stora, O M Monval, P Poulin, J Bibette *Phys. Rev. Lett.* **72** 2959 (1994)
204. C Menager, V Cabuil *Colloid Polym. Sci.* **272** 1299 (1994)
205. C Menager, V Cabuil *J. Colloid Interface Sci.* **169** 251 (1995)
206. J-C Bacri, V Cabuil, S Menager, R Perzynski *Europhys. Lett.* **33** 235 (1996)
207. P Fabre, C Cassagrande, M Veyssie, V Cabuil, R Massart *Phys. Rev. Lett.* **64** 539 (1990)
208. C Menager, V Cabuil, L Belloni, M Dubois, Th Zemb *Langmuir* **12** 3516 (1996)
209. C Binns *Surf. Sci. Rep.* **44** 1 (2001)
210. M Heemeier, A F Carlsson, M Naschitzki, M Schmal, M Bäumer, H-J Freund *Angew. Chem., Int. Ed.* **41** 4073 (2002)
211. V Dupuis, J Tuaillon, B Prevel, A Perez, P Melinon, G Guiraud, F Parent, L B Steren, R Morel, A Barthelemy, A Fert, S Mangin, L Thomas, W Wernsdorfer, B Barbara *J. Magn. Magn. Mater.* **165** 42 (1997)
212. S Honda, F A Modine, A A Meldrum, J D Budai, T E Haynes, L A Boatner *Appl. Phys. Lett.* **77** 711 (2000)
213. S Sun, S Anders, H F Hamann, J-U Thiele, J E E Baglin, T Thomson, E E Fullerton, C B Murray, B D Terris *J. Am. Chem. Soc.* **124** 2884 (2002)
214. F J Lázaro, J L Garcia, G V Schünemann, Ch H Butzlaff, A Larrea, M A Zaluska-Kotur, *Phys. Rev. B* **53** 13 934 (1996)
215. Z Zhang, Y D Zhang, W A Hines, J I Budnick, W M H Sachtler *J. Am. Chem. Soc.* **114** 4843 (1992)
216. H M Ziethen, H Winkler, A Schiller, V Schünemann, A X Trautwein, A Quazi, F Schmidt *Catal. Today* **8** 427 (1991)
217. K Lazar, H K Beyer, G Onyesnyak, B J Jönsson, L K Varga, S Pronier *Nanostruct. Mater.* **12** 155 (1999)
218. C Garcia, Y Zhang, F DiSalvo, U Wiesner *Angew. Chem., Int. Ed.* **42** 1526 (2003)
219. F Jiao, B Yue, K Zhu, D Zhao, H He *Chem. Lett.* **32** 770 (2003)
220. Y Hayakawa, S Kohiki, M Sato, Y Sonda, T Babasaki, H Deguchi, A Hidaka, H Shimooka, S Takahashi *Physica E (Amsterdam)* **9** 250 (2001)
221. S Roy, B Roy, D Chakravorty *J. Appl. Phys.* **79** 1642 (1996)
222. D Sunil, J Sokolov, M H Rafailovich, H D Gafney, X Duan *Inorg. Chem.* **32** 4489 (1993)
223. F Bentivegna, J Ferre, M Nyvlit, J P Jamet, D Imhoff, M Canva, A Brun, P Veillet, S Visnovsky, F Chaput, J P Boilot *J. Appl. Phys.* **83** 7776 (1998)
224. F Bentivegna, M Nyvlit, J Ferre, J P Jamet, A Brun, S Visnovsky, R Urban *J. Appl. Phys.* **85** 2270 (1999)
225. A K Santra, D W Goodman *J. Phys.: Condens. Matter* **14** 31 (2002)
226. K S Suslick, T Hyeon, M Fang *Chem. Mater.* **8** 2172 (1996)
227. A A Khassin, V F Anufrienko, V N Ikorskii, L M Plysova, G N Kustova, T V Larina, I Yu Molina, V N Parmon *Phys. Chem. Chem. Phys.* **4** 4236 (2002)
228. X Chuanyun, Y Jinlong, D Kaiming, W Delin *Phys. Rev. B* **55** 3677 (1997)
229. L Dimesso, G Miehe, H Fuess, H Hahn *J. Magn. Magn. Mater.* **191** 162 (1999)
230. M Jamet, M Negrier, V Dupuis, J Tuaillon-Combes, P Mélinon, A Perez, W Wernsdorfer, B Barbara, B Baguenard *J. Magn. Magn. Mater.* **237** 293 (2001)
231. S Mørup, S Linderoth, J Jacobsen, M Holmbland *Hyperfine Interact.* **69** 489 (1991)
232. G N Glavee, K Easom, K J Klabunde, C M Sorensen, G C Hadjipanayis *Chem. Mater.* **4** 1360 (1992)
233. D Zhang, K J Klabunde, C M Sorensen, G C Hadjipanayis *Phys. Rev. B* **58** 14167 (1998)
234. F Budker, S Murup *Nucl. Instrum. Methods Phys. Res. Sect. B* **108** 413 (1996)
235. S P Gubin, I D Kosobudskii *Dokl. Akad. Nauk SSSR, Ser. Khim.* **272** 1155 (1983) [d]
236. I D Kosobudskii, L V Kashkina, S P Gubin, G A Petrakovskii, V P Pienorskii, N M Svirepaya *Vysokomol. Soedin.* **27** 689 (1985) [h]
237. R F Ziolo, E P Giannelis, B A Weinstein, M P O'Horo, B N Ganguly, V Mehrotra, M W Russell, D R Huffman *Science* **257** 219 (1992)
238. T Ji, H Shi, J Zhao, Y Zhao *J. Magn. Magn. Mater.* **212** 189 (2000)
239. A M Testa, S Foglia, L Suber, D Fiorani, L Casas, A Roig, E Molins, J M Greneche, J Tejada *J. Appl. Phys.* **90** 1534 (2001)
240. P C Morais, R B Azevedo, D Rabelo, E C Lima *Chem. Mater.* **15** 2485 (2003)
241. J K Vassiliou, V Mehrotra, M W Russell, E P Giannelis, R D McMichael, R D Shull, R F Ziolo *J. Appl. Phys.* **73** 5109 (1993)

242. D Prodan, V V Grecu, M N Grecu, E Tronc, J P Jolivet *Meas. Sci. Technol.* **10** 41 (1999)
243. J Osuna, D de Caro, C Amiens, B Chaudret, E Snoeck, M Respaud, J M Broto, A R Fert *J. Phys. Chem.* **100** 14571 (1996)
244. D Zitoun, C Amiens, B Chaudret, M-C Fromen, P Lecante, M-J Casanove, M Respaud *J. Phys. Chem. B* **107** 6997 (2003)
245. J Ramos, A Millan, F Palacio *Polymer* **41** 8461 (2000)
246. T W Smith, D Wychick *J. Phys. Chem.* **84** 1621 (1980)
247. D L Leslie-Pelecky, X Q Zhang, R D Rieke *J. Appl. Phys.* **79** 5312 (1996)
248. A K Giri *J. Appl. Phys.* **81** 1348 (1997)
249. S P Gubin *Colloids Surf., A* **202** 155 (2002)
250. S P Gubin, M S Korobov, G Yu Yurkov, A K Tsvetnikov, V M Buznik *Dokl. Akad. Nauk, Ser. Khim.* **388** 493 (2003) [d]
251. S P Gubin, G Yu Yurkov, M S Korobov, Yu A Koksharov, A V Kozinkin, I V Pirog, S V Zubkov, V V Kitaev, D A Sarichev, V M Bouznik, A K Tsvetnikov *Acta Mater.* **53** 1407 (2005)
252. T O Ely, C Amiens, B Chaudret, E Snoeck, M Verelst, M Respaud, J-M Broto *J. Chem. Mater.* **11** 526 (1999)
253. H Liu, X Ge, Y Zhu, X Xu, Z Zhang, M Zhang *Mater. Lett.* **46** 205 (2000)
254. C Castro, J Ramos, A Millan, J Gonzalez-Calbet, F Palacio *Chem. Mater.* **12** 3681 (2000)
255. V Yu Petukhov, F G Vagizov, M I Ibragimova, N R Khabibullina, E P Zheglov, S V Shulyndin, in *Tezisy Mezhdunarodnoi Konferentsii 'Effekt Messbauera: Magnetizm. Materialovedenie, Gamma-optika', Kazan', 2000* [Abstracts of Reports of the International Conference 'Mössbauer Effect: Magnetism. Materials Science, Gamma Optics', Kazan', 2000] p. 155
256. I W Hamley *Nanotechnology* **14** 39 (2003)
257. B H Sohn, R E Cohen, G C Papaefthymiou *J. Magn. Magn. Mater.* **182** 216 (1998)
258. I Šafařik, M Šafařiková *Monatsh. Chem.* **133** 737 (2002)
259. M Allen, D Willits, J Mosolf, M Young, T Douglas *Adv. Mater.* **14** 1562 (2002)
260. E C Theil *Annu. Rev. Ser. Biochem.* **56** 289 (1987)
261. P M Harrison, A Treffy, T H Lilley *J. Inorg. Biochem.* **27** 287 (1986)
262. G C Ford, P M Harrison, D W Rice, M A Smith, A Treffry, J L White, J Yariv *Philos. Trans. R. Soc. London B* **304** 551 (1984)
263. E R Bauminger, P M Harrison, D Hechel, I Nowik, A Treffry *Biochim. Biophys. Acta* **1118** 48 (1991)
264. S M Heald, E A Stern, B Bunker, E M Holt, S L Holt *J. Am. Chem. Soc.* **101** 67 (1979)
265. J Yang, K Takeyasu, A P Somlyo, Z Shao *Ultramicroscopy* **45** 199 (1992)
266. S A Makhlouf, F T Parker, A E Berkowitz *Phys. Rev. B* **55** 14717 (1997)
267. F C Meldrum, B R Heywood, S Mann *Science* **257** 522 (1992)
268. D P E Dickson *J. Magn. Magn. Mater.* **203** 46 (1999)
269. U Hafeli, W Schutt, J Teller, M Zborowski *Scientific and Clinical Applications of Magnetic Carriers* (New York: Plenum, 1997)
270. M Fang, P S Grant, M J McShane, G B Sukhorukov, V O Golub, Y M Lvov *Langmuir* **18** 6338 (2002)
271. M N Antipina, R V Gainutdinov, A A Rachnyanskaya, A L Tolstikhina, T V Yurova, G B Khomutov *Surf. Sci.* **532–535** 1025 (2003)
272. M N Antipina, R V Gainutdinov, A A Rakhnyanskaya, A N Sergeev-Cherenkov, A L Tolstikhina, T V Yurova, V V Kislov, G B Khomutov *Biofizika* **48** 998 (2003) [i]
273. G B Khomutov, M N Antipina, A N Sergeev-Cherenkov, T V Yurova, A A Rakhnyanskaya, V V Kislov, R V Gainutdinov, A L Tolstikhina *Mater. Sci. Eng., C* **23** 903 (2003)
274. G B Khomutov, V V Kislov, M N Antipina, R V Gainutdinov, S P Gubin, A Yu Obydenov, S A Pavlov, A A Rakhnyanskaya, A N Sergeev-Cherenkov, E S Soldatov, D B Suyatin, A L Tolstikhina, A S Trifonov, T V Yurova *Microelectron. Eng.* **69** 373 (2003)
275. S Mornet, A Vekris, J Bonnet, E Duguet, F Grasset, J-H Choy, J Portier *Mater. Lett.* **42** 183 (2000)
276. U Hafeli, G J Pauer *J. Magn. Magn. Mater.* **194** 76 (1999)
277. M H Sousa, J C Rubim, P G Sobrinho, F A Tourinho *J. Magn. Magn. Mater.* **225** 67 (2001)
278. F Caruso *Adv. Mater.* **13** 11 (2001)
279. Z G M Lacava, R B Azevedo, E V Martins, L M Lacava, M L L Freitas, V A P Garcia, C A Rebula, A P C Lemos, M H Sousa, F A Tourinho, M F DaSilva, P C Morais *J. Magn. Magn. Mater.* **201** 431 (1999)
280. P Vavassori, E Angeli, D Bisero, F Spizzo, F Ronconi *Appl. Phys. Lett.* **79** 2225 (2001)
281. J B Kortright, D D Awschalom, J Stlhr, S D Bader, Y U Idzerda, S S P Parkin, I K Schuller, H-C Siegmann *J. Magn. Magn. Mater.* **207** 7 (1999)
282. M Murayama, J M Howe, H Hidaka, S Takaki *Science* **295** 2433 (2002)
283. S Mürup, in *Mössbauer Spectroscopy Applied to Inorganic Chemistry* Vol. 2 (Ed. G J Long) (New York: Plenum, 1987) p. 89
284. S Mürup, J A Dumestic, H Topsüe, in *Applications of Mössbauer Spectroscopy* Vol. 2 (Ed. R L Cohen) (New York: Academic Press, 1980) p. 1
285. S Mürup, in *Magnetic Properties of Fine Particles* (Eds J L Dormann, D Fiorani) (Amsterdam: Elsevier, 1992) p. 125
286. S P Gubin *Khimiya Klasterov. Osnovy Klassifikatsii i Stroeniya* (The Chemistry of Clusters. Foundation of Classification and Structure) (Moscow: Nauka, 1987)
287. A V Kozinkin, O V Sever, S P Gubin, A T Shuvaev, I A Dubovtsev *Neorg. mater.* **30** 678 (1994) [c]
288. E I Kondorskii *Zh. Eksp. Teor. Fiz.* **10** 420 (1940) [g]
289. E Kondorskii *Dokl. Akad. Nauk SSSR* **82** 365 (1952) [d]
290. C Kittel *Phys. Rev.* **70** 965 (1946)
291. E C Stoner, E P Wohlfarth *Philos. Trans. R. Soc. London, A* **240** 599 (1948)
292. L Néel *C.R. Hebd. Seances Acad. Sci.* **224** 1488 (1947)
293. L Néel *C.R. Hebd. Seances Acad. Sci.* **224** 1550 (1947)
294. L Néel *C.R. Hebd. Seances Acad. Sci.* **228** 664 (1949)
295. L Néel *C.R. Hebd. Seances Acad. Sci.* **5** 99 (1949)
296. W F Brown Jr *J. Appl. Phys.* **29** 470 (1958)
297. W F Brown Jr *J. Appl. Phys.* **30** 130 (1959)
298. W F Brown Jr *J. Appl. Phys.* **34** 1319 (1963)
299. W F Brown Jr *Phys. Rev. B* **130** 1677 (1963)
300. I Antik, T Kubyshkina *Uchen. Zap. Mosk. Univ.* **11** 143 (1934)
301. V H Gottschalk *Physics* **6** 127 (1935)
302. W C Elmor *Phys. Rev.* **54** 309 (1938)
303. W C Elmor *Phys. Rev.* **54** 1092 (1938)
304. F Bitter, A Kaufmann, C Starr, S Pan *Phys. Rev.* **60** 134 (1941)
305. A Mayer, E Vogt *Z. Naturforsch., A* 334 (1952)
306. W Heukolom, J J Broeder, L L Van Reijen *J. Chim. Phys.* **51** 51 (1954)
307. C P Bean *J. Appl. Phys.* **26** 1381 (1955)
308. C P Bean, I S Jacobs *J. Appl. Phys.* **27** 1448 (1955)
309. E F Kneller, F E Luborsky *J. Appl. Phys.* **34** 656 (1963)
310. J L Dormann, D Fiorani, E Tronc *Adv. Chem. Phys.* **98** 283 (1997)
311. D Leslie-Pelecky, R D Rieke *Chem. Mater.* **8** 1770 (1996)
312. R Skomski *J. Phys.: Condens. Matter* **15** R841 (2003)
313. C Chen, O Kitakami, Y Shimada *J. Appl. Phys.* **84** 2184 (1998)
314. R D Gomez, T V Luu, A O Park, K J Kirk, J N Chapman *J. Appl. Phys.* **85** 6163 (1999)
315. H Koo, T V Luu, R D Gomez, V V Metlushko *J. Appl. Phys.* **87** 5114 (2000)
316. W Wernsdorfer, K Hasselbach, D Mailly, B Barbara, A Benoit, L Thomas, G Suran *J. Magn. Magn. Mater.* **145** 33 (1995)

317. W Wernsdorfer, D Mailly, A Benoit *J. Appl. Phys.* **87** 5094 (2000)
318. J I Martìn, J Nogués, K Liu, J L Vicent, I K Schuller *J. Magn. Magn. Mater.* **256** 449 (2003)
319. B Sadeh, M Doi, T Shimizu, M J Matsui *J. Magn. Soc. Jpn.* **24** 511 (2000)
320. V I Nikolaev, A M Shipilin *Fiz. Tv. Tela* **45** 1029 (2003) [a]
321. I S Jacobs, C P Bean, in *Magnetism* Vol. 3 (Eds G T Rado, H Suhl) (New York: Academic Press, 1963) p. 271
322. X Batlle, A Labarta *J. Phys. D* **35** R15 (2002)
323. S Chikazumi *Physics of Ferromagnetism, Magnetic Characteristics and Engineering Applications* Vol. 2 (Tokyo: Shokabo Publ. Co., 1984)
324. W T Coffey, D S Crothers, J L Dormann, L J Geoghegan, Yu P Kalmykov, J T Waldron, A W Wickstead *J. Magn. Magn. Mater.* **145** L263 (1995)
325. W T Coffey, D S Crothers, J L Dormann, L J Geoghegan, Yu P Kalmykov, J T Waldron, A W Wickstead *Phys. Rev. B* **52** 15951 (1995)
326. E P Wohlfarth *J. Phys.* **10** 241 (1980)
327. L E Wenger, J D Mydosh *Phys. Rev. B* **29** 4156 (1984)
328. R W Chantrell, K O'Grady, in *Applied Magnetism* (Eds R Gerber, C D Wright, G Asti) (Dordrecht, Boston, London: Kluwer Academic, 1992) p. 113
329. G Yu Yurkov, S P Gubin, D A Pankratov, Yu A Koksharov, A V Kozinkin, Yu I Spichkin, T I Nedoseikina, I V Pirog, V G Vlasenko *Neorg. Mater.* **38** 186 (2002) [c]
330. S P Gubin, Yu I Spichkin, Yu A Koksharov, G Yu Yurkov, A V Kozinkin, T A Nedoseikina, V G Vlasenko, M S Korobov, A M Tishin *J. Magn. Magn. Mater.* **265** 234 (2003)
331. R Sappey, E Vincent, N Hadacek, F Chaput, J P Boilot, D Zins *Phys. Rev. B* **56** 14 551 (1997)
332. M F Hansen, S Mørup *J. Magn. Magn. Mater.* **203** 214 (1999)
333. R W Chantrell, E P Wohlfarth *Phys. Status Solidi A* **91** 619 (1985)
334. P A Joy, P S A Kumar, S K Date *J. Phys.: Condens. Matter.* **10** 11049 (1998)
335. J Jakubowicz, M Giersig *J. Alloys Compd.* **349** 311 (2003)
336. G C Hadjipanayis *J. Magn. Magn. Mater.* **200** 373 (1999)
337. J Fidler, T Schrefl *J. Magn. Magn. Mater.* **177 – 181** 970 (1998)
338. R Fischer, H Kronmuller *J. Magn. Magn. Mater.* **184** 166 (1998)
339. R H Kodama, A E Berkowitz, E J McNiff, S Foner *Phys. Rev. Lett.* **77** 394 (1996)
340. R H Kodama, A E Berkowitz, E J McNiff, S Foner *J. Appl. Phys.* **81** 5552 (1997)
341. O Iglesias, A Labarta *Phys. Rev. B* **63** 184416 (2001)
342. H Kachkachi, M Noguès, E Tronc, D A Garanin *J. Magn. Magn. Mater.* **221** 158 (2000)
343. P V Hendriksen, S Linderoth, P-A Lindgsrd *Phys. Rev. B* **48** 7259 (1993)
344. F Liu, M R Press, S N Khanna, P Jena *Phys. Rev. B* **39** 6914 (1989)
345. S-K Ma, J T Lue *Solid State Commun.* **97** 979 (1996)
346. T Taniyama, E Ohta, T Sato *Physica B* **237** 286 (1997)
347. T Nakano, Y Ikemoto, Y Nozue *J. Magn. Magn. Mater.* **226 – 230** 238 (2001)
348. B V Reddy, S N Khanna, B I Dunlap *Phys. Rev. Lett.* **70** 3323 (1993)
349. S V Vonsovskii *Magnetizm* (Magnetism) (Moscow: Nauka, 1971)
350. K O'Grady, R W Chantrell, in *Magnetic Properties of Fine Particles* (Eds J L Dormann, D Fiorani) (Amsterdam: Elsevier, 1992) p. 93
351. J L Dormann, F D'Orazio, F Lucari, E Tronc, P Prené, J P Jolivet, D Fiorani, R Cherkaoui, M Noguès *Phys. Rev. B* **53** 14291 (1996)
352. E P Wohlfarth *J. Magn. Magn. Mater.* **39** 39 (1983)
353. J Geshev, M Mikhov, J E Schmidt *J. Appl. Phys.* **85** 7321 (1999)
354. J L Dormann, L Bessais, D Fiorani *J. Phys. C: Solid State Phys.* **21** 2015 (1988)
355. M F Hansen, S Mørup *J. Magn. Magn. Mater.* **184** 262 (1998)
356. J Dai, J-Q Wang, C Sangregorio, J Fang, E Carpenter, J Tang *J. Appl. Phys.* **87** 7397 (2000)
357. S Mørup *Europhys. Lett.* **28** 671 (1994)
358. W Luo, S R Nagel, T F Rosenbaum, R E Rosensweig *Phys. Rev. Lett.* **67** 2721 (1991)
359. P Allia, M Coisson, P Tiberto, F Vinai, M Knobel, M A Novak, W C Nunes *Phys. Rev. V* **64** 144420 (2001)
360. D C Douglass, J P Bucher, D B Haynes, L A Bloomfield, in *Physics and Chemistry of Finite Systems: from Cluster to Crystals* Vol. 1 (Eds P Jena, S N Khanna, B K Rao) (Amsterdam: Kluwer Academic, 1992) p. 759
361. D C Douglass, J P Bucher, L A Bloomfield *Phys. Rev. Lett.* **68** 1774 (1992)
362. Y B Pithawalla, M S El-Shall, S C Deevi, V Strom, K V Rao *J. Phys. Chem. B* **105** 2085 (2001)
363. J D Aiken, R G Finke *J. Mol. Catal. A: Chem.* **145** 1 (1999)
364. F J Himpsel, J E Ortega, G J Mankey, R F Willis *Adv. Phys.* **47** 511 (1998)
365. K O'Grady, H Laider *J. Magn. Magn. Mater.* **200** 616 (1999)
366. R M White *J. Magn. Magn. Mater.* **226 – 230** 2042 (2001)
367. Y N Konan, R Gurny, E Allemann *J. Photochem. Photobiol.* **66** 89 (2002)
368. M Shinkai *J. Biosci. Bioeng.* **94** 606 (2002)
369. H Kronmüller, R Fischer, M Bachmann, T Leineweber *J. Magn. Magn. Mater.* **203** 12 (1999)
370. M E McHenry, D E Laughlin *Acta Mater.* **48** 223 (2000)
371. G A Prinz *J. Magn. Magn. Mater.* **200** 57 (1999)
372. D D Awschalom, N Samarth *J. Magn. Magn. Mater.* **200** 130 (1999)
373. F M Peeters, J DeBoeck, in *Hybrid Magnetic Semiconductor Nanostructures. Handbook of Nanostructured Materials and Nanotechnology* Vol. 3 (Ed. H S Nalwa) (New York: Academic Press, 2000) p. 345
374. J Shen, J Kirschner *Surf. Sci.* **500** 300 (2002)
375. D Das, M Pal, E Di Bartolomeo, E Traversa, D Chakravorty *J. Appl. Phys.* **88** 6856 (2000)
376. W J Parak, D Gerion, T Pellegrino, D Zanchet, C Micheel, S C Williams, R Boudreau, M A Le Gros, C A Larabell, A P Alivisatos *Nanotechnology* **14** 15 (2003)
377. B K Middleton *J. Magn. Magn. Mater.* **193** 24 (1999)
378. D E Speliotis *J. Magn. Magn. Mater.* **193** 29 (1999)
379. J Li, M Mirzamaani, X Bian, M Doerner, S Duan, K Tang, M Toney, T Arnoldussen, M Madison *J. Appl. Phys.* **85** 4286 (1999)
380. D Jiles, in *Introduction to Magnetism and Magnetic Material* (London: Chapman and Hall, 1996)
381. F Li, X Bao, R M Metzger, M Carbucicchio *J. Appl. Phys.* **79** 4869 (1996)
382. D Goll, H Kronmüller *Naturwissenschaften* **87** 423 (2000)
383. A H Morrish *The Physical Principles of Magnetism* (New York, London, Sydney: Wiley, 1965)
384. J M D Coey *J. Magn. Magn. Mater.* **140 – 144** 1041 (1995)
385. K Zhang, D R Fredkin *J. Appl. Phys.* **79** 5762 (1996)
386. P Morales, M Andres-Vergés, S Veintemillas-Verdaguer, M I Montero, C J Serna *J. Magn. Magn. Mater.* **203** 146 (1999)
387. G Xiao, C L Chien *J. Appl. Phys.* **61** 3308 (1987)
388. J P Chen, C M Sorensen, K J Klabunde, G C Hadjipanayis, E Devlin, A Kostikas *Phys. Rev. B* **54** 9288 (1996)
389. S Linderoth, L Balcells, A Laborta, J Tejada, P V Hendriksen, S A Sethi *J. Magn. Magn. Mater.* **124** 269 (1993)
390. D L Hou, X-F Nie, H-L Luo *J. Magn. Magn. Mater.* **188** 169 (1998)
391. D Kumar, J Narayan, A V Kvit, A K Sharma, J Sankar *J. Magn. Magn. Mater.* **232** 161 (2001)
392. B J Jönsson, T Turkki, V Ström, M S El-Shall, K V Rao *J. Appl. Phys.* **79** 5063 (1996)
393. L Maya, J R Thompson, K J Song, R J Warmack *J. Appl. Phys.* **83** 905 (1998)
394. C J O'Connor, V Kolesnichenko, E Carpenter, C Sangregorio, W Zhou, A Kumbhar, J Sims, F Agnoli *Synth. Met.* **122** 547 (2001)
395. Y Otani, H Miyajima, M Yamaguchi, Y Nazaki, T Manago, A J Fagan, J M D Coey *J. Magn. Magn. Mater.* **140 – 144** 403 (1995)
396. H Ohno *Science* **281** 951 (1998)

397. T Dietl *J. Appl. Phys.* **89** 7437 (2001)
398. E I Rashba, A L Efros *Phys. Rev. Lett.* **91** 126405 (2003)
399. S A Wolf, D D Awschalom, R A Buhrman, J M Daughton, S von Molnár, M L Roukes, A Y Chtchelkanova, D M Treger *Science* **294** 1488 (2001)
400. I Zutic, J Fabian, S D Sarma *Rev. Mod. Phys.* **76** 323 (2004)
401. J M Slaughter, R W Dave, M DeHerrera, M Durlam, B N Engel, J Janesky, N D Rizzo, S Tehrani *J. Supercond.* **15** 19 (2002)
402. W Prellier, A Fouchet, B Mercey *J. Phys.: Condens. Matter* **15** 1583 (2003)
403. S J Pearton, W H Heo, M Ivill, D P Norton, T Steiner *Semicond. Sci. Technol.* **19** 59 (2004)
404. T Dietl *Semicond. Sci. Technol.* **17** 377 (2002)
405. P A M Rodrigues, P Y Yu, G Tamulaitis, S H Risbud *J. Appl. Phys.* **80** 5963 (1996)
406. N Feltin, L Levy, D Ingert, E Vincent, M P Pileni *J. Appl. Phys.* **87** 1415 (2000)
407. J M Slaughter, E Y Chen, S Tehrani *J. Appl. Phys.* **85** 4451 (1999)
408. J F Gregg, I Petej, E Jouguelet, C Dennis *J. Phys. D: Appl. Phys.* **35** R121 (2002)
409. D P Di Vincenzo, D Loss *J. Magn. Magn. Mater.* **200** 202 (1999)
410. D Loss, G Burkard, D P Di Vincenzo *J. Nanoparticle Res.* **2** 401 (2000)
411. J Slaughter, in *The 1st Annual CNS Nanotechnology Symposium* (Ithaca: Cornell University, 2004)
412. J-G Zhu, Y Zheng, G A Prinz *J. Appl. Phys.* **87** 6668 (2000)
413. Z Cui, J Rothman, M Klaui, L Lopez-Diaz, C A F Vaz, J A C Bland *Microelectron. Eng.* **61–62** 577 (2002)
414. J M D Coey *Solid State Commun.* **102** 101 (1997)
415. I Šafařík, M Šafaříková *J. Chromatogr. B* **722** 33 (1999)
416. C Suryanarayana, C C Koch *Hyperfine Interact.* **130** 5 (2000)

[a] — *Phys. Solid State (Engl. Transl.)*
[b] — *Mendeleev J. (Engl. Transl.)*
[c] — *Inorg. Mater. (Engl. Transl.)*
[d] — *Dokl. Chem. (Engl. Transl.)*
[e] — *Russ. J. Phys. Chem. (Engl. Transl.)*
[f] — *Chem. Sust. Devel. (Engl. Transl.)*
[g] — *J. Exp. Theor. Phys. (Engl. Transl.)*
[h] — *Polym. Sci. (Engl. Transl.)*
[i] — *Biophysics (Engl. Transl.)*